

University of Nottingham

UK | CHINA | MALAYSIA

The Role of Survivin in Autophagy

Thesis submitted to the University of Nottingham

for the Degree of Doctor of Philosophy

Nicola Humphry BSc

September 2018

ABSTRACT

Survivin is a highly conserved protein with important roles in cell death and mitosis; deletion of the survivin gene is embryonically lethal. It is highly expressed in most cancers, making it a promising target for cancer therapy. Autophagy, an important homeostatic cellular recycling system, promotes cell survival under stresses such as DNA damage, nutrient starvation and hypoxia.

Recent research has begun to identify a link between survivin and autophagy, and therefore the aim of this thesis was to clarify the role of survivin in autophagy and to study the reported interaction between survivin and the autophagic protein microtubule-associated protein light chain 3 (LC3).

To achieve this aim, a variety of cell biology and molecular biology techniques were employed. Cultured human cells were modified to express survivin and LC3 with fluorescent tags and studied with fluorescence microscopy to investigate the localisation and characteristics of both survivin and autophagic bodies. Co-immunoprecipitation was used to study the interaction between survivin and LC3, and gene manipulation was used to identify the critical amino acid residues.

This thesis reports that high levels of survivin reduce the rate of autophagy and are associated with smaller autophagic bodies and larger acidic bodies. In addition, this study reveals that survivin interacts with LC3 through a canonical LC3-interaction region at residues 61-64, but this interaction is not critical to the role of survivin in regulating autophagosome or acidic body size. Finally, it raises the possibility that survivin-LC3 interaction may affect the mitotic role of survivin.

PUBLICATIONS ARISING FROM THIS THESIS

Survivin inhibits excessive autophagy in cancer cells but does so independently of its interaction with LC3

Nicola J. Humphry and Sally P. Wheatley

Biology Open (2018) 7, bio037374. doi:10.1242/bio.037374

Full manuscript included at the end of this thesis.

ACKNOWLEDGEMENTS

My thanks go to Sally Wheatley for providing me with this amazing opportunity; Lucia Dunajova and Aysha Aljaberi for holding my hand at the beginning; James Grey and Amelia Townley – my comrades in arms; Sophie Rochette and Jess Winfield for their assistance in the lab; Nur Mohd Rashid (Aida) for performing survival assays under my guidance; Alan Huett, Alistair Hume, Ian Kerr, Bill Wickstead, Nick Holliday and Rob Layfield for advice and consumables, my sister Jenny for proof-reading and last but never least, Martin, Izzie, Sarah and Jill for their unfailing support and encouragement.

This thesis is dedicated

to Martin, for believing in me,

and to my parents, for everything.

CONTENTS

Abstract ii
Publications arising from this thesis iii
Acknowledgements iv
1 Introduction 1
1.1 Overview 1
1.2 Survivin / BIRC5 2
1.2.1 History / Discovery 2
1.2.2 Physical structure 2
1.2.3 Post-translational modifications 4
1.2.4 Localisation 5
1.2.5 Function in cell division 6
1.2.6 Function in apoptosis 9
1.2.7 Dysregulation of Survivin in disease 11
1.3 Autophagy 15
1.3.1 History / Discovery 15
1.3.2 Mechanism. 15
1.3.3 Dysregulation of Autophagy in disease 21
1.4 LC3 22
1.4.1 History / Discovery 22
1.4.2 Physical structure. 22
1.4.3 Function. 23
1.4.4 Dysregulation of LC3 in disease 25
1.5 Rationale 26
1.5.1 Survivin and mTOR 27
1.5.2 Survivin and clathrin 28

1.5.3 Survivin and c-Src (proto-oncogene tyrosine-kinase of the sarcoma-family of kinases). 29
1.6 Hypothesis and aims: 30
2 Materials and methods 31
2.1 Molecular biology techniques. 31
2.1.1 Bacterial transformation with plasmid DNA purification 31
2.1.2 Polymerase Chain Reaction (PCR) 31
2.1.3 DNA agarose electrophoresis 32
2.1.4 Site-directed mutagenesis 32
2.1.5 Restriction digestion 33
2.1.6 Ligation 33
2.2 Cloning strategies for individual plasmid constructs 33
2.2.1 Generation of survivin^{pent}-RFP 34
2.2.2 Generation of survivin^{F61A,L64A} constructs 34
2.3 Mammalian cell culture techniques. 35
2.3.1 Cell lines 35
2.3.2 Growth conditions and media. 35
2.3.3 Passaging cells 35
2.3.4 Transfection. 36
2.3.5 Generation of stable cell lines 36
2.3.6 Freezing cells 36
2.3.7 Drug treatments. 37
2.4 Biochemical assays 37
2.4.1 Bradford protein assay 37
2.5 Microscopy techniques. 38
2.5.1 Fixation and immunostaining 38

2.5.2 Live cell imaging. 38
2.5.3 Imaging. 39
2.5.4 Measurement of puncta 39
2.6 SDS PAGE and Immunoblotting 40
2.6.1 SDS Polyacrylamide gel electrophoresis 40
2.6.2 Immunoblotting 40
2.7 P62 degradation assay for autophagic flux 41
2.8 Viability Assay 42
2.9 Clonogenic Survival Assay 42
2.10 Co-immunoprecipitation. 42
Flag-tagged co-immunoprecipitation 42
GFP-tagged co-immunoprecipitation. 43
2.11 Statistical analysis 44
3 Results 46
3.1 Survivin associates with LC3 through an LC3-interacting Region 46
3.1.1 Sequence analysis 46
3.1.2 Generation of survivin mutants. 50
3.1.3 Co-Immunoprecipitation of survivin and lc3 54
3.1.4 Co-localisation of survivin and LC3 56
3.2 Survivin inhibits autophagy via an LC3-independent mechanism. 59
3.2.1 Autophagic flux 59
3.2.2 Autophagosome / lysosome characteristics 63
3.2.3 Survival under autophagic stress 67
3.3 Residues F61 and L64 are required for mitotic localisation of survivin 71
3.3.1 Localisation of survivin^{F61A,L64A} 71

3.3.2 Co-immunoprecipitation of survivin and histone H3 pT3 75

4 Discussion 77

4.1 Conclusions 77

4.1.1 Survivin regulates autophagic flux, autophagosome and acidic puncta size independent of its association with LC3. 78

4.1.2 Survivin does not co-localise with autophagic puncta. 79

4.1.3 Survivin contains an LIR at residues 61-64 which is essential to the association with LC3. 79

4.1.4 Survivin increases sensitivity to RAP treatment in a manner that is dependent upon residues F61 and L64. 80

4.2 Understanding the mechanism and purpose of autophagic inhibition by survivin. 81

4.3 Understanding and purpose of the association between survivin and LC3. 84

4.4 Outlook 86

References 87

Appendix 100

Cloning primers 100

Buffers and solutions. 100

Reagent 100

Fixation solution 100

Triton X-100 solution 100

Blocking solution 100

Towbin transfer buffer 100

SDS sample buffer 101

Antibiotic concentrations 101

Methodologies 102

Co-immunoprecipitation 105

Macros 107

Batch Processing images to measure red puncta, green puncta and co-localised puncta 107

Batch processing to measure red lysosome puncta 109

Abbreviations 110

5 Publications ..... **Error! Bookmark not defined.**

INTRODUCTION

OVERVIEW

Survivin is a small evolutionarily-conserved protein with dual roles in the regulation of mitosis and apoptosis. Expressed at the G2 and M phases of the cell cycle, survivin is required to regulate chromosomal congression, segregation and cytokinesis, to maintain genomic stability of daughter cells. Deletion of the survivin gene in mice results in lethality during embryonic development, with cells displaying mitotic failure and giant cells with irregular nuclei and micronuclei after just one week of growth[1]. In most tumours, survivin is aberrantly expressed throughout the cell cycle, with highest levels found in breast and lung cancers[2], where expression is associated with resistance to oncotherapies and poor prognosis for survival. The mechanism for the anti-apoptotic activity of survivin is more complex than the direct inhibition of caspases and may require co-factors.

Autophagy, a process to degrade sequestered cytoplasmic material, is closely associated with cell death, and many examples exist where autophagy protects cells against apoptosis[3].

A link between survivin and autophagy was recently discovered suggesting that survivin can protect cells from autophagic cell death[4] and this raises the possibility that inhibition of apoptosis by survivin may involve the regulation of autophagy.

SURVIVIN / BIRC5

History / Discovery

The human survivin protein was first described in 1997 by Ambrosini, Adida and Altieri, who identified survivin as a member of the Inhibitor of Apoptosis (IAP) family by the presence of a Baculovirus IAP Repeat (BIR) domain, and recognised that it was expressed during foetal development but also in many human cancers[5].

Physical structure

A single copy of the survivin gene BIRC5 is located at the chromosomal position 17q25[5]. This chromosome is rich in protein-coding genes, having the second highest gene density in the genome[6].

The survivin gene promoter contains three cell cycle-dependent elements (CDE's) and one cell cycle gene homology region (CHR)[7]. These G1 transcriptional repressor elements are also found in other G2/M-regulated genes where they control cell-cycle periodicity[8]. As this suggests, endogenous survivin is expressed predominantly in the G2 and M phases of the cell cycle[7]. It has a short half-life of 30 minutes, with polyubiquitination and subsequent proteasome degradation causing a sharp fall in protein levels after mitosis[9].

The tertiary structure of survivin is a c-terminal alpha-helix; a 70-amino-acid zinc finger fold and a single N-terminal BIR domain, making it a member of the inhibitor of apoptosis (IAP) gene family[10]. The alpha-helix contains hydrophobic clusters with the potential for protein-protein interaction[11,12]. A summary of the two dimensional structure and function of survivin, along with the effect of experimental mutations is shown in figure 1.2.1.

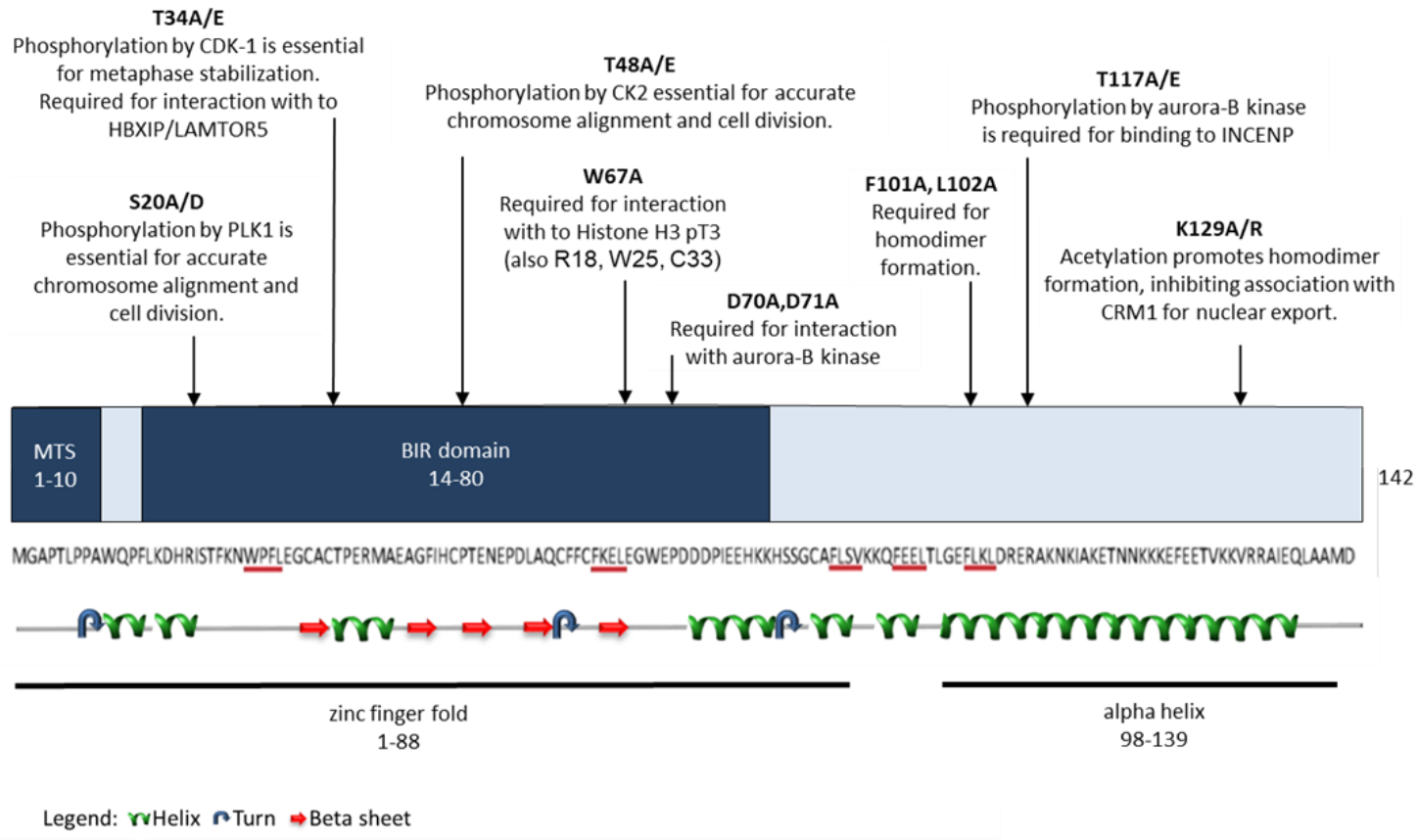


Figure 1.2.1 Summary of the two dimensional structure and function of survivin. Sources: Mitochondrial Targetting Sequence (MTS)[13], BIR domain[10], T34[14], T48[15] ,D70-D71[16] T97[17], L98[17], F102-L102[18], T117[19], K129[20,21].

Survivin readily forms a bow-tie-shaped homodimer in solution[11] (figure 1.2.2) through an intermolecularly-bound zinc atom. Dimerisation appears to mask a nuclear export sequence in the central region of survivin[18]. Apart from itself, survivin forms binary interactions with inner centromere protein (INCENP)[22], aurora kinase[23] and borealin[22] to form the chromosomal passenger complex (CPC); ran[24], a small GTPase involved in mitotic spindle formation; CDK1[25] which phosphorylates survivin at T34 during mitosis; beclin1[26], a protein with roles in autophagy and apoptosis; second mitochondria-derived activator of caspase (SMAC/DIABLO)[27], a mitochondrial protein involved in apoptosis and GAS2-like protein 3 (GAS2L3)[28], a tubulin- and actin-binding protein.

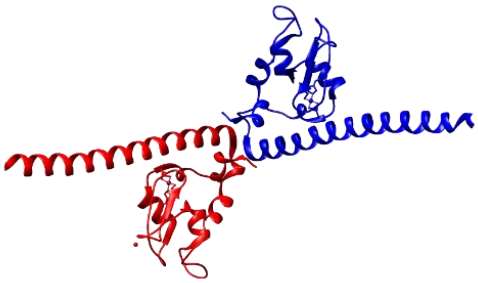


Figure 1.2.2: Structure of the survivin homodimer. Ribbon diagram illustrating the crystal structure of the survivin homodimer[11](RCSB PDB:IE31). Molecular graphic generated with the UCSF Chimera package[29].

Post-translational modifications

Survivin is subject to multiple post-translational modifications which regulate its localization and function. For example, acetylation of K129 enhances survivin homodimerization, preventing exportation from the nucleus in association with chromosome region maintenance 1 (CRM1)[20]. Phosphorylation by cyclin-dependent kinase (CDK-1) at T34 has been implicated in stabilizing survivin during metaphase[25]. Phosphorylation of residue T48 by casein kinase 2 (CK2) and residue S20 by polo-like kinase 1 (PLK1) are essential for accurate chromosome alignment and cell division[15,30,31]. Residue T117 is phosphorylated by aurora-B kinase at pro-metaphase, yet dephosphorylation stabilises centromere association and is critical for chromosome bio-orientation[32].

Localisation

Full length wild type survivin is predominantly cytoplasmic, suggesting either active transport out of the nucleus or restricted entry into the nucleus. Several studies have attempted to explain this localisation, but evidence has been somewhat conflicting, with several research groups suggesting alternative mechanisms for nuclear export, see figure 1.2.3.

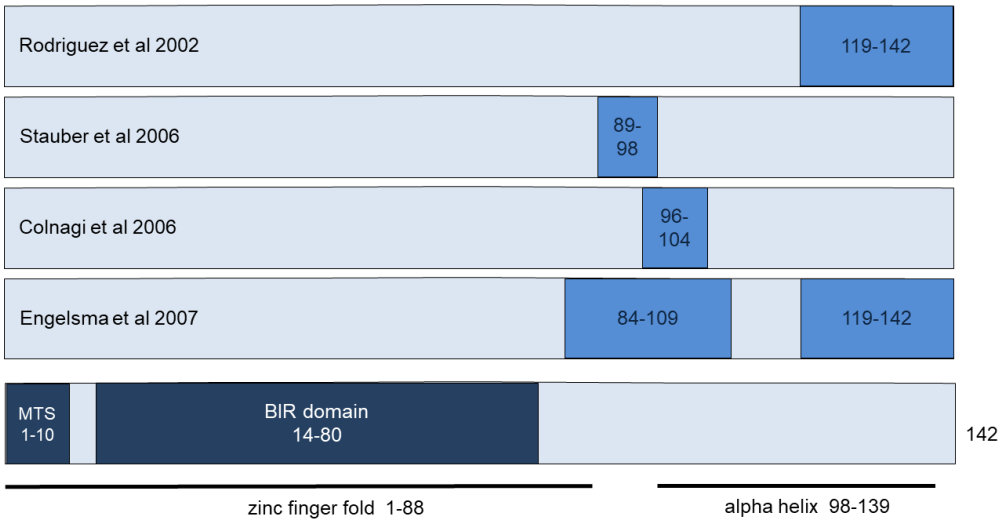


Figure 1.2.3: Regions of survivin identified as important for nuclear export.

The 23 c-terminal amino acids of survivin were initially identified as critical residues for CRM1-mediated nuclear export[33], yet a few years later nuclear export sequences (NES) at residues 89-98[34] and 96-104[17] were reported by different research groups. Later research found that CRM1-dependent nuclear export can be achieved by either the C-terminal region or by a region within residues 84-109 where a L98 is critical[18]. Though not part of a canonical NES, the first five hydrophobic residues of this sequence do appear to increase cytoplasmic localisation. In addition, mutation of residues 101 and 102 restricted survivin to the monomeric form, and this significantly improved the affinity for CRM1, presumably because this NES lies within the dimer interface of the protein[18]. This suggests that the NES in the central region of survivin is monomer-specific and that nucleocytoplasmic shuttling of survivin may be regulated by dimerisation.

Though survivin is pre-dominantly cytoplasmic in cultured cells, pools are also found in the nucleus[35,36], mitochondria[13,37], and localised to polymerised microtubules[7,38]. Survivin localizes to mitochondria in tumour cells via a mitochondrial-targeting sequence at residues 1-10[13] and is rapidly released into the cytosol following apoptotic stimuli where it suppresses caspase processing[37]. Nuclear survivin expression markedly increases in squamous cell carcinoma (SCC) tissues, as compared with normal epithelia, and it is highest in poorly differentiated SCCs[36]. Nuclear survivin in HeLa cells is not anti-apoptotic[35], yet it is still an unfavourable prognostic marker in several cancer tissues[39]. This apparent contradiction can be explained by the finding that nuclear survivin increases cell migration in SCCs, suggesting that while cytoplasmic survivin is anti-apoptotic, nuclear survivin has a role to play in tumour invasion[36].

Function in cell division

Survivin performs an essential role in mitosis, where chromosomes align along the midzone formed between two spindle poles. This alignment requires the binding of the kinetochores of sister chromatids to microtubules from opposite poles of the cell during metaphase. Shortening of these microtubules then separate the chromatids which migrate to the spindle poles during anaphase. At telophase the plasma membrane at the midzone pinches together segregating both DNA and cytoplasmic organelles into daughter cells with identical copies of genetic material in each (figure 1.2.4).

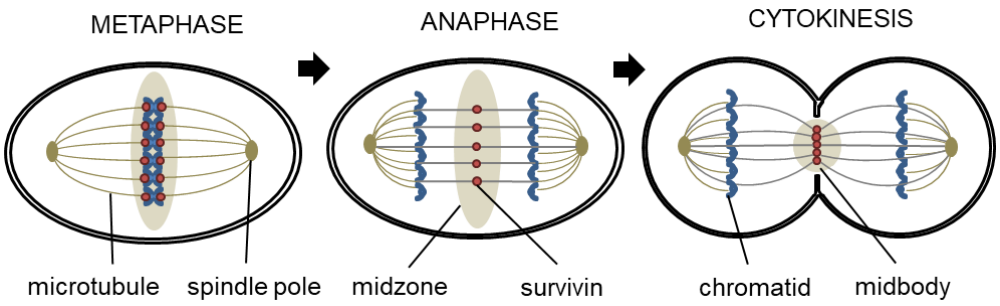


Figure 1.2.4: An overview of mitosis. Sister chromatids align at the midzone of the mitotic spindle at metaphase and are drawn to opposite spindle poles during anaphase. Duplicated DNA is segregated into daughter cells when the midbody contracts and splits the cell through a process termed cytokinesis.

The concentration of survivin at G2/M -phase of the cell cycle is around 40 times that found at G1, where it is almost undetectable[7]. During G2, survivin associates with the proteins borealin, INCENP and aurora-B kinase to form the chromosomal passenger complex (CPC)[19,22]. The CPC associates with the centromeres at metaphase. During anaphase the CPC transfers to the spindle midzone, and at cytokinesis it localises to the midbody[40]. The structure of the CPC is illustrated in figure 1.2.5.

Within the CPC, survivin is bound to borealin[22]. All four components of the CPC complex are required for cell division: without INCENP, survivin does not localise to the centromeres[41]; binding of aurora-B to survivin is required for its full kinase activity[42]; phosphorylation of survivin by Aurora-B at T117 in its carboxyl alpha-helical coil is required for binding to INCENP[19] and survivin depletion prevents localisation of aurora-B and INCENP to the centromere[43]. Survivin anchors the CPC to the centromeres at prophase and metaphase by interacting with histone H3 phosphorylated at T3 via a discrete pocket in the BIR-domain[44,45]. As mentioned previously, phosphorylation of survivin by CDK1, CK2 and PLK1 are also essential for accurate chromosome alignment and cell division[15,30,31].

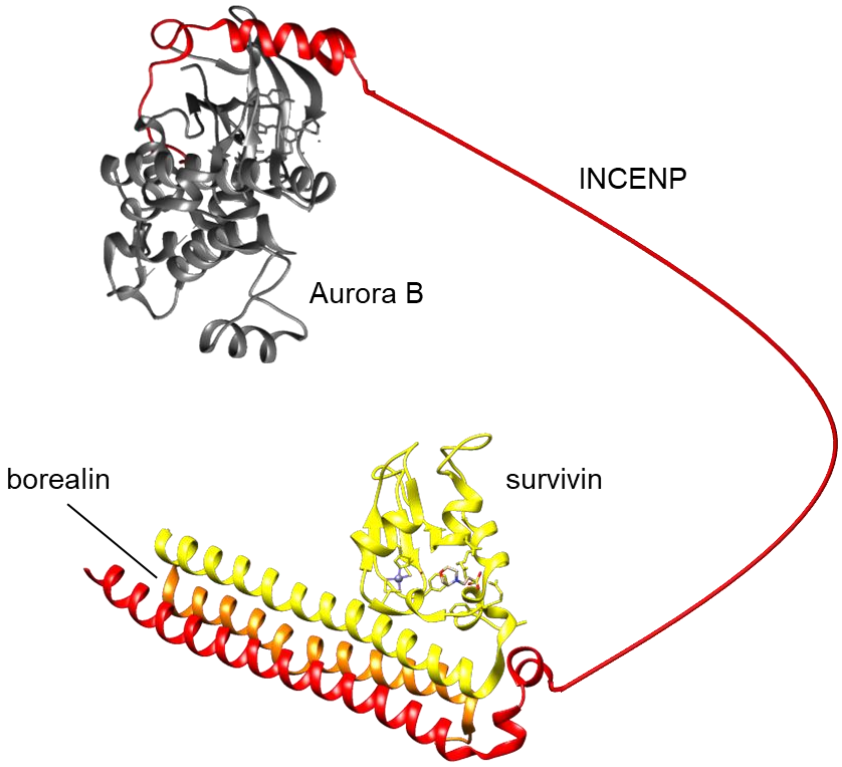


Figure 1.2.5: Structure of the Chromosomal Passenger Complex (CPC). Borealin (orange), Survivin (yellow) and the N-terminus of INCENP (red) form a triple coiled coil (UniProt 2QFA[22]). The C-terminus of INCENP binds to aurora B kinase (grey) (UniProt 4AF3[23]). The central domain of INCENP, a single alpha helix, is thought to provide flexibility to the CPC while tethering aurora B to centromere – regulating phosphorylation of kinetochore substrates when bipolar microtubule attachment creates kinetochore tension[46].

Misaligned chromosomes do not segregate correctly into daughter cells and resulting chromosomal instability can cause genetic and phenotypic variability leading to cancer[47]. To guard against this, metaphase to anaphase transition can be delayed in the event of chromosome misalignment, by a surveillance mechanism named the mitotic spindle checkpoint (reviewed in [48]). When kinetochores are not attached to microtubules, or are attached but not under tension, Mitotic arrest-deficient protein 2 (MAD2) and Budding uninhibited by benzimidazole-related protein 1 (BUBR1) inhibit CDC20, an accessory protein for the anaphase promoting complex (APC). Without APC activity, CDK1 remains active, and cohesion complexes at the centromere cannot be cleaved, preventing progression to anaphase.

Survivin plays a role in the mitotic spindle checkpoint by stabilising the association of BUBR1 with kinetochore and therefore sustaining checkpoint signalling in response to a lack of tension[43]. In this way, survivin reduces the risk of chromosomal instability in dividing cells. However, during mitotic arrest, transcription is absent, which means that short-lived proteins like survivin gradually become depleted. Depletion of other anti-apoptotic proteins such as induced Myeloid leukemia cell differentiation protein (MCL1) can trigger apoptosis during prolonged mitotic arrest[49] and it is highly likely that depletion of survivin during such an event would also trigger apoptosis, a final measure by the cell to prevent chromosomal instability.

Function in apoptosis

Apoptosis is a normal process during development and aging and maintains tissue homeostasis. As a cell death mechanism, it is carefully regulated; too much apoptosis results in tissue necrosis or impaired growth, too little results in tumour development. There are two main apoptosis activation pathways: the extrinsic and the intrinsic (reviewed in [50]). The extrinsic pathway is initiated by the binding of ligands such as Tumour Necrosis Factor (TNF), Fas, and TNF-Related Apoptosis-Inducing Ligand (TRAIL) to cell-surface receptors, or the delivery of granzyme-B through perforin channels. These signals lead to the activation of caspase-3 and a cascade of activation of effector caspase enzymes leading to cell death. The intrinsic pathway is initiated by internal signals such as p53 upregulation following DNA damage. These signals result in the depolarisation of the mitochondrial membrane and subsequent release of apoptosis effectors cytochrome c, SMAC/DIABLO which leads to the activation of caspase-3, and Apoptosis-Inducing Factor (AIF) which translocates to the nucleus where it induces nuclear fragmentation. Both pathways involve the activation of caspases resulting in a cascade of events ultimately leading to cell death.

The ectopic expression of survivin in cell culture can counteract apoptosis[10], and interference with survivin can lead to apoptotic cell death[51] making it clear that survivin plays a role in apoptotic regulation. The BIR domains of other human IAP family members such as x-linked inhibitor of apoptosis protein (XIAP) have been shown to inhibit caspase-3 and caspase-7, and they are regulated by SMAC/DIABLO. Whether survivin can inhibit caspase-3 or caspase-7 activity remains controversial, with a number of papers citing evidence that it can[2,52,53], and others claiming the opposite[54,55], though there is evidence to suggest that survivin can inhibit caspase-9[56], and several other indirect mechanisms for apoptotic inhibition have been suggested. First, a direct interaction between survivin and SMAC/DIABLO has been identified as a critical factor in the inhibition of apoptosis, suggesting that the association of these proteins inhibits the pro-apoptotic activity of SMAC/DIABLO[57,27]. Second, survivin binds to XIAP during apoptotic stimulation and protects XIAP from polyubiquitination and subsequent proteosomal-degradation[58]. Finally, depletion of survivin appears to induce the translocation of AIF from mitochondria to the nucleus, causing DNA fragmentation in a caspase-independent process[59]. An illustration of the mechanisms by which survivin may inhibit apoptosis is shown in figure 1.2.6

In addition to its well-established roles in mitosis and apoptosis, a new role in autophagy is emerging, and this is discussed further in section 1.5.

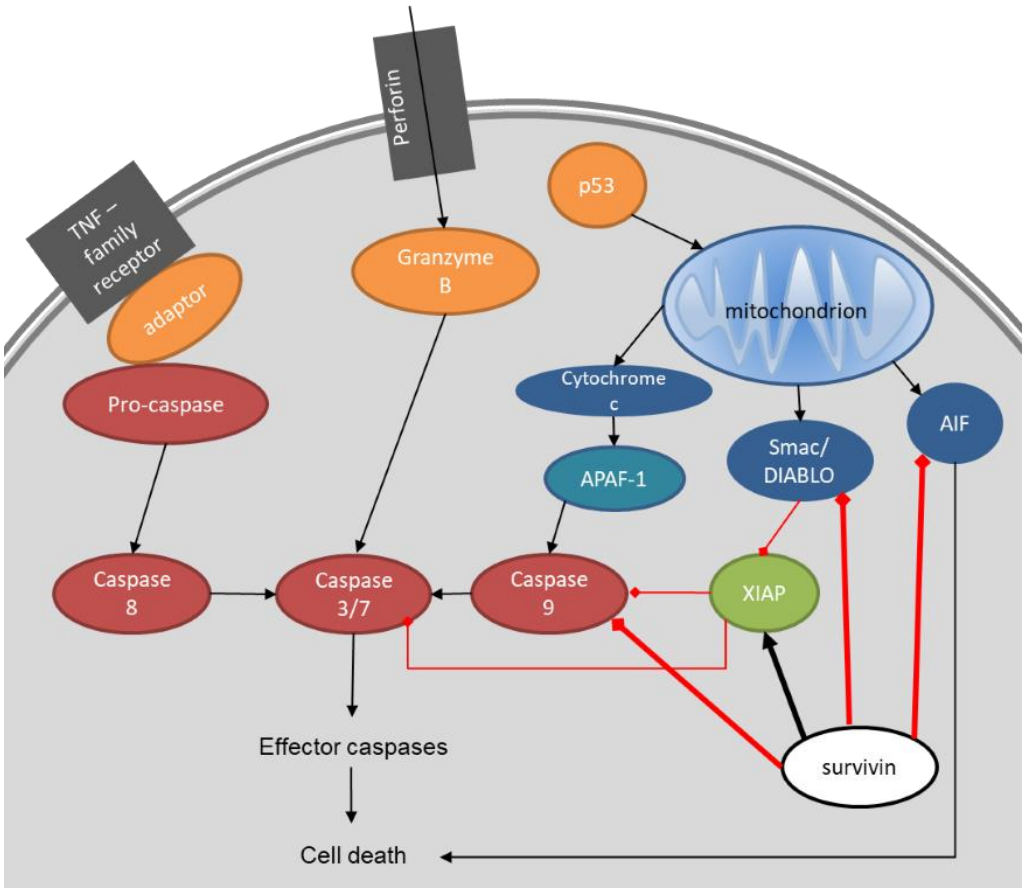


Figure 1.2.6: Overview of the role of survivin in apoptosis. External signals for apoptosis are received through TNF-family receptors and Granzyme-B which enters the cell through perforin channels. These signals lead to the activation of caspase-3 and a cascade of activation of effector caspase enzymes leading to cell death. Internal signals for apoptosis such as p53 upregulation following DNA damage, result in depolarisation of the mitochondrial membrane and subsequent release of apoptosis effectors cytochrome c, SMAC/DIABLO and AIF. Survivin stabilises XIAP, inhibits caspase-9 and interferes with the SMAC/DIABLO and AIF pathways to inhibit apoptosis.

Dysregulation of Survivin in disease

Unlike the cell-cycle-dependent expression in normal dividing cells, survivin is expressed throughout the cell-cycle in most cancers[10]. High levels of survivin correlate with increased resistance to chemotherapy[60] and irradiation[17], and therefore poor prognosis for the patient. Because survivin is overexpressed in most cancers, yet found in very low levels in most human cells[61] it is a promising target for cancer therapy.

The Clinical Trials database (https://clinicaltrials.gov/ct2/) lists 19 completed trials which targeted survivin. The majority of these studies relate to the use of survivin inhibitors such as LY2181308, an antisense oligonucleotide that binds to survivin mRNA to inhibit its expression in tumour tissue, and YM-155 (sepantronium bromide), a small molecule that suppresses the translation of survivin through direct binding to its promoter. A total of eight clinical trials have investigated the use of these inhibitors in combination therapy but published results indicate that they did not provide any clinical improvement (NCT01107444, NCT01038804, NCT01100931, NCT01009775, NCT00642018)[62–65]. A less direct approach to regulating survivin is more promising; a phase-I trial of CWP232291, a small molecule which blocks the proliferation of cancer cells via activation of caspases and downregulates survivin, found that this agent was effective against acute myeloid leukaemia[66] (NCT01398462) and recruitment for a phase-II trial is now underway (NCT03055286).

In addition, six trials have used dendritic cell (DC) vaccines which take advantage of the essential role of DCs in activating T cells to promote antitumor responses. These vaccines supply the patient with DCs transfected with the mRNA of tumour-associated antigens such as survivin. Published data indicate that DC vaccines using survivin mRNA showed promising results in phase-I trials (NCT00197860, NCT00197912, NCT01410968)[67–69]. Three phase-I trials investigated the potential of survivin-peptide vaccines and published data indicates that survivin peptide vaccination produced positive effects in both anaplastic astrocytoma and multiple myeloma (NCT01250470, NCT00499577)[70,71]. Finally, a trial using the DPX-Survivac vaccine (IMV Inc.), a T-cell-activating immunotherapy targets survivin found that the vaccine produced sustained immune responses in ovarian cancer (NCT01416038)[72].

There are currently five ongoing clinical trials that target survivin: two peptide vaccines, of which one is now in phase-II (NCT00470015, NCT00834665); a DC vaccine in phase-II (NCT01197625), a DPX-survivac vaccine trial looking at efficacy in different forms of cancer (NCT03332576); a SurVaxM (MimiVax) vaccine using a peptide mimic (NCT02455557), and a trial investigating tumour-associated antigen (TAA)-specific cytotoxic T lymphocytes, including lymphocytes specific to survivin, in solid tumours (NCT02239861).

In addition to the strong association with cancer, dysregulation of survivin plays a role in several other diseases. In autoimmune disease, survivin enhances antigen presentation, maintains the persistence of autoreactive cells, and supports the production of autoantibodies[73]. In Crohn's disease for example, levels of survivin are increased in T cells of the small intestine due to reduced proteasome degradation, and this protects T cells from apoptosis[74]. A recent clinical trial found that the level of survivin in circulating blood is associated with rheumatoid arthritis (RA, NCT02851056)[75,76] and this led to an active clinical trial to investigate whether current RA treatment reduces survivin levels (NCT03440892)[75,76]. Survivin has also been identified as a potential cardiac biomarker in elderly patients with heart disease where high levels of expression are associated with poor outcomes[77]. High levels are also associated with pathogenesis of acne and acne scarring[78], and with human adipose-derived stem cells from obese patients[79].

Unusually low levels of survivin are associated with a severe pathology in women with chronic obstructive pulmonary disease (COPD)[80], and also characterise cysts in polycystic kidney disease (PKD) where it is associated with chromosomal instability, cytokinesis defects and nuclear polyploidy or aneuploidy[81]. In non-alcoholic fatty liver disease, survivin expression is progressively lower in advanced stages[82].

Abnormal levels of survivin may play a role in disease through disruption of the cell cycle. Mouse models demonstrate that survivin knockout induces mitotic catastrophe[1], yet on the other hand, high levels of survivin during prolonged

mitotic arrest will favour mitotic exit rather than apoptosis, which will also lead to aneuploidy and chromosomal instability. High levels of survivin may also allow cells to survive apoptotic stimuli causing unrestrained cell growth and division.

AUTOPHAGY

History / Discovery

Autophagy is a conserved catabolic process induced by cell stress such as hypoxia, nutrient deprivation, and DNA damage (caused by irradiation or chemotherapy for example). While the ubiquitin/proteasome system degrades the majority of short-lived, damaged proteins, autophagy targets long-lived or aggregated proteins and cellular organelles[83].

The lysosome was the first autophagic vesicle to be identified in 1949 by Belgian scientist Christian de Duve, who also coined the term 'autophagy' from the Ancient Greek auto (self) and phagia (eat)[84]. The full autophagic process was not observed in mammalian cells for another 50 years, when fluorescence microscopy enabled visualisation of the process in live cells[85].

The primary purpose of autophagy is cellular homeostasis which promotes cell survival, yet excessive levels can lead to cell death[86] and therefore it is a highly regulated process. During mitosis for example, the breakdown of the nuclear envelope and fission of mitochondrial networks leaves chromosomes and mitochondria vulnerable to degradation by the autophagic machinery, and inhibition of autophagy by CDK-1 during mitosis is likely to be protective[87,88].

Considerable research has been focussed on autophagy over the past few years, expanding our understanding of the process in human cells, and discovering how its deregulation is associated with disease.

Mechanism.

Autophagy is a process whereby proteins and organelles are sequestered into double-membraned vesicles (autophagosomes) which then fuse with lysosomes to degrade their contents, releasing metabolic components back into the cytoplasm. There are three main forms of autophagy: macroautophagy, involving the generation of an autophagosome enclosing a portion of the cytoplasm, and fusion of this vesicle with a lysosome;

microautophagy, involving invagination of the lysosomal membrane – directly taking cytoplasm into the lysosome[89] and chaperone-mediated autophagy, involving the transportation to, and translocation across, the lysosomal membrane of a targeted protein[90]. Macroautophagy is the subject of this study and will be referred to simply as 'autophagy' hereinafter.

Early-stages of autophagy

The molecular components of the early autophagic process are summarised in figure 1.3.1. Autophagy can be induced by low levels of energy, nutrients, growth factors or DNA damage, through AMP:ATP ratio or the PI3K-I/Akt, MAPK/Erk or p53 signalling pathways respectively. These signals activate AMP kinase (AMPK) or inhibit mammalian-target of rapamycin (mTOR) to activate unc-51-like autophagy activating kinase 1 (ULK-1). ULK-1 phosphorylates beclin-1 to enhance the activity of VPS34, the mammalian class III phosphatidylinositol 3-kinase (PI3K). Along with co-factors Atg14 and survivin, PI3K phosphorylates phosphatidylinositol to generate phosphatidylinositol-3-phosphate (PI3P)[91–93].

A double-membrane lipid bilayer pre-autophagosomal structure called a phagophore is generated at the phagophore assembly site (PAS) in the presence of PI3P[94]. Several different sources for the origin of this membrane have been proposed, including *de-novo* synthesis and formation from the membrane of the golgi, endoplasmic reticulum or mitochondria (reviewed in [95]). The phagophore extends to engulf cytoplasmic proteins and organelles. Extension of the phagophore requires the activation of Atg12 by Atg7, and conjugation of Atg12 with Atg5 and Atg16L to form a large complex of approximately 800kDa[96]. This complex is thought to form a scaffold upon which microtubule-associated protein light chain 3 I (LC3-I) is lipidated with phosphatidylethanolamine (PE) forming LC3-II, and bound to the phagophore in a process catalysed by Atg3[97]. The phagophore eventually forms a complete vesicle termed an autophagosome, enclosing selectively targeted material

bound to LC3-II on the inner membrane via cargo proteins. For example p62 binds to both poly-ubiquitinated proteins[98] and LC3-II, and optineurin binds to damaged mitochondria[99] and LC3-II.

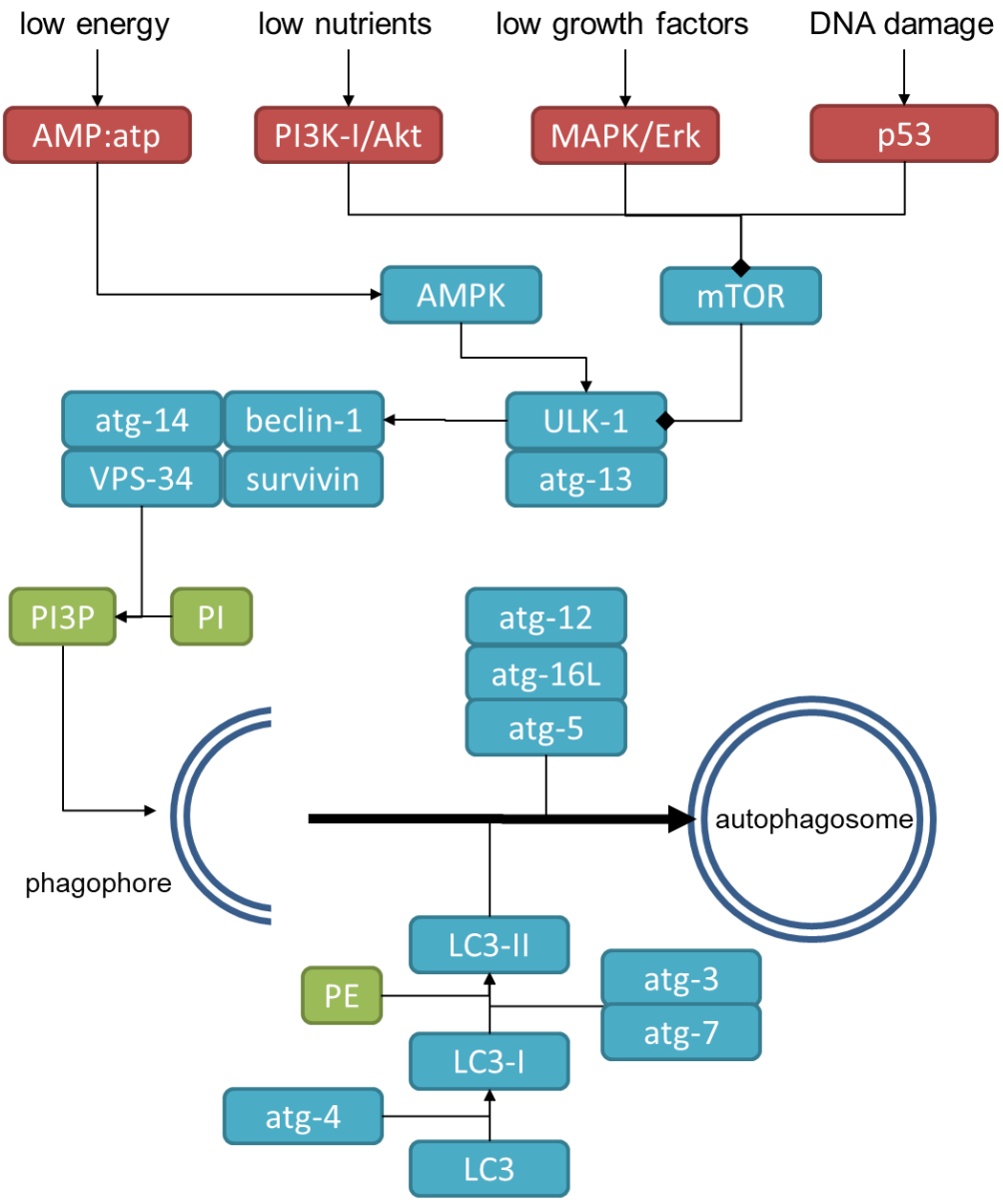


Figure 1.3.1: An overview of early autophagy. Autophagy can be induced by low levels of energy, nutrients, growth factors or DNA damage through a high AMP:ATP ratio or the PI3K-I/Akt, MAPK/Erk or p53 signalling pathways respectively. These signals result in the activation of ULK-1 resulting in the generation of PI3P which is required for nucleation of the phagophore. Phagophore extension to form the autophagosome requires PE-conjugated LC3-II, and a complex of Atg12, Atg16L and Atg5.

Late-stage autophagy

Once the closed autophagic vesicle is formed, it may fuse with endosomes, forming an amphisome[100] (see figure 1.3.2). The autophagosome or amphisome will then fuse with a lysosome to form an autolysosome[101], where the target material will be degraded by acid hydrolases and the constituent components released back into the cytoplasm via membrane permeases[102].

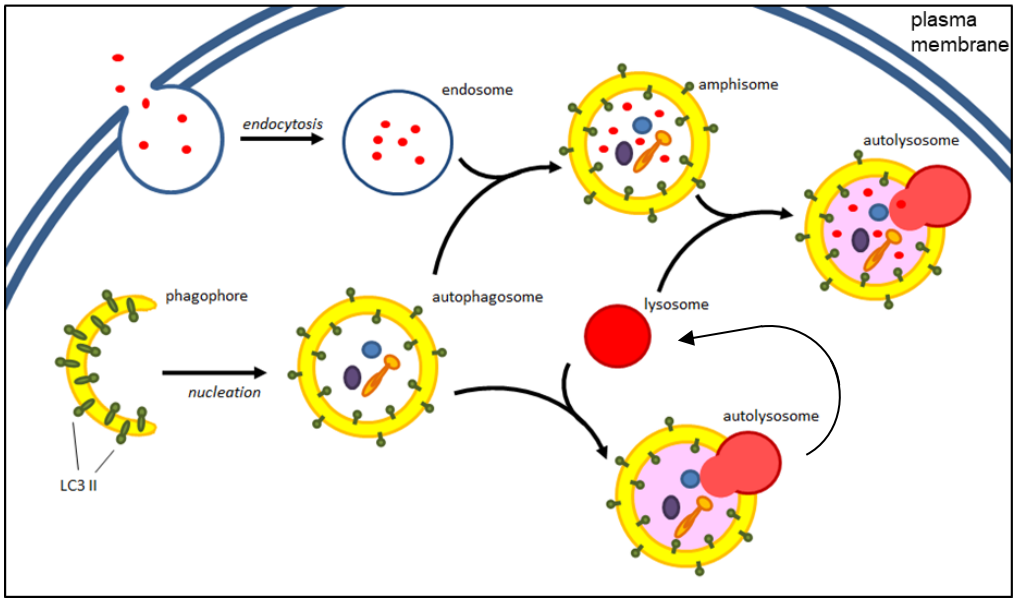


Figure 1.3.2: Vesicular compartments in autophagy. The autophagic vesicle may fuse with endosomes to form an amphisome[100] followed by fusion with a lysosome to form an autolysosome[101], where the target material will be degraded.

Lysosomes and autophagosomes need to migrate to the nuclear periphery to fuse together, and in mammals the microtubule network is required for this to occur efficiently[103]. Mature autophagosomes can be tethered to dynein motors for transport to the perinuclear area by the membrane-bound small GTPase Rab7[104]. To position them accurately for fusion, they also need to be able to move in the opposite direction, and this is achieved by kinesin motors which bind Rab7 and LC3 on the autophagosome membrane through the FYVE and coiled-coil domain-containing 1 (FYCO1) mediator[105].

When nutrients are scarce, kinesins maintaining lysosomes at the cell periphery are released, allowing lysosomes to move towards the nucleus[106]. Though it is unclear how nutrient availability affects autophagosome positioning, one potential regulatory factor could be the lipid complement of the autophagosomal membrane. A recent study found that when lipids are limited, autophagosomes are tethered to ER contact sites, preventing their movement towards the nucleus for fusion with lysosomes. The authors of this study suggest that perhaps the lipid components of the outer autophagosome membrane are a measure of maturity and only mature autophagosomes are released for transport to the perinuclear area to fuse with lysosomes[104].

Once they come into contact, lysosomes and autophagosomes are tethered together in a complex process involving many proteins, summarised in figure 1.3.3. Ectopic p-granules protein 5 (EPG5) binds to LC3 and the syntaxin17-SNAP29 protein complex on the autophagosome membrane, and to VAMP8 and rab7 on the lysosome[107,108]. Lysosomal rab7 is tethered to Syntaxin17 (STX17) on the autophagosome by the homotypic fusion and protein sorting (HOPS) complex[107,109], and to LC3-II and HOPS by Pleckstrin homology domain-containing family M member 1 (PLEKHM1) Along with Atg14L[110], EPG5 facilitates the assembly of the soluble N-ethylmaleimide-sensitive factor attachment protein receptor (SNARE) complex of syntaxin17, SNAP29 and VAMP8 to drive fusion[111]. Starvation stimulates autophagosome-lysosome fusion by suppressing O-GlcNAcylation of SNAP-29 to increase its binding affinity for other SNARE proteins[112].

The fusion of autophagosomes to lysosomes can be transient, involving a transfer of autophagic luminal material to the lysosome, followed by detachment of the two separate organelles, or it can be stable, resulting in a loss of the inner autophagosomal membrane, and the formation of a hybrid organelle[113]. In both cases the resulting organelle is termed the ‘autolysosome’.

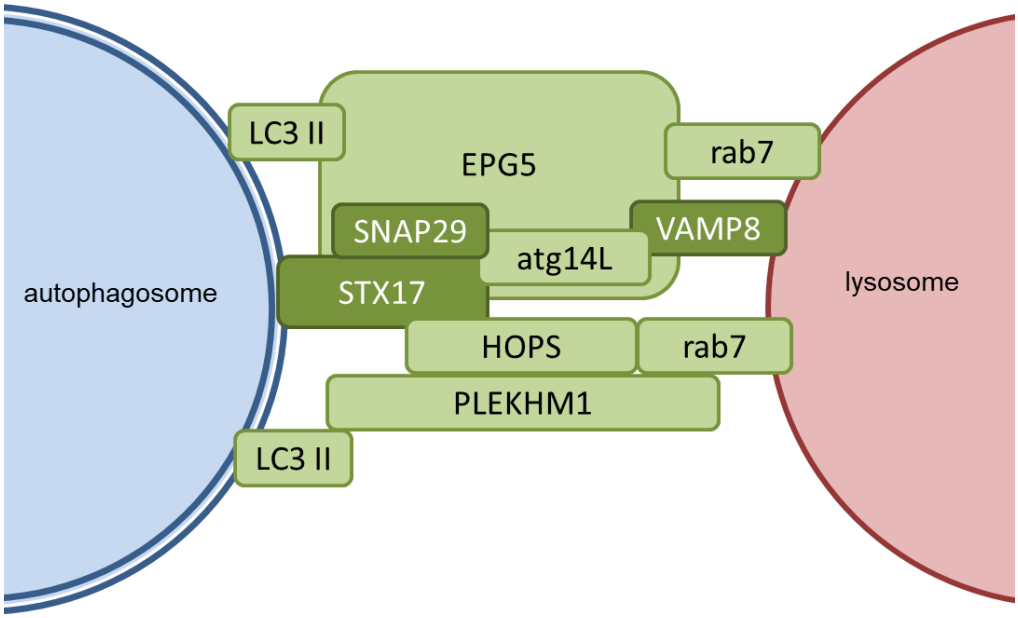


Figure 1.3.3: Fusion of the autophagosome and lysosome. Autophagosomes and lysosomes are tethered together in a complex process involving many different proteins. EPG5 binds to LC3 and the syntaxin17-SNAP29 protein complex on the autophagosome membrane, and to VAMP8 and Rab7 on the lysosome. The HOPS complex binds to lysosomal rab7 and STX17 on the autophagosome[107,109]. PLEKHM1 binds to LC3-II on the autophagosome, HOPS, and rab7 on the lysosome. Atg14L[110] and EPG5 facilitate the assembly of the SNARE complex highlighted in dark green, to drive fusion of the two vesicles[111].

Autophagy is a cyclical process since components of late-stage autophagy are recycled to produce new autophagosomes and lysosomes. LC3 is cleaved from PE in autolysosomal membranes by Atg4, releasing LC3-I into the cytoplasm, and lysosomes can be reformed from autolysosomes by a process termed autolysosomal reformation (ALR). ALR is triggered by the release of nutrients from an autolysosome which reactivates mTORC1 on the lysosomal surface. During this process, proto-lysosomal tubules extrude from autolysosomes and bud off to eventually mature into functional lysosomes[112].

Dysregulation of Autophagy in disease

Autophagy is deregulated in a number of human diseases, including neurodegenerative disorders, inflammatory disease and cancer reviewed in [114].

Alzheimer's disease, Parkinson's disease and Huntington's disease have all been reported to be associated with high levels, or suppression, of autophagy[115], though whether autophagy is protective or detrimental in these diseases is unclear. For example, patients with Alzheimer's disease have been shown to have high numbers of autophagic vesicles[116], yet in mice with early Alzheimer's disease, the suppression of beclin- 1, an autophagy promoter, was associated with pathology[117].

In the chronic inflammatory disorder cystic fibrosis, protein aggregates accumulate in airway epithelial cells. Cystic fibrosis transmembrane conductance regulator is mutated in this disorder, and its overexpression in cell culture is associated with beclin-1 downregulation and defective autophagy[118]. In Crohn's disease, another chronic inflammatory disorder, clearance of bacteria which have invaded cells is impaired. Susceptibility to this disease is increased in patients with mutations in the autophagy protein Atg16L1 which is involved in the elongation of the autophagosome membrane[119].

It is likely that autophagy has dual roles in cancer, since it can both degrade oncogenic material, inhibiting tumourigenesis, yet also promote tumour survival in hypoxic or low nutrient conditions reviewed in[120]. For example, beclin-1 is commonly deleted in one allele in human breast, prostate and ovarian cancers[121] and a number of studies have indicated that downregulation of this protein leads to increased tumorigenesis[92]. Aberrant expression of LC3 has also been identified in cancer, though studies report opposing correlations with pathology.

LC3

History / Discovery

Autophagy protein Atg8 was identified from the autophagy protein gene 8 (*apg8*) yeast mutant; *apg8-1* in 1993[122] and the protein (originally called Apg8 or Aut7) was described a few years later as critical for autophagy[123]. Though microtubule-associated protein light chain 3 (MAP-LC3) was discovered in mammals at a similar time[124], it was not recognised as an Atg8 homologue associated with the autophagosome membrane until 2000[125].

MAPs are involved in microtubule-assembly regulation, cytoskeletal organization, and organelle transport. They are often associated with light chain proteins, of which LC3 is perhaps the most studied[126].

Physical structure.

LC3 is encoded by a gene on human chromosome 20q13[124] and transcription is regulated by several factors including activating transcription factor 4 (ATF4), CCAAT-enhancer-binding protein β (CEBP-β), C/EBP homologous protein (CHOP), E2F Transcription Factor 1 (E2F1), forkhead box O3 (FOXO 1/3), GATA Binding Protein 1 (GBP-1) , jun, transcription factor EB (TFEB), sterol regulatory element-binding protein 2S (SREBP2) and Zinc finger protein with KRAB and SCAN domains 3 (ZKSCAN3)[127.]

Newly synthesised LC3 (often termed pro-LC3) is cleaved by Atg4 to form LC3-I. LC3-I can be bound to a lipid molecule, phosphatidyl ethanolamine (PE), to form LC3-II[125] in a process requiring Atg3 and Atg7. A protein complex formed by Atg12, Atg5 and Atg16L serves as a scaffold on the phagophore membrane to which LC3-I is localised for lipidation[97]. LC3-II exists as a membrane-bound protein on both the inside and outside surfaces of autophagosomes and the amount of LC3-II expressed in a cell correlates with the extent of autophagosome formation[125]. The crystal structure of MAPLC3B is shown in figure 1.4.1.

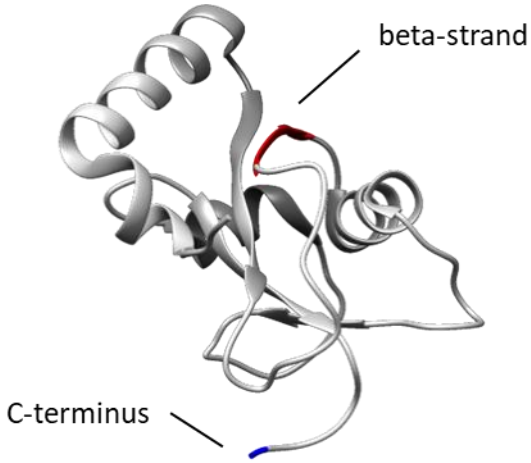


Figure 1.4.1: MAP-LC3 crystal structure. from www.ebi.ac.uk Protein Data Bank id:3vtu. The beta strand commonly used as a binding site for adaptor proteins is highlighted in red. The C-terminal glycine exposed during post-translational cleavage by Atg4 is highlighted in blue. Ribbon diagram generated with Chimera[29].

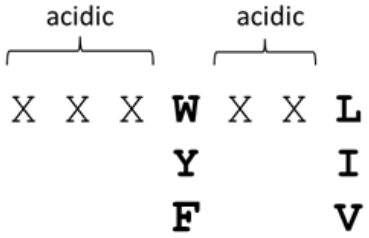
It is now considered that there are six mammalian orthologs of yeast Atg8 which can be divided into the MAP1LC3 (LC3) family, consisting of LC3A, LC3B and LC3C, and the GABARAP-like family, consisting of GABARAP, GABARAPL1 and GABARAPL2/GATE-16. All of these Atg8-homologues associate with autophagosomes, are lipidated post-translation[128–131], and show considerable overlap in their binding partners[128]. Both LC3A and LC3B are expressed in higher levels than LC3C across various tissues, and have been shown to accumulate on autophagosome membranes, though they show minimal co-localisation, suggesting that autophagosomes are formed from a single isoform[130,131].

Function.

LC3 proteins have long been considered to be necessary for autophagosome formation[123,132], yet a recent study demonstrated that when all human Atg8 orthologues are knocked out, the main defect observed is in autophagosome-lysosome fusion[133]. This suggests that LC3 proteins are required for fusion, but are not essential for autophagosome formation, though they must play a role

in the latter since autophagosomes were formed at a slower rate and are smaller in these experiments[133].

Multiple binding partners for LC3 have been discovered which act either by tethering LC3 to autophagic machinery or targeting particular cargos for degradation in selective autophagy[134]. Binding partners typically contain a canonical sequence of amino-acids used to interact with LC3, termed an LC3-interacting-region (LIR) or Atg8-interacting motif (AIM)[135]. The LIR motif consists of a tryptophan (Trp, W) or less commonly a tyrosine (Tyr, Y) residue followed by two further amino acids (xx, where x is any amino acid) and terminates with a leucine (Leu,L), an isoleucine (Ile,I) or in one instance, a valine (Val,V) forming a WxxL pattern illustrated in figure 1.4.2. The preceding three N-terminal residues to W, and the two residues separating the W and L tend to be acidic which complements the basic nature of the binding site on Atg8/LC3, making the interaction stronger. The residues preceding W also tend to be hydrophilic, whereas the residue immediately preceding the L tends to be hydrophobic[135]. LC3-binding partners form an intermolecular parallel beta-sheet with β2 of LC3 family members, which means that a functional LIR requires a WxxL-like sequence with an extended β-conformation[135].



	AIM/LIR sequence	Binding partner
Atg19	ALT**W**EE**L**	Atg8
Atg3	VGD**W**ED**L**QD	Atg8
Atg4B	TLT**Y**DT**L**RF	LC3
P62	DDD**W**TH**L**SS	LC3
NBR1	SED**Y**II**I**LP	LC3
Nix	NSS**W**VE**L**PM	GABARAP

Figure 1.4.2: AIM/LIR canonical sequence and its form in several known LC3-interacting proteins. Adapted from [135]. X represents any amino-acid.

LC3 also interacts with tubulin either through MAP1A or MAP1B[124], or directly via its N-terminal domain[136] and stabilizes microtubule networks by promoting growth over shortening events[137]. In this capacity, LC3 is contributes to intracellular transport during autophagy[105], phagocytosis[138] and viral infection[139].

Dysregulation of LC3 in disease

Aberrant expression of LC3 has also been identified in cancer, though studies report opposing correlations with pathology. For example, LC3 is highly expressed in gastrointestinal cancers[140] and correlates with stage, tumour size and poor overall survival in patients with oral squamous cell carcinoma (OSCC)[141]. In contrast, both beclin-1 and LC3-II have reduced expression in lung cancer tissues[142], and their downregulation correlates with poor prognosis in hypopharyngeal squamous cell carcinoma (HSCC)[143]. Reduced expression of LC3 is also associated with the progression of renal cancer[144]. It is likely that the relationship between LC3 and cancer depends on the stage and type of cancer and the co-expression of other proteins.

RATIONALE

A number of studies have demonstrated that there is considerable cross-talk between apoptosis and autophagy, and survivin is not the first protein to have a role in both processes. For example, beclin-1, which is required for the nucleation of the phagophore, also interacts with the anti-apoptotic Bcl-2 proteins[145]. These two proteins disassociate during autophagy and prolonged autophagy disrupts the anti-apoptotic function of Bcl-2 leading to cell death. Another example is the inhibitory interaction of Atg12, required for the expansion of the phagophore, with the anti-apoptotic protein mcl-1[146]. Finally, p53 is a pro-apoptotic protein, which in the cytoplasm can inhibit autophagy through the activation of mTOR[147].

Evidence pointing to a role for survivin in autophagy has been gradually accumulating over the past few years. An inverse relationship between survivin and autophagy was indicated by research on glioma cells, where the depletion of beclin-1, a key promoter of autophagy, led to the downregulation of survivin and sensitization to TRAIL-induced apoptosis[26]. In support of this, the suppression of survivin using the inhibitor YM155 induced autophagy-dependent cell death in prostate cancer cells[148] and adenoid cystic carcinoma cells[149]. In addition, several cancer cell lines treated with the tumourigenic chemokine CCL2 demonstrated an increase in survivin expression associated with a decrease in autophagy[4].

Interactions have been identified between survivin and autophagy proteins beclin-1[26], Atg5[150], LAMTOR(HBXIP)[14] and of particular relevance to this thesis, LC3B[4]. The interaction with LC3B was reported by Roca, et al (2008) and is the sole paper to date to demonstrate an interaction between these two proteins[4]. Other potential mechanisms for the regulation of autophagy by survivin are discussed in more detail below.

Survivin and mTOR

The primary inhibitor of autophagy, mTOR, can promote the translation of survivin mRNA[151], and survivin has been shown to associate with LAMTOR5/HBXIP[14] which forms part of the ragulator complex responsible for tethering mTORC1 at the lysosome surface for activation when amino acids are abundant. mTOR activation at the lysosome surface is illustrated in figure 1.5.1. In addition, overexpression of p70S6K1, a phosphorylation target of mTORC1, is sufficient to upregulate survivin[152]. Together, these data suggest reciprocal regulation occurs between mTOR and survivin.

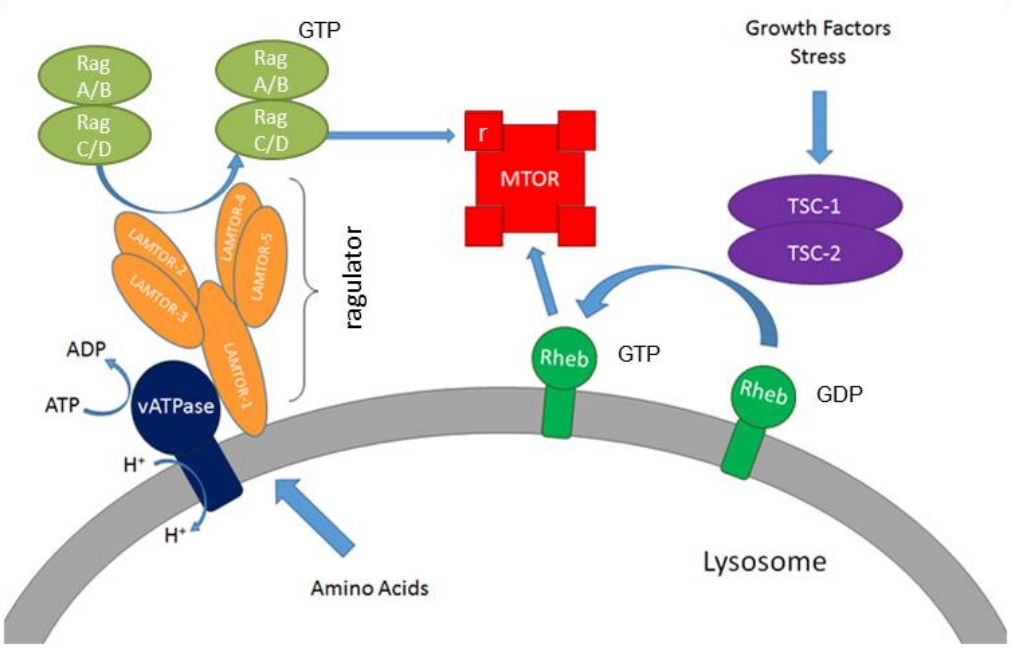


Figure 1.5.1: Activation of mTOR at the lysosome surface: Small GTPase 'Rag' proteins interact with a pentameric 'ragulator' complex on the lysosome surface. Ragulator is comprised of LAMTOR1 (p18/C11orf59), itself anchored to the lysosome surface by lipidation; LAMTOR2 (p14); LAMTOR3 (MAPKSP1/MP1), LAMTOR4 (C7orf59), and LAMTOR5 (HBXIP/XIP). Abundant amino acids induce the guanine nucleotide exchange factor (GEF) -activity of ragulator, to load RagB with GTP, enabling rag A/B heterodimers to interact with raptor (r) in mTORC1, essentially tethering mTORC1 to the lysosome. This allows mTORC1 to be activated by lysosome-bound protein Rheb. Growth factor and energy signals are transmitted to mTORC1 via a different mechanism, whereby TSC1 and TSC2 proteins form a tumor suppressor complex which regulates the GTP-loading state of Rheb[153,154].

Survivin and clathrin

Other potential links with autophagy include the interaction of survivin with clathrin, a protein that plays a major role in the formation of coated vesicles[151]. During normal enucleation, large vacuoles resembling autolysosomes form, yet when survivin is knocked-down, enucleation is inhibited and smaller vacuoles resembling autophagosomes are formed, suggesting that autophagosome-lysosome fusion is affected[151]. Clathrin also plays a role in the regulation of ALR, a process crucial to autophagosome homeostasis[155], and clathrin-coated vesicles are used to transport acid hydrolases from the golgi apparatus to the lysosome [156] (figure 1.5.2).

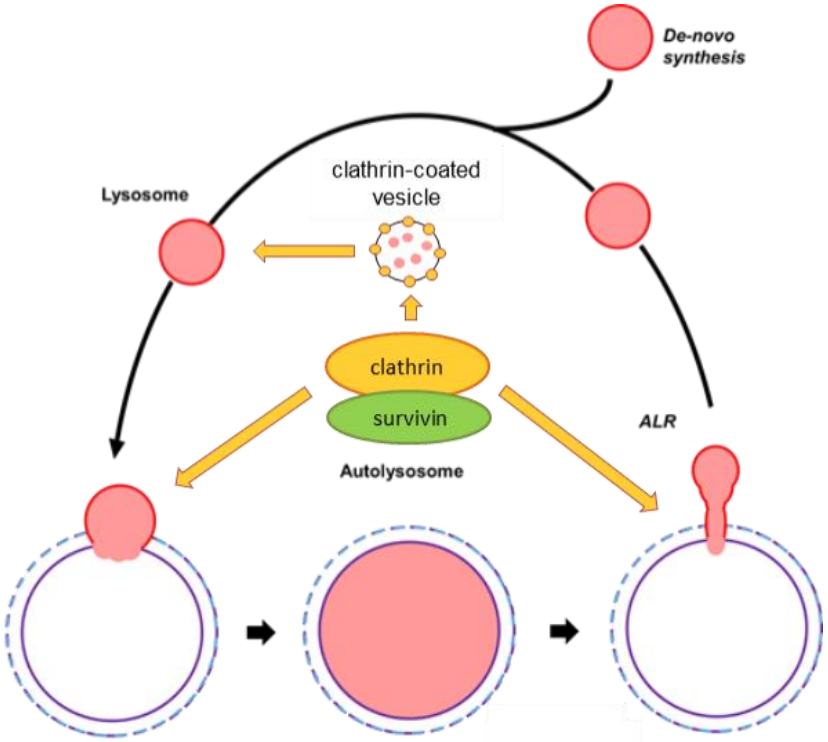


Figure 1.5.2: Clathrin and the lysosome. Clathrin plays a role in autophagic lysosome reformation (ALR)[155], coats vesicles used to deliver acid hydrolases to the lysosome[156], and associates with survivin (CO-IP) in enucleating erythroblasts where survivin knockdown may affect autophagosome-lysosome fusion[151]. Image not to scale.

Survivin and c-Src (proto-oncogene tyrosine-kinase of the sarcoma-family of kinases).

When cells migrate, the focal adhesion (FA) sites anchoring them to their substrate need to be assembled at the leading-edge of the cell and disassembled at the trailing-edge. FA disassembly requires the interaction of c-Src, integrins, and LC3-II[157] (figure 1.5.3). Survivin has recently been shown to interact with c-Src[13], and expression of survivin is related to cancer metastasis[158], suggesting the possibility of a connection between survivin and autophagic disassembly of FAs.

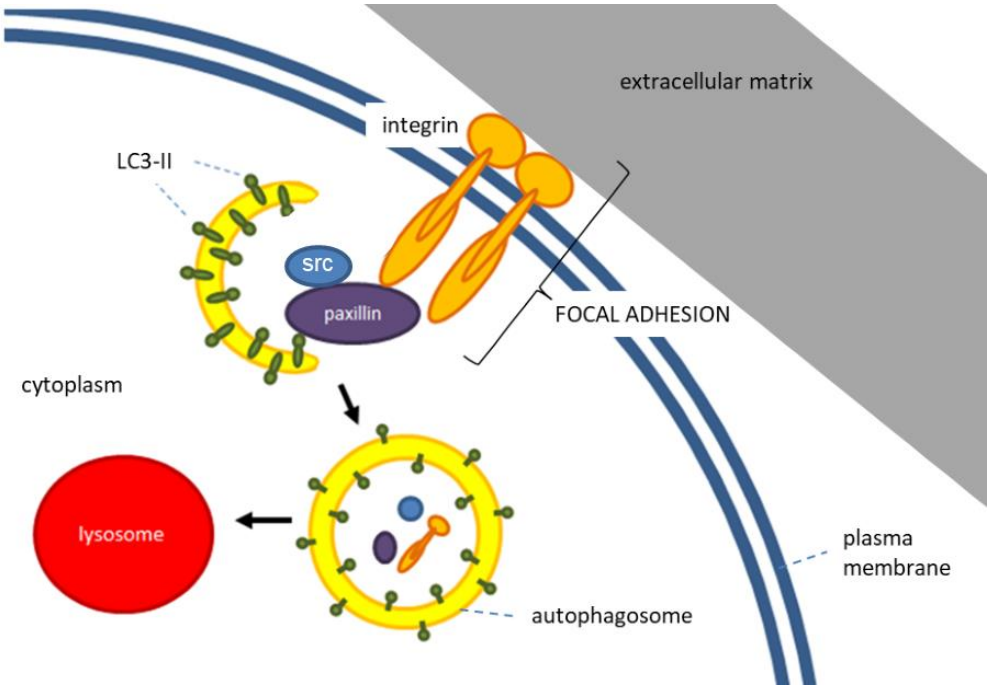


Figure 1.5.3: Focal adhesion (FA) disassembly. The key FA protein, paxillin, is degraded by autophagy. Paxillin interacts with LC3 through an LIR in a c-Src-regulated manner[157].

HYPOTHESIS AND AIMS:

This study tests the following hypothesis: Interaction between survivin and LC3 inhibits autophagy.

The aims of this thesis are two-fold:

To confirm interaction between survivin and LC3 and to identify the critical amino-acid residues responsible.

To determine the impact of survivin expression on autophagy in cultured human cells.

MATERIALS AND METHODS

MOLECULAR BIOLOGY TECHNIQUES.

All reagents were from New England Biolabs (NEB) unless otherwise stated.

Bacterial transformation with plasmid DNA purification

Approximately 1µg plasmid DNA was added to 100ul $CaCl_2$-chemically-competent *E.coli* DH5α bacteria and incubated on ice for 30 min. Cells were heat-shocked for 45 seconds at 42^{o}C and returned to ice for 2 min. 750 µl Luria Broth (LB) (0.17 M NaCl with 1% tryptone (w/v) and 0.5% yeast extract (w/v), pH 7) was added and the cells incubated at 37^{o}C with shaking for 1 hour. Cells were then pelleted by centrifugation at 17,000 xg for 1 min and resuspended in 100 µl LB broth then streaked onto LB-agar with either 100 µg/ml ampicillin or 30 µg/ml kanamycin and incubated overnight at 37^{o}C. Selected colonies were resuspended in 5 ml LB with antibiotic and grown-on overnight at 37^{o}C with shaking. Plasmid DNA was purified using the QIAprep Spin Miniprep kit (QIAGEN). Overnight cultures were centrifuged at 3,220 xg (4^{o}C) and supernatant discarded. Plasmid DNA was extracted from bacterial pellets into 30 µl sterile distilled water by centrifugation through filter cartridges according to manufacturer's instructions. DNA samples were stored at -20^{o}C.

Polymerase Chain Reaction (PCR)

A 50 µl reaction was prepared in sterile distilled water in a thin-walled 0.2 ml PCR tube (Thermo Fisher Scientific) on ice, consisting of ThermoPol reaction buffer (10x, 5 ul), 200 µM deoxynucleotides, 0.4 µM forward primer, 0.4 µM reverse primer, 50 ng plasmid DNA template, 1 U of Vent DNA Polymerase. Reaction mixtures were incubated in a thermocycler (T100 Thermocycler, BioRad) where they were subjected to cycles of temperature described in the following table:

Temperature (°C)		Duration (minutes)	Purpose
95	30 cycles	3	initial denaturation
95		0.5	denaturation
60		0.5	annealing
72		1 minute per kb template	extension
72		5	final extension

Confirmation of amplification was achieved by subjecting 5 µl of the PCR reaction product and negative control to agarose gel electrophoresis.

DNA product was purified from the PCR reaction using the QIAquick PCR Purification kit according to manufacturer's instructions, and eluted with 30 µl sterile distilled water.

DNA agarose electrophoresis

DNA samples were analysed by agarose gel electrophoresis (0.8% w/v agarose in TAE buffer [40 mM tris-acetate, 1 mM EDTA]) containing SYBR Safe DNA stain (ThermoFisher Scientific) at 100 V (45 min). DNA bands were visualised with UV light.

Site-directed mutagenesis

A PCR reaction was performed using mutagenesis primers (see appendix). Purified plasmids were then treated with 20U Dpn1 at 37°C for 3 h. The reaction was terminated by heat-inactivation of the Dpn1 enzyme at 80°C for 20 min. 10 µl reaction mixture was used to transform *E.coli* DH5α cells.

Mutagenesis of the plasmid construct was confirmed by sequencing using an appropriate primer at the Nottingham University DNA Sequencing Facility. The DNA sequence of the mutant construct was aligned with the template DNA construct using NCBI:BLAST[159] to confirm successful mutagenesis.

Restriction digestion

Plasmids were cleaved at unique restriction sites by incubation with specific restriction endonucleases and CutSmart buffer for 1 hour (37^{o}C). Gel Loading Dye (6x) was added to terminate the digestion reaction. Digested DNA was separated by agarose gel electrophoresis and the amplified fragment of interest identified by size and excised. DNA was extracted from the gel using QIAquick Gel Extraction Kit (Qiagen) according to manufacturer's instructions.

Ligation

Restriction enzyme-digested plasmid backbone (vector) and insert (PCR product) were ligated together at a molar ratio of 1:3 using the following equation:

$$\frac{vector\ (ng) \times\ insert\ (kb)}{vector\ (kb)} \times 3$$

A 20ul reaction mixture was prepared with 2 µl T4 DNA Ligase Buffer (10x), 100 ng vector DNA, insert DNA as determined by the above equation, 400U T4 DNA ligase for 1 h (16^{o}C). A control reaction without the DNA insert was also performed to confirm that significant vector re-ligation did not occur. The reaction mixture (5 µl) was used to transform *E.coli* DH5α cells.

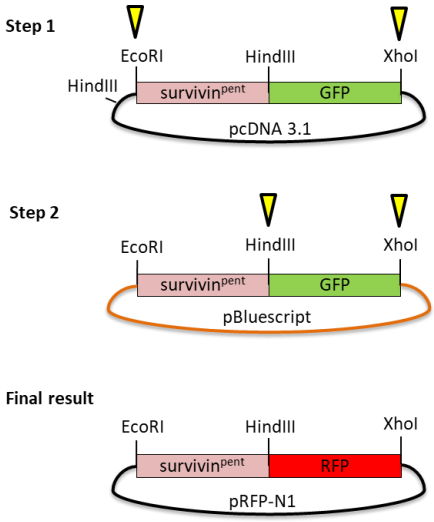
CLONING STRATEGIES FOR INDIVIDUAL PLASMID CONSTRUCTS

To express mutant forms of survivin in mammalian cells, plasmids were required containing the cDNA for survivin^{L28A,L64A,V89A,L96A,L104A} (survivin^{pent}) or survivin^{F61A,L64A} tagged with GFP, RFP, flag, or untagged. Plasmids generated prior to this study were survivin^{pent}-GFP, survivin^{L64A}, survivin^{L64A}-GFP, and flag-survivin.

For all mutants, the target amino-acid was replaced with an alanine (Ala,A).

Generation of survivin^{pent}-RFP

Survivin^{pent}GFP was extracted from pre-existing plasmid pcDNA3.1 Survivin^{pent}-GFP by digestion with EcoRI and XhoI and ligated into an empty pBluescript vector digested with the same restriction sites. This new plasmid; pBluescript survivin^{pent}GFP was then digested EcoRI and HindIII, both of which were now unique, and ligated into pDsRed1-N1 digested with the same restriction sites.



Generation of survivin^{F61A,L64A} constructs

These plasmids were generated by site-directed mutagenesis of survivin^{L64A} constructs in pcDNA3.1 mammalian expression vectors created previously in this laboratory. Overlapping primers were designed and used for site-directed mutagenesis of the survivin^{F61A,L64A}, and back-to-back primers were used with the Q5 site-directed mutagenesis kit for GFP, RFP or flag -tagged constructs. Primers sequences are listed below:

Template plasmid	Desired construct	Primer nucleotide sequence
pcDNA3.1 survivin^{L64A}	survivin^{F61A,L64A}	Forward: CTTCTGCGCCAAGGAGGCGCAAGGCTGGG Reverse: CCCAGCCTTCCGCCTCCTTGGCGCAGAAG
pcDNA3.1 survivin^{L64A}GFP	survivin^{F61A,L64A}GFP	Forward: TTTCTTCTGCGCCAAGGAGGCGG Reverse: CACTGGGCCAAGTCTGGC
pDsRed1-N1 survivin^{L64A}RFP	survivin^{F61A,L64A}RFP	Forward: TTTCTTCTGCGCCAAGGAGGCGG Reverse: CACTGGGCCAAGTCTGGC
pcDNA3.1 survivin^{L64A}	flag-survivin^{F61A,L64A}	Forward: TTTCTTCTGCGCCAAGGAGGCGG Reverse: CACTGGGCCAAGTCTGGC

MAMMALIAN CELL CULTURE TECHNIQUES.

All reagents were from Sigma-Aldrich unless otherwise stated.

Cell lines

U2OS – a human osteosarcoma cell line with epithelial adherent morphology. These cells display a flattened phenotype in cell culture which makes them ideal for microscopy.

Hek293T cells - human embryonic kidney or adrenal cells. These cells have excellent transfection efficiency and expression of ectopic genes making them ideal for transient transfection and immunoprecipitation.

Growth conditions and media.

Cell lines were cultured in tissue culture flasks at 37°C and 5% CO_2 in a humidified incubator. Culture medium consisted of Dulbecco's Modified Eagle's Medium with 4500 mg/L glucose, L-glutamine, sodium pyruvate, and sodium bicarbonate (DMEM, D6429) supplemented with 10% foetal calf serum (FCS, HyClone), herein referred to as 'complete medium'.

To maintain the expression of plasmid DNA in stable cell lines, media was supplemented with 50 µg/ml Geneticin (G418, Acros organics).

Cells cultures were passaged at approximately 80% confluence and maintained in a TriMat2 Class 2 Microbiological Safety Unit.

Passaging cells

To maintain a healthy population of cells, adherent cell lines were passaged in log-phase of growth. Cells were dissociated from the tissue culture surface with trypsin solution (0.5% Trypsin, 0.2% EDTA) in PBS. Harvested cells were diluted 1:10 with fresh complete media, applied to a fresh tissue culture flask, and cultured as described previously.

Transfection.

Cells were transfected with plasmids using Torpedo^{DNA} transfection reagent (ibidi) at a ratio of 1µg plasmid DNA : 3 µl reagent. Plasmid DNA and reagent were diluted individually with PBS and then combined with gentle pipetting and incubated for 15 minutes to form complexes. The DNA/reagent complex was applied to adherent cells at an exponential phase of growth in complete media using a drop-wise technique and cells incubated overnight. Transfections were performed in eight-well tissue culture dishes (ibidi) for microscopy or six-well tissue culture dishes for molecular biology and respective reagent quantities are shown below.

	8 well	6 well
Surface area per well (cm^2)	1	9
Media volume per well (µl)	200	2000
Plasmid DNA (µg)	0.3	2
Torpedo^{DNA} (µl)	0.9	6
Total PBS (µl)	60	200

Generation of stable cell lines

To generate a Hek 293T cell line stably expressing GFP or GFP-LC3 for immunoprecipitation experiments, Hek cells were transfected with pcDNA3.1_GFP or pcDNA3.1_GFP-LC3 and the following day 50 µg/ml Geneticin (G418, Acros organics) was added to the complete medium. Surviving adherent cells were harvested 7-10 days later using trypsin/EDTA in PBS, and FACS sorted with a Beckman Coulter MoFlo XDP, to filter out cells not expressing the fluorescent tag. Positive cells were then maintained in media supplemented with Geneticin (50 µg/ml) to maintain selection pressure.

Freezing cells

To maintain low passage number and therefore cell phenotype, cells were batch frozen in liquid nitrogen following stable line generation and woken as

required. Cultured cells were harvested during log phase growth using trypsin/EDTA solution (0.5% Trypsin, 0.2% EDTA) in PBS, pelleted by centrifugation at approximately 500 xg for five minutes and resuspended in FCS supplemented with 10% DMSO at a concentration of approximately 2 million cells per ml. Cell suspension was aliquoted into cryovials in volumes of 500 µl and gradually frozen to -200°C and stored in liquid nitrogen.

Drug treatments.

Chloroquine (CQ) diphosphate salt (C6628) was dissolved in water to a concentration of 100 mM and aliquots stored at -20°C and used at a final concentration of 50 µM or 120 µM.

Lyophilized Rapamycin (RAP, ThermoFisher Scientific) was dissolved in DMSO to a concentration of 200 µM and stored in aliquots at -20°C and used at a final concentration of 200 nM.

Dimethylenastron (DMA, Calbiochem) was dissolved in DMSO to a concentration of 10mM and stored in aliquots at -20°C. and used at a final concentration of 1 uM.

BIOCHEMICAL ASSAYS

Bradford protein assay

To determine the protein concentration in cell lysates, a 2 µl sample of lysate was diluted with dH_2O (800ul) and mixed by vortex with 200 µl dye reagent concentrate (Bio-Rad). After 10 min at room temperature, the absorbance of each sample was measured at 595nm using a spectrophotometer.

BSA protein standards of 1, 2.5, 5, 10, 15 and 25 µg were used to construct a standard curve of absorbance.

MICROSCOPY TECHNIQUES.

Fixation and immunostaining

Cells in the log phase of growth were seeded onto sterile coverslips at 30,000 cells per well in a 24 well tissue culture plate and incubated overnight. If mitotic cells were required, adhesion was promoted by pre-treating coverslips with a layer of 10% poly-L-lysine in PBS, followed by evaporation and three washes in PBS. Cells on the coverslips were washed gently with PBS to remove media and cell debris. Fixation solution (0.5 ml per well, 4% formaldehyde in PBS at 37^{o}C) was applied for 5 min followed by 3x 5 min washes with PBS. Cells were permeablised using 0.15% Triton X-100 in PBS (37^{o}C) for 2 min.

To reduce non-specific antibody binding, coverslips were incubated with blocking solution (1% BSA in PBS) for 15 min. Primary antibodies were diluted in blocking solution and applied to the coverslips for 1 h followed by a 15 min wash in blocking solution. Species-specific secondary antibodies conjugated to a fluorescent dye (Vector) were diluted (see appendix) in blocking solution and applied to coverslips with a DAPI (1 μg/ml) counter-stain for 1 hour before washing cells gently in PBS, leaving to dry and mounting on glass slides with Mowiol 4.88 mounting medium (Polysciences Inc.) and sealing with nail polish.

Live cell imaging.

Exponentially growing cells (50,000) were seeded onto chambered coverslips (μSlide 8-well, Ibidi) and allowed to adhere to the surface overnight at 37°C and 5% CO_2 in a humidified incubator.

The following day, growth medium was aspirated and replaced with live imaging medium consisting of DMEM (phenol-red-free, D1145) supplemented with 4 mM l-glutamine, 10% FCS and buffered with 25 mM HEPES.

Imaging.

All images were acquired using an inverted, wide-field fluorescence microscope (Olympus IX-71, DeltaVision Elite) with 100x (1.40 NA, oil-immersion) or 60x (1.42 NA, oil-immersion) objectives. The incubation chamber and objectives were pre-heated to 37°C. Microscope control was provided by Lenox Softworks software and images captured with an integrated CoolSnap HQ^2 camera (Photometrics). Images were deconvolved and 0.3 µm z-stacks projected using maximum signal from each slice.

For live imaging, cells were grown in phenol red-free, HEPES-buffered media to maintain physiological pH in the absence of a 5% CO_2 environment.

Measurement of puncta

Fluorescent puncta were measured using ImageJ software[160]. To achieve this, deconvolved and projected z-stack images were masked to restrict images to a single cell expressing the protein construct(s) of interest. Macros were created to automatically measure the number of puncta in the cell, and the diameter of each puncta (see appendix). Briefly, this macro first split the colour channels of each image, then selecting the channel relevant to the puncta being measured, enhanced the contrast, subtracted any background and thresholded the image, creating a mask of the puncta. Identified puncta were then measured and counted by the ImageJ Analyse Particles program, excluding any puncta above $2um^2$, below 0.1 um^2, or that did not form an oval or circular shape. Data for each image was saved to a text file as the macro opened, analysed and closed each file in turn in the target directory, which increased throughput and reduced observer bias.

SDS PAGE AND IMMUNOBLOTTING

SDS Polyacrylamide gel electrophoresis

Cell lysates were prepared by washing adherent cells in log-phase of growth with 1 ml ice-cold tris-buffered saline (TBS) twice before scraping into 1 ml cold TBS and centrifuging at 500 xg for 3 min at 4^{o}C to pellet the cells. The cell pellet was resuspended in 1 ml ice-cold lysis buffer (10 mM Tris-Cl pH 7.5; 150 mM NaCl; 0.5 mM EDTA; 0.5% NP40; 1 µg/ml CLAP containing chymostatin, leupeptin, antipain and pepstatin A; 1 mM PMSF) and kept on ice for 30 minutes with gentle pipetting. Lysates were then centrifuged at 17,000 xg for 10 min to pellet cell debris and DNA.

Lysate samples were boiled in sample buffer as detailed in specific methods and applied to hand cast 15% polyacrylamide gels. Proteins were drawn through the gel in Laemmli running buffer (25 mM Trizma, 192 mM Glycine, 0.1% SDS) using Bio-Rad apparatus at 200 constant volts for 45 mins at room temperature. Separated proteins were transferred to PVDF (Immobilon-P) in Towbin transfer buffer (24 mM Trizma, 195 mM Glycine, 0.5% SDS, 10% methanol) using Bio-Rad apparatus at 350 constant amps for 90 minutes at room temperature. An ice-block was used to prevent over-heating of the buffer and gel during electrophoresis.

Immunoblotting

PVDF membranes from SDS-PAGE were soaked in blocking buffer consisting of PBS with 5% w/v dry non-fat milk (Marvel) and 0.1% Tween 20 for 1 hour with agitation at room temperature to reduce non-specific binding. Primary antibodies were diluted in blocking buffer as detailed below and applied to the membranes which were sealed in plastic and incubated overnight at 4^{o}C with agitation.

Antibody	Manufacturer	Host	Dilution
Polyclonal anti-LC3 (recognises LC3A and LC3B)	Sigma-Aldrich L8918	rabbit	1:2000
Polyclonal anti-survivin	Novus	rabbit	1:1000
Monoclonal anti-tubulin clone B512	Sigma-Aldrich T5168	mouse	1:2000
Monoclonal histone H3 pT3 clone 159	Novus	Rabbit	1:2000
GFP	Sigma-Aldrich	Mouse	1:2000
Polyclonal p62	Enzo Life Sciences	rabbit	1:1000

Membranes were washed three times for 5 min each in PBST (PBS with 0.1% Tween 20). HRP-conjugated secondary antibodies (DAKO) raised against the primary antibody species of origin were diluted 1:2000 in blocking buffer and applied to the membranes, sealed in plastic and incubated for 45 min at room temperature with agitation. Membranes were washed three times for 5 min each in PBST and bands detected using enhanced chemiluminescence (Amersham ECL; GE Healthcare) and X-ray film (Amersham Hyperfilm; GE Healthcare).

P62 DEGRADATION ASSAY FOR AUTOPHAGIC FLUX

For these experiments, U2OS cells stably expressing GFP or survivin-GFP were seeded onto 6 well plates at a density of 1 x 10^5 per well in complete medium and left overnight to adhere. The following day medium was aspirated and replaced with complete medium with or without 50 uM CQ or 200 nM RAP. Cells were harvested at 1, 2, 3 and 6 hr after treatment and lysates analysed by SDS-PAGE and immunoblotting for P62, GFP and tubulin (see section 2.6.2 for antibody details). Relative p62 abundance was quantified using ImageJ

software to measure the density of p62 bands relative to tubulin bands at each time-point.

VIABILITY ASSAY

Cell culture media in a 96-well-plate was supplemented with resazurin (R7017) to a final concentration of 10 µg/ml and cells incubated for 1 hour (37°C, 5% CO_2). Fluorescence was measured with an excitation wavelength of 530 nm and an emission wavelength of 590 nm to detect resorufin using a FLUOstar Galaxy Spectrophotometer (BMG Lab technologies).

CLONOGENIC SURVIVAL ASSAY

U2OS cells expressing GFP or survivin-GFP were seeded at 500 cells per 10 cm^2 tissue culture dish, allowed to adhere overnight and then incubated in starvation media (Hanks' balanced salt solution) for 24 h. The following day, starvation media was replaced with complete media and the cells left to grow in standard cell culture conditions for two weeks. Cells were washed gently with warm PBS, stained with 2ml methylene blue dye (1% methylene blue (w/v) in ethanol) per dish for 1 h, rinsed with water and inverted to dry.

Percentage survival was calculated by expressing the colony number on each treated plate as a percentage of the mean colony number on untreated dishes for the same cell line.

CO-IMMUNOPRECIPITATION.

Flag-tagged co-immunoprecipitation

Exponentially growing Hek293T cells stably expressing GFP-LC3 were seeded at a density of 1 x 10^5 per well on a 6 well tissue culture plate and allowed to adhere to the surface overnight at 37°C and 5% CO_2 in a humidified incubator. The following day, cells were transfected with plasmids for the expression of flag, flag-survivin, or flag-survivin^{F61A,L64A}. After 16-24 h cells were washed gently with ice-cold PBS and harvested by scraping into 700 µl freshly made ice-cold lysis buffer (50 mM TrisHCl pH 4, 150 mM NaCl, 1 mM EDTA, 1% Triton x-

100, 1 µg/ml CLAP containing chymostatin, leupeptin, antipain and pepstatin A, and 100 µM AEBSF) and lysed on ice for 30 min with gentle pipetting. DNA and cell debris were pelleted by centrifuging the lysate at 17,000 xg for 10 min at 4^{o}C and the supernatant lysate retained. 20 µl of this lysate was removed as an input sample and boiled in 20µl 2x sample buffer (125 mM TrisHCl pH 6.8, 4% SDS, 20% glycerol, 0.004% bromophenol blue) in a heat block at 90^{o}C for 3 min.

Anti-Flag M2 Affinity Gel (25 µl per condition, 50:50 slurry) was washed 3x in cold TBS (50 mM TrisHCl pH 7.4, 150 mM NaCl) made fresh from 10x stock, and centrifuged at 5,000 xg for 30 seconds at 4^{o}C. Remaining cell lysate was incubated with M2 gel for 2 h at 4^{o}C with end-over-end rotation before washing 3x with 1 ml TBS at 500 xg and 4^{o}C to remove unbound species. M2 gel was then boiled in 30 µl 2x SDS loading buffer (125 mM TrisHCl pH 6.8, 4% SDS, 20% glycerol, 0.004% bromophenol blue) and stored at -20^{o}C.

GFP-tagged co-immunoprecipitation.

Exponentially growing Hek293T cells were seeded as per flag-tagged co-immunoprecipitation. The following day cells were transfected with plasmids for the expression of GFP-LC3 and either survivin or survivin^{F61A,L64A}. After 16-24 h cells were harvested and re-seeded onto 10 cm tissue culture plates and grown on until a confluence of 80% was reached. Cells were then washed with 1 ml ice-cold tris-buffered saline (TBS) twice before scraping into 1 ml cold TBS and centrifuging at 500 xg for 3 min at 4^{o}C to pellet the cells. The cell pellet was resuspended in 1 ml ice-cold lysis buffer (10 mM Tris-Cl pH 7.5; 150 mM NaCl; 0.5 mM EDTA; 0.5% NP40; 1 µg/ml CLAP containing chymostatin, leupeptin, antipain and pepstatin A; 1 mM PMSF) and kept on ice for 30 minutes with gentle pipetting. DNA and cell debris were pelleted as per flag-tagged co-immunoprecipitation. A sample of supernatant lysate (20 µl) was removed as an input sample and the remaining lysate supplemented with 300 µl dilution buffer (10 mM Tris-Cl pH 7.5; 150 mM NaCl; 0.5 mM EDTA).

GFP-Trap A beads (25 µl per condition, 50:50 slurry, Chromotek) were washed twice in 500µl cold dilution buffer, centrifuging at 2,500 xg for 2 min at 4°C to pellet beads between washes. Lysate samples were added to the beads and the mixture incubated at 4°C for 1 h with end-over-end rotation. Beads were washed with 500 µl cold dilution buffer, centrifuging at 2,500 xg for 2 min at 4°C to pellet beads and the supernatant removed. Bead pellets were resuspended in 100 ul of 2x sample buffer (120 mM Tris/Cl pH 6.8; 20% glycerol; 4% SDS; 0.04% bromophenol blue; 10% β-mercaptoethanol), boiled for 10 min at 90°C to dissociate immunocomplexes from beads and stored at -20°C.

STATISTICAL ANALYSIS

Experimental data was collated using MS Excel software. Graphs were generated, and statistical analyses performed with GraphPad Prism software.

To ensure reproducibility, experiments were repeated independently three times where possible. For each experiment, clonogenic and resazurin experiments were performed in triplicate, and 15-30 cells were imaged per well for fluorescence microscopy experiments.

All error bars shown indicate standard error of the mean (SEM) calculated by the following equation:

$$\mathbf{SEM = SD / \sqrt{n}}$$

where SD = standard deviation of the sample mean, n = sample size.

The sample size of measurements taken for autophagosome and lysosome analyses was considerable, increasing the chance of introducing outliers due to experimental error. For these experiments, outliers were identified and removed using GraphPad Prism ROUT method with a coefficient Q of 1%. The ROUT method combines robust regression and outlier removal techniques and coefficient Q defines how aggressively the technique defines outliers. The sample size indicated on graphs excludes values by the ROUT method.

To assess whether a difference between two datasets was representative of the difference in the true population, the student's t-test was used to compare data sets. The t-test used was a Welch's unpaired, two-tailed t-test, which means that the variance within each data set is not assumed to be the same between data sets, the data sets being compared were samples from different populations (unpaired), and the distribution of data about the mean was normal (two-tailed).

Where multiple datasets needed to be compared, a one-way ANOVA test was used, followed by a post-hoc Dunnett's test for multiple comparisons, to assess the significance of any difference between a dataset mean and the experimental control mean. This method applies corrects for multiple comparison bias, whereby the more comparisons an investigator makes, the more likely they are to identify a significant difference.

RESULTS

SURVIVIN ASSOCIATES WITH LC3 THROUGH AN LC3-INTERACTING REGION

Sequence analysis

A significant number of LC3 binding partners contain an LC3-interacting-region (LIR)[128]. This region is a consensus sequence of amino acid residues following the pattern xxxWxxL/where x represents any amino acid – usually acidic, W represents a tryptophan or less commonly a tyrosine residue, and L represents a leucine or isoleucine residue. In addition, the preceding three N-terminal residues to W, and the two residues separating the W and L are frequently acidic and the residue immediately preceding the L is often hydrophobic[135].A functional LIR motif needs to be exposed on the outer surface of a folded protein, specifically on an exposed flexible strand which could potentially form a beta sheet[135], and is likely to be evolutionarily conserved.

To investigate whether survivin has an LIR by which it interacts with LC3, the primary, secondary and tertiary structures of survivin were analysed.

Sequence analysis of the survivin peptide identified five putative LIR motifs: $WPFL_{25}$; $FKEL_{64}$; $FLSV_{89}$; $FEEL_{96}$ and $FLKL_{104}$, illustrated in figure 3.1.1. Only motif one has a hydrophobic residue immediately N-terminal from the L; a phenylalanine (phe, F). Motifs two and four have an acidic residue N-terminal to the L. Motif five alone has an acidic residue N-terminal to the W position; a glutamic acid (glu, E). By sequence alone, no single putative LIR stood out as more likely to be a true LIR.

To identify whether these putative LIR motifs are conserved across vertebrates, the human survivin protein sequence was compared with that of cat, mouse, chicken and frog homologues identified using the protein sequence similarity search program FASTA[161], provided by EMBL-EBI and aligned using the BLAST[159] tool provided by NCBI (table 3.1.1). Putative LIR motifs at sites 2, 3 and 5 are more conserved than the others, making them more likely to be true LIRs.

To extend this investigation to other kingdoms, a sequence logo was produced from alignments of survivin homologues CSC1_CAEEL (nematode); BIR1_YEAST; BIRC5_HUMAN; BIRC5_PONAB (orangutan); BIRC5_PIG; BIRC5_FELCA (cat); BIRC5_BOVIN (cow); BIRC5_CANFA (dog); BIRC5_MOUSE and BIRC5_RAT. A sequence logo is a graphical representation of an amino acid or nucleic acid multiple sequence alignment developed by Schneider and Stephens[162]. One stack on the logo represents a single position in the sequence. The height of the stack represents the sequence conservation, and the height of each symbol in the stack indicates the relative frequency of each amino acid at that position. The sequence logo was generated with the multiple alignment tool ClustalW2[163] (10 iterations, EMBL-EBI) and WebLogo[164] software as shown in figure 3.1.2.

The results from analyses of primary sequence, secondary structure and sequence alignment suggested that site two, FKEL[64], was the most likely candidate for a functional LIR in survivin since it alone is located at a flexible strand capable of forming a beta sheet and is well conserved in other mammals.

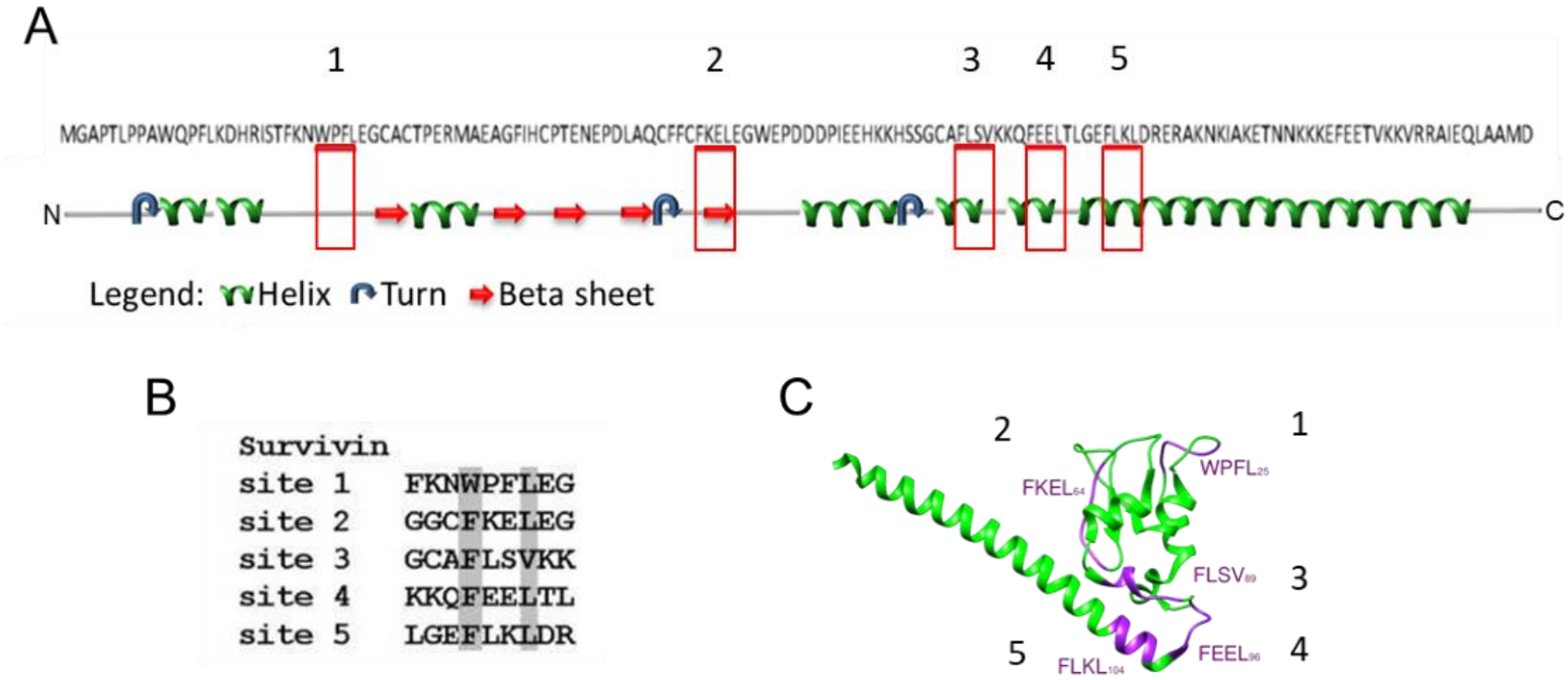


Figure 3.1.1: Putative LIR motifs in survivin. (A) Amino acid sequence of survivin with putative LIRs underlined in red, above the its secondary structure (UniProt O15392). (B) Putative LIR sites with critical aromatic and hydrophobic residues highlighted. (C) Crystal structure of survivin with putative LIRs indicated in purple (UCSF Chimera from www.ebi.ac.uk Protein Data Bank id 1e31)

	1	2	3	4	5	6	7	8	9	10	11	12	13	14	15	16	17	18	19	20	21	22	23	24	25	26	27	28	29	30	31	32	33	34	35	36	37	38	39	40
human	M	G	A	P	T	L	P	P	A	W	Q	P	F	L	K	D	H	R	I	S	T	F	K	N	**W**	P	F	**L**	E	G	C	A	C	T	P	E	R	M	A	E
cat	M	G	A	S	S	L	P	P	A	W	Q	L	Y	L	K	D	H	R	I	S	T	F	K	N	**W**	P	F	**L**	E	G	C	A	C	T	P	E	R	M	A	E
mouse	M	G	A	P	A	L	P	Q	I	W	Q	L	Y	L	K	N	Y	R	I	A	T	F	K	N	**W**	P	F	**L**	E	D	C	A	C	T	P	E	R	M	A	E
wolf	M	G	A	S	S	L	P	P	A	W	Q	L	Y	L	K	D	H	R	V	S	T	F	K	N	**W**	P	F	**L**	E	G	C	A	C	T	P	D	R	M	A	E
chick			A	E	M	L	P	K	E	W	L	V	Y	L	V	S	T	R	A	A	T	F	R	N	W	P	F	T	E	G	C	A	C	T	P	E	R	M	A	A
frog				P	S	M	P	D	E	W	R	L	Y	K	L	A	S	R	L	R	T	F	S	N	W	P	F	T	E	D	C	A	C	T	P	E	R	M	A	E
	41	42	43	44	45	46	47	48	49	50	51	52	53	54	55	56	57	58	59	60	61	62	63	64	65	66	67	68	69	70	71	72	73	74	75	76	77	78	79	80
human	A	G	F	I	H	C	P	T	E	N	E	P	D	L	A	Q	C	F	F	C	**F**	K	E	**L**	E	G	W	E	P	D	D	D	P	I	E	E	H	K	K	H
cat	A	G	F	I	H	C	P	T	E	N	E	P	D	L	A	Q	C	F	F	C	**F**	K	E	**L**	E	G	W	E	P	D	D	D	P	I	E	E	H	K	K	H
mouse	A	G	F	I	H	C	P	T	E	N	E	P	D	L	A	Q	C	F	F	C	**F**	K	E	**L**	E	G	W	E	P	D	D	N	P	I	E	E	H	R	K	H
wolf	A	G	F	I	H	C	P	T	E	N	E	P	D	L	A	Q	C	F	F	C	**F**	K	E	**L**	E	G	W	E	P	D	D	D	P	I	E	E	H	K	K	H
chick	A	G	F	V	H	C	P	S	E	N	S	P	D	V	V	Q	C				**F**	F	C	**L**	K	E	L	E	G	W	E	P	D	D	D	P	L	E	E	H
frog	A	G	F	V	H	C	P	T	D	N	S	P	D	V	V	K	C				**F**	F	C	**L**	K	E	L	E	G	W	Q	P	E	D	D	P	M	D	E	H
					81	82	83	84	85	86	87	88	89	90	91	92	93	94	95	96	97	98	99	100	101	102	103	104	105	106	107	108	109	110	111	112	113	114	115	116
human					S	S	G	C	A	**F**	L	S	**V**	K	K	Q	**F**	E	E	**L**	T	L	G	E	**F**	L	K	**L**	D	R	E	R	A	K	N	K	I	A	K	E
cat					S	S	G	C	A	**F**	L	S	**V**	K	K	Q	**F**	E	E	**L**	T	L	S	E	**F**	L	K	**L**	D	K	E	R	A	K	N	K	I	A	K	E
mouse					S	P	G	C	A	**F**	L	T	**V**	K	K	Q	M	E	E	**L**	T	V	S	E	**F**	L	K	**L**	D	R	Q	R	A	K	N	K	I	A	K	E
wolf					S	S	G	C	A	**F**	L	S	**V**	K	K	Q	**F**	E	E	**L**	T	L	S	E	**F**	L	K	**L**	D	K	E	R	A	K	N	K	I	A	K	E
chick		K	K	H	S	A	G	C	A	**F**	A	A	**L**	Q	K	D	P	S	N	L	T	V	Q	E	**F**	L	K	**L**	D	K	K	R	T	K	N	V	I	K	K	A
frog	K	K	H	S	P		S	C	L	**F**	I	A	**L**	K	K	K	A	E	E	L	T	L	S	E	**F**	L	K	**L**	D	L	E	H	T	K	I	K	M	Q	K	Q
	117	118	119	120	121	122	123	124	125	126	127	128	129	130	131	132	133	134	135	136	137	138	139	140	141	142														
human	T	N	N	K	K	K	E	F	E	E	T	V	K	K	V	R	R	A	I	E	Q	L	A	A	M	D														
cat	T	N	H	K	Q	K	E	F	E	E	T	A	K	R	V	R	C	A	I	E	Q	L	A	A	L	E														
mouse	T	N	N	K	Q	K	E	F	E	E	T	A	K	T	T	R	Q	S	I	E	Q	L	A	A																
wolf	T	N	N	K	Q	K	E	F	E	E	T	A	K	K	V	R	C	A	I	E	Q	L	A	A	A	E														
chick	I	S	Q	K	E	T	D	I	E	D	V	A	K	G	V	R	H	A	I	E	N	M	G																	
frog	M	N	L	H	I	E	R	F	Q	A	K	A	N	E	V	R	G	H	L	E	K	L	D	A																

Table 3.1.1: Conservation of LIR motifs in survivin. Alignment of the human survivin protein sequence with homologues in other species. Grey shading indicates putative LIR found in human survivin and matching sequences in other vertebrate species.

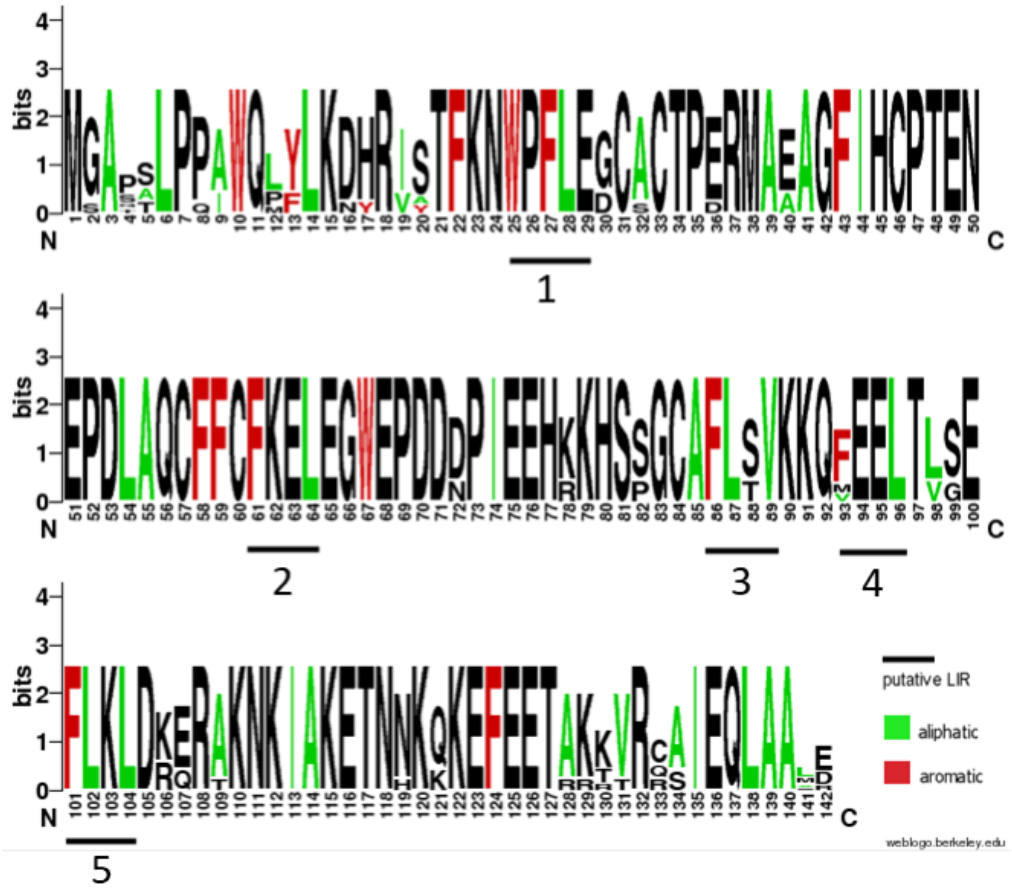


Figure 3.1.2: Sequence Logo for mammalian survivin homologue alignments. Putative LIRs are shown as black bars. Developed using WebLogo (http://weblogo.berkeley.edu).

Generation of survivin mutants.

To investigate the relevance of the five putative LIR sites of survivin in a biological context, plasmids were generated to express survivin with point mutations at these sites.

Initially, mutations were made in all the LIR sites to eliminate any possibility of LC3 interaction. Position 1 in each LIR was replaced with an alanine (ala,A) which is a relatively small amino-acid lacking a reactive side chain. A mutant was generated in a pcDNA3.1 plasmid outside of this study and designated survivin^{pent} to represent the five point-mutations L25A, L64A, V89A, L96A and L104A. A GFP-tagged construct was also generated. For this study, restriction digestion techniques were used to generate two additional plasmids – pcDNA 3.1-flag-survivin^{pent} and pDsRed1-N1-survivin^{pent}.

In addition, mutant constructs were generated in pcDNA where the 'W' and 'L' residues of the most likely LIR, FKEL[64] were both mutated to alanines. These mutants were designated survivin^{F61A,L64A} and constructs were made with GFP, RFP (dsRed1) and flag tags.

The localization of survivin^{pent} was assessed by transient transfection of U2OS cells with the RFP-tagged construct, alongside survivin$^{wild\text{-}type}$. At interphase, survivin$^{wild\text{-}type}$ was predominantly cytoplasmic, but survivin^{pent} adopted a diffuse localisation throughout the cytoplasm and nucleus, and lobular nuclei were commonly observed (figure 3.1.3A). After treatment with RAP/CQ for 2 hours, survivin^{pent} but not survivin$^{wild\text{-}type}$ showed a marked accumulation around the nucleus, potentially at the nuclear lamina (figure 3.1.3B). In mitotic cells, visualised after release from prometaphase arrest with the Eg5-inhibitor dimethynestron, survivin^{pent} failed to localise to the centromeres of the chromosomes, yet survivin$^{wild\text{-}type}$ localised normally (figure 3.1.3C).

To assess the level of survivin^{pent} mutant expression, Hek 293T cells were transiently transfected with flag-survivin^{pent} (figure 3.1.3D) and U2OS cells with survivin^{pent}-GFP (figure 3.1.3E). Cell lysates were analysed by immunoblotting which suggested that both flag-survivin^{pent} and survivin^{pent}-GFP were expressed at much lower levels than flag-survivin$^{wild\text{-}type}$.

To investigate the localisation of survivin^{F61A,L64A}, an RFP-tagged construct was transiently transfected into U2OS cells alongside survivin$^{wild\text{-}type}$-RFP. At interphase, survivin^{F61A,L64A} was predominantly cytoplasmic, and did not display any unusual localisation after RAP/CQ treatment similar survivin$^{wild\text{-}type}$ (figure 3.1.4A-B). However, like survivin^{pent}, survivin^{F61A,L64A} failed to localise to the centromeres during mitosis.

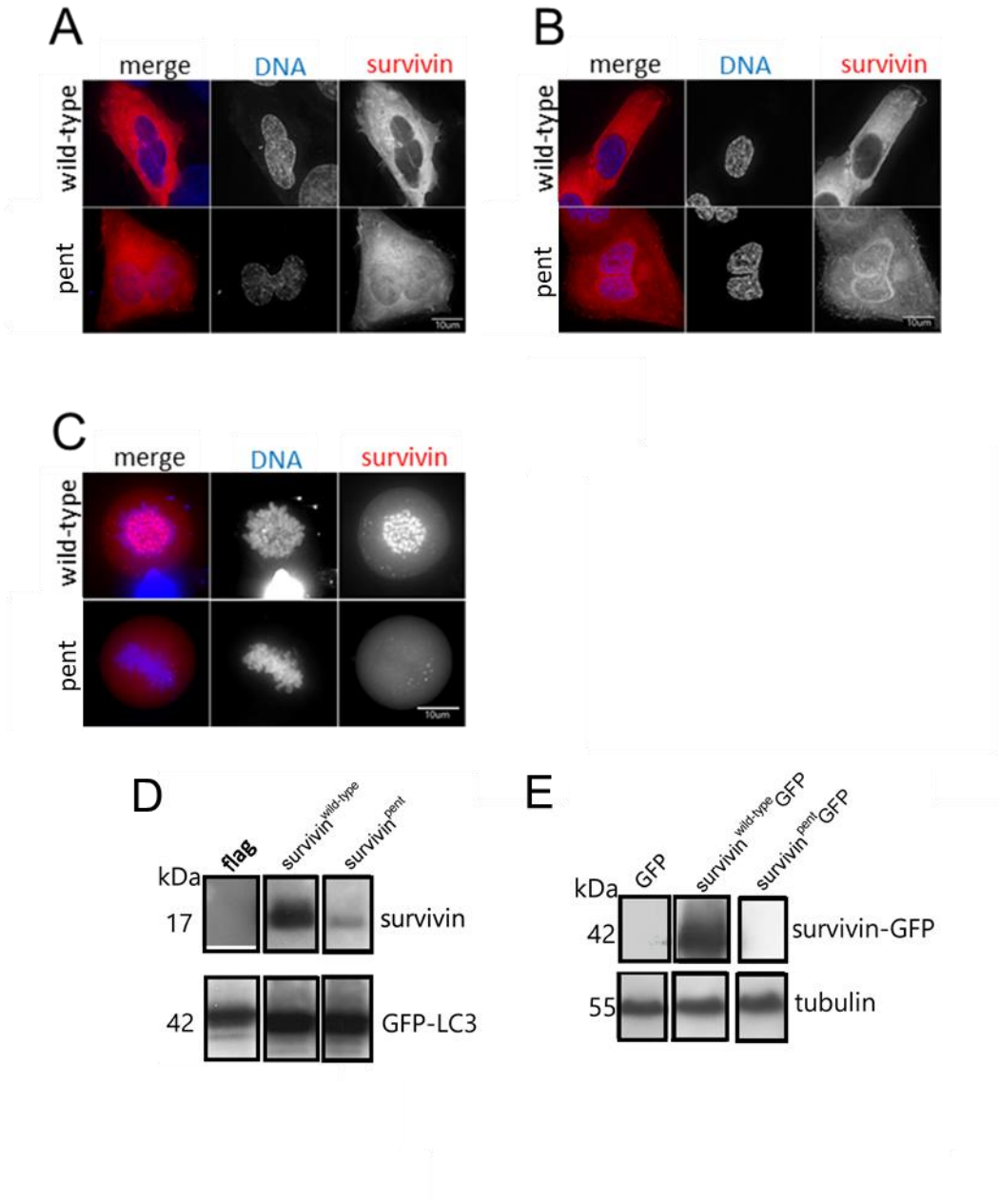


Figure 3.1.3: Survivin^{pent} expression in mammalian cells. U2OS cells were transiently transfected with survivin$^{wild\text{-}type}$-RFP or survivin^{pent}-RFP (A), and either treated with RAP/CQ for two hours (B) or with dimethylnestron overnight (C) before imaging live. (D) Hek 293T cells expressing GFP-LC3 were transiently transfected with flag-survivin$^{wild\text{-}type}$ or flag-survivin^{pent} before SDS-PAGE and immunoblotting with anti-survivin and anti-lc3. (E) U2OS cells were transiently transfected with survivin$^{wild\text{-}type}$-GFP or survivin^{pent}-GFP before SDS-PAGE and immunoblotting with anti-survivin and anti-tubulin. Figures are representative of three independent experiments. Scale bars 10 µm

Hek 293T cells transiently transfected with flag-survivin^{F61A,L64A} expressed lower levels of the protein than cells transfected with flag-survivin$^{wild\text{-}type}$ (figure 3.1.4D), though the mutant construct did show improved expression compared to flag-survivin^{pent}.

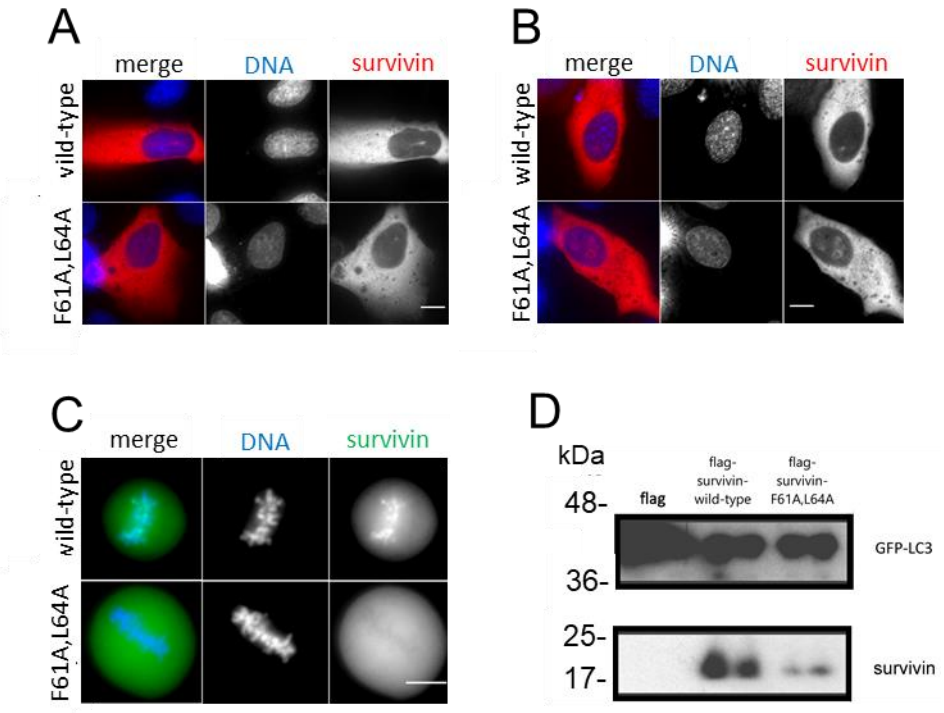


Figure 3.1.4: Survivin^{F61A,L64A} expression in mammalian cells. U2OS cells were transiently transfected with survivin$^{wild\text{-}type}$-RFP or survivin^{F61A,L64A}-RFP (A) and treated with RAP/CQ for 2h (B) before imaging live. (C) U2OS cells were transiently transfected with survivin$^{wild\text{-}type}$-GFP or survivin^{F61A,L64A}-GFP and imaged live. (D) Hek 293T cells expressing GFP-LC3 were transiently transfected with flag-survivin$^{wild\text{-}type}$ or flag-survivin^{F61A,L64A} and expression analysed by immunoblotting with anti-LC3 and anti-survivin. Scale bars 10 µm. Figures are representative of three independent experiments.

The poor expression of survivin^{pent} constructs, along with the unusual cellular localization at interphase and lack of centromeric association at mitosis led to the conclusion that this mutant was a poor choice for studying the LC3-survivin interaction in an autophagic context as it would be difficult to distinguish whether the effects of mutant expression were due to interference with other

functions of survivin. For this reason, the survivin^{F61A,L64A} mutant was selected for further investigation.

Co-Immunoprecipitation of survivin and lc3

To investigate the importance of the $FKEL_{64}$ LIR motif in the association of survivin with LC3, co-immunoprecipitation was performed with both wild-type survivin, and survivin^{F61A,L64A}.

Co-immunoprecipitation experiments were performed on Hek 293T cell lysates, using agarose beads coated with antibodies, to confirm published data on the interaction of survivin and LC3. As shown in figure 3.5A, GFP-LC3 associates with flag-tagged survivin, but not flag alone, when co-immunoprecipitated with anti-flag agarose beads. In the reciprocal experiment shown in figure 3.5B, survivin associates with GFP-LC3 but not GFP alone, when co-immunoprecipitated with anti-GFP agarose beads. These experiments were performed in triplicate and band intensity of immunoblots quantified using ImageJ software (figure 3.5C and D).

In contrast to wild-type survivin, figure 3.1.5A and B illustrates that survivin^{F61A,L64A} does not associate with LC3 when co-immunoprecipitated with either flag-survivin or GFP-LC3.

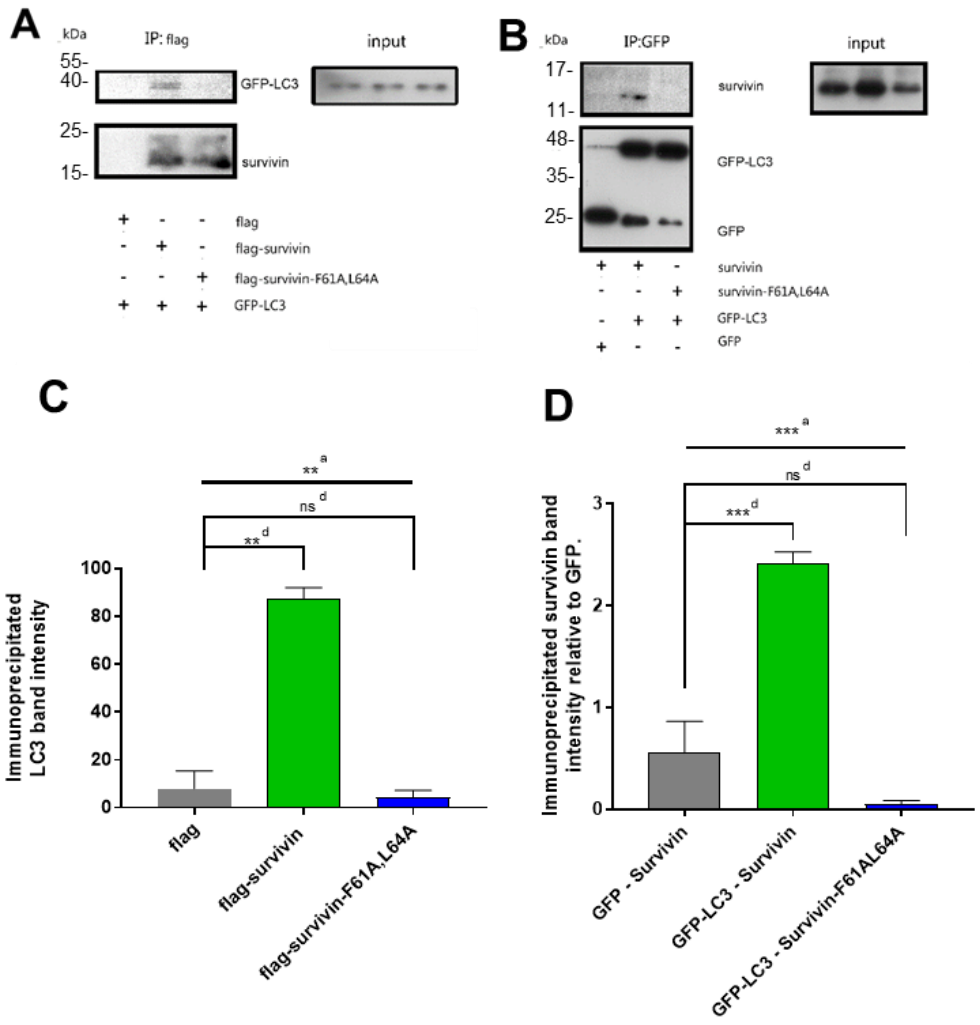


Figure 3.1.5: F61A,L64A mutation prevents survivin-LC3 co-immunoprecipitation: (A) Hek 293T cells expressing GFP-LC3 were transiently transfected with either flag, flag-survivin $^{wild\text{-}type}$ or flag-survivin^{F61A,L64A}. Lysates were immunoprecipitated with anti-flag antibodies and analysed by immunoblotting for survivin and LC3. Blot shown is representative of 2 experiments. (B) Hek 293T cells expressing GFP or GFP-LC3 were transiently transfected with survivin$^{wild\text{-}type}$ or survivin^{F61A,L64A}. Lysates were immunoprecipitated with anti-GFP antibodies and analysed by immunoblotting for survivin and GFP. Blot shown is representative of 3 experiments. (C) Quantitation of western blots illustrated in (A) using ImageJ. (D) Quantitation of western blots illustrated in (B) using ImageJ. All error bars indicate SEM. **P<0.005, **P<0.005. a=one-way ANOVA, d=Dunnett's multiple comparisons test.

The results from these experiments confirm the findings by Roca et al (2008)[4] that survivin associates with LC3 in human cells. Importantly, they also indicate that this association occurs through a canonical LIR motif at F_{61}KEL, which suggests that this is a direct interaction.

Co-localisation of survivin and LC3

Lipidated LC3 (LC3-II) is strongly associated with autophagosomes and is commonly used to label these cell compartments in fluorescence microscopy. To determine whether survivin interacts preferentially with autophagosome-associated LC3, rather than LC3 freely in the cytoplasm, U2OS cells stably expressing RFP or RFP-survivin were transfected with plasmids for the expression of GFP-tagged LC3. ImageJ software was used to generate a 'mask' of RFP puncta, and a 'mask' of GFP puncta, and co-localised puncta were defined as areas where RFP and puncta significantly overlapped. To generate substantial numbers of autophagosomes, so that co-localisation could be easily visualized, cells were treated with both rapamycin and chloroquine (RAP/CQ).

GFP-LC3 puncta were observed in all cell lines and RAP/CQ treatment significantly increased the number and size of these puncta (figure 3.1.6). Individual RFP puncta and survivin-RFP puncta were observed in some cells, with a small minority displaying a cluster of several puncta (figure 3.1.7A), where masked puncta results from ImageJ analysis are also shown. Analysis of GFP and RFP puncta indicated that it was rare for these puncta to co-localise, with less than one occurrence per cell on average, in treated and untreated cells. Statistically, differences between the mean number of co-localised puncta per cell for each cell line and treatment were not significant (figure 3.1.7B)

Survivin-RFP did not form a significant number of puncta in most cells, and this is consistent with current literature that suggests it has a diffuse cytoplasmic localisation at interphase. The lack of co-localization found between survivin and LC3 puncta indicates that the autophagosome is unlikely to be the main site of survivin-LC3 interaction. This finding implies that survivin may preferentially associate with the LC3-I, since it is the lipidated form (LC3-II) that is enriched on the autophagosome membrane.

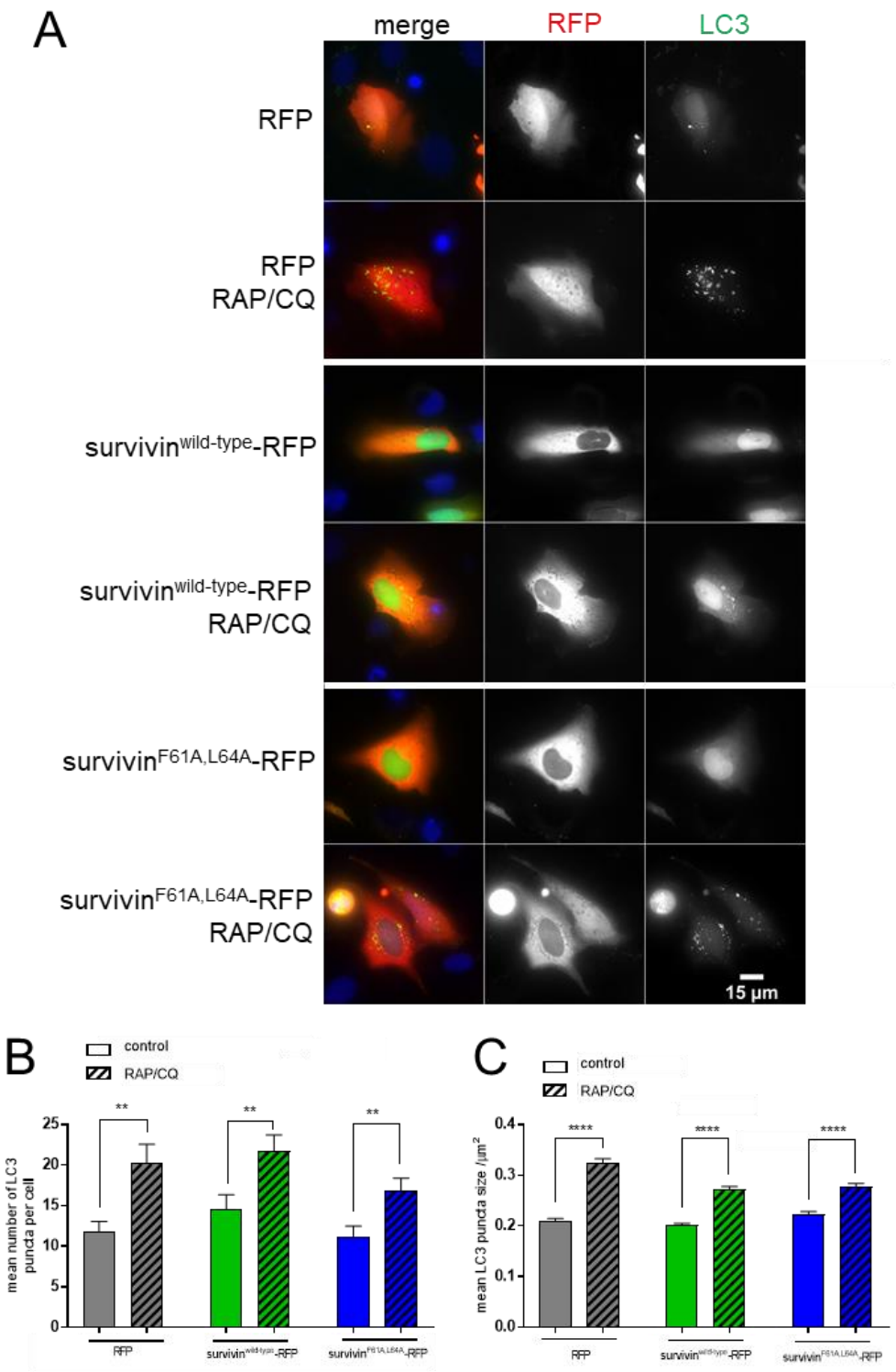


Figure 3.1.6. Localisation of RFP and GFP-LC3: (A) U2OS cells were transiently transfected with GFP-LC3 and RFP constructs and treated with 200 nM RAP and 120 µM CQ for 2 hours. At least 45 live cells were imaged per condition over 5 independent experiments. Puncta were identified using ImageJ software. (B) Mean number of LC3 puncta per cell from(A). (C) Mean size of LC3 puncta per cell from (A). Error bars show SEM. **P<0.05, ****P<0.0001.

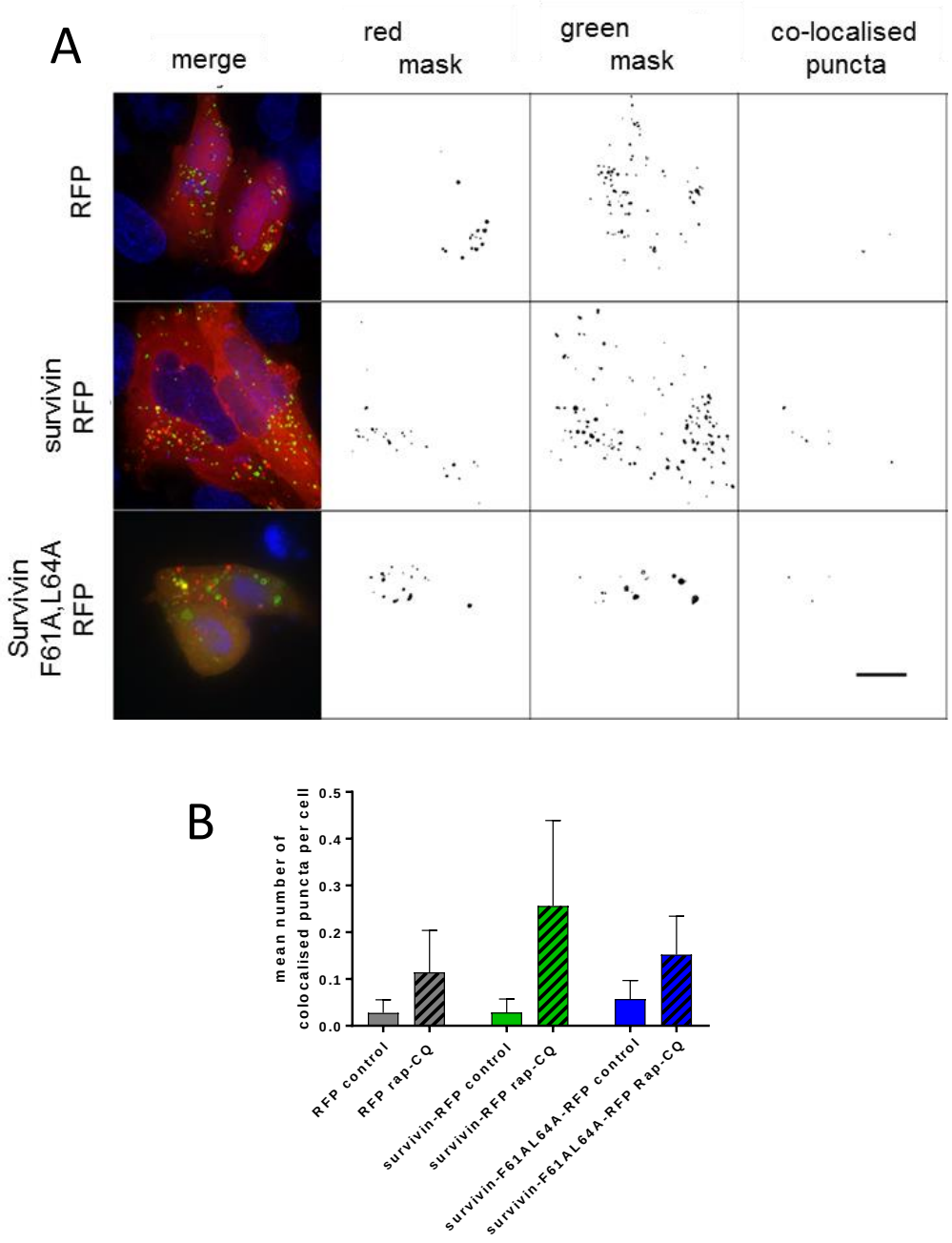


Figure 3.1.7. Co-localisation of RFP and GFP-LC3: U2OS cells were transiently transfected with GFP-LC3 and RFP constructs and then treated with 200 nM RAP and 120 µM CQ for 2 h. At least 45 live cells were imaged per condition over 5 independent experiments. Puncta were identified using ImageJ software. (A) Examples of punctate RFP phenotypes and associated analysis of co-localisation with GFP-LC3. (B) Mean number of co-localised red and green puncta per cell from (A). Error bars show SEM. Differences between cell lines were not significant. Scale bar 15 µm.

SURVIVIN INHIBITS AUTOPHAGY VIA AN LC3-INDEPENDENT MECHANISM.

Autophagic flux

Autophagy is a process that occurs at a variable rate known as 'autophagic flux'. Assessing the abundance of autophagic proteins at any single stage of this process is not sufficient to determine how rapidly cell components are being degraded by autophagy. The two main methods used to measure autophagic flux are 1, to compare the abundance of an autophagic target protein with and without autophagic inhibition, and 2, to monitor the abundance of an autophagic target protein over time in the presence of an autophagic inhibitor.

LC3-II levels were assessed with and without autophagic inhibition to measure autophagic flux. U2OS cells stably expressing either GFP or survivin$^{wild\text{-}type}$-GFP were treated with RAP to induce autophagy, CQ to inhibit degradation of autophagosomes, or a combination of these treatments for 2 h then analyzed by immunoblotting.

Cells expressing survivin-GFP showed higher LC3-II levels in general (figure 3.2.1A -B), with reduced autophagic flux under rapamycin-induced conditions compared to cells expressing GFP (figure 3.2.1C). Survivin levels changed very little following autophagic inhibition by CQ, and this was significantly different from the accumulation seen for LC3-II ($P>0.005$, figure 3.2.D).

A p62 degradation assay was also performed to monitor the accumulation of autophagic protein p62 over time in the presence of autophagic induction or inhibition. U2OS cells stably expressing GFP or survivin$^{wild\text{-}type}$GFP were treated with RAP or a low dose of CQ (50 µM) over a period of 8 hours, and p62 level assessed at regular intervals by immunoblotting.

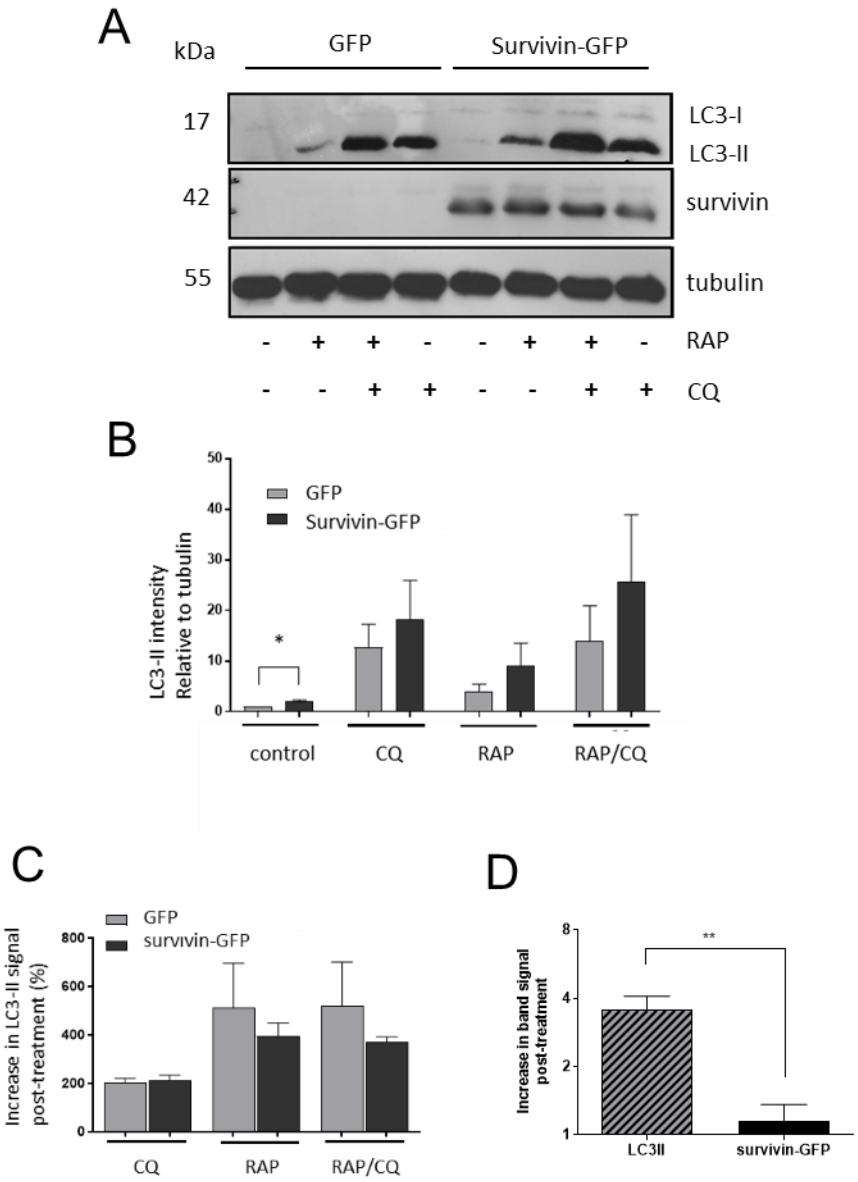


Figure 3.2.1. LC3 expression: (A) U2OS cells were treated with 200nM RAP and or 120uM CQ for 2 h before SDS PAGE and immunoblotting. (B) Quantitation of LC3-II levels. (C) LC3-II levels in treated cells expressed as a percentage of LC3-II in untreated cells. (D) LC3-II and survivin levels in CQ-treated cells relative to untreated cells, 4 independent experiments, SE, *P<0.05, **P<0.005.

Cells treated with RAP maintained stable levels of p62 over the 8 h time period in both cell lines (figure 3.2.2A and B). This was comparable to the stability of p62 in untreated cells.

In the presence of CQ, cells overexpressing survivin accumulated p62 more slowly than cells expressing GFP (figure 3.2.2-C and D) and this was confirmed by linear regression analysis which showed that the difference between the lines of best-fit for p62 accumulation in survivin$^{wild\text{-}type}$-GFP and GFP cells could not be attributed to chance, with a probability of $P<0.0001$ (figure 3.2.2-E).

Importantly, these experiments also demonstrate that survivin does not accumulate following autophagic inhibition, which excludes the possibility that survivin is either an adaptor protein like P62, or a degradation target.

Cells overexpressing survivin showed higher LC3-II levels than control cells, yet when CQ was used to block autophagy, LC3-II levels did not increase to the same degree. This suggests that survivin is restricting autophagic flux via a mechanism that causes LC3-II (and therefore autophagosome) accumulation.

P62 degradation experiments confirmed this finding by indicating that in conditions of autophagic inhibition, p62 accumulates more slowly in cells overexpressing survivin than in control cells. Both cell lines maintained stable levels of p62 during autophagic induction with RAP, suggesting that an increase in autophagic flux and therefore p62 degradation, is accompanied by an increase in p62 expression to maintain homeostasis.

Together these results suggest that survivin is associated with reduced autophagic flux.

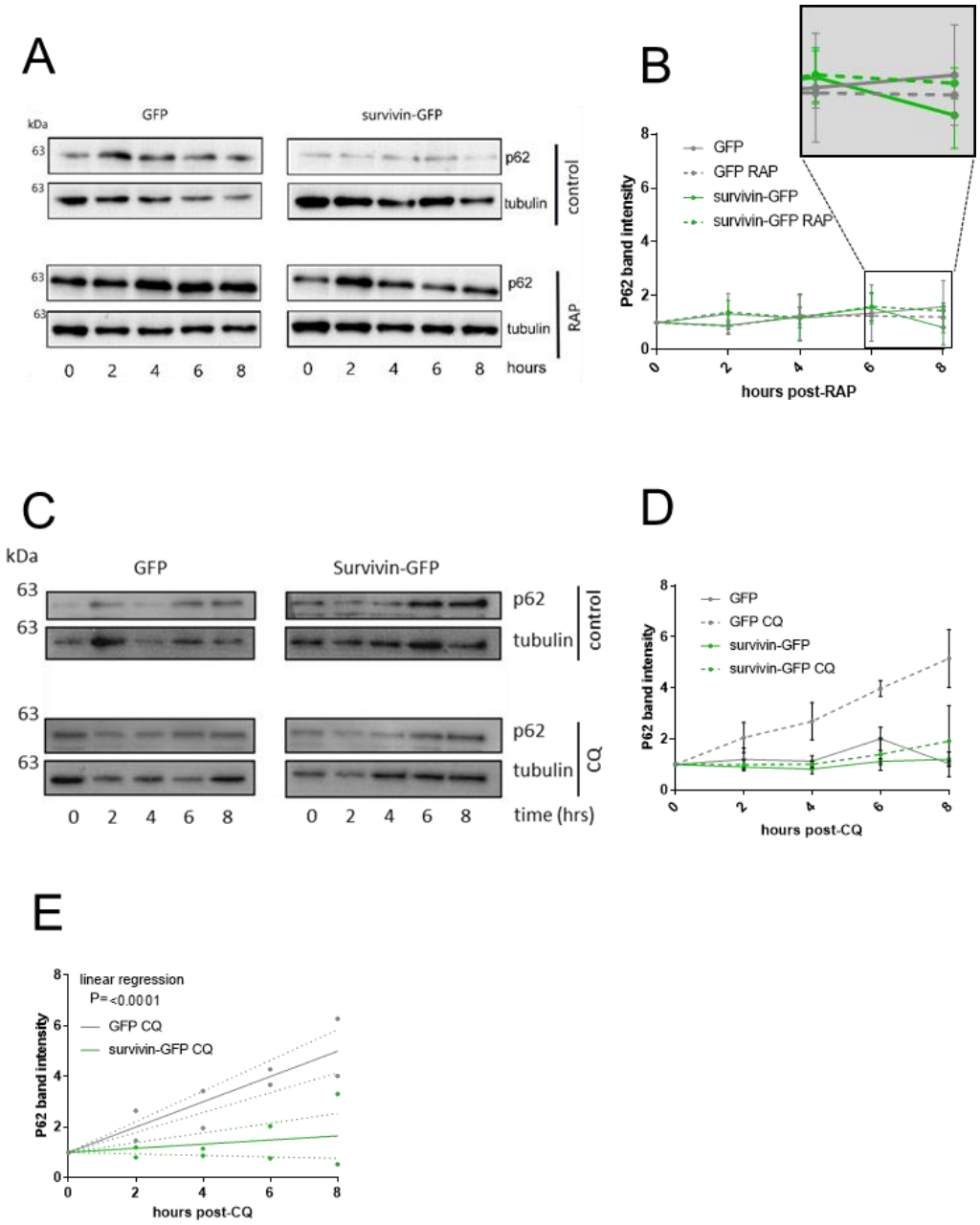


Figure 3.2.2. P62 degradation. U2OS cells stably expressing survivin-GFP or GFP were treated with RAP (A and B) or CQ (C-E) for 8 hours and p62 levels assessed by immunoblotting at 2-hour intervals. (B) Quantitation of p62 signals relative to tubulin and intensity at time 0 are shown in (B) and (D). (E) Linear regression of p62 accumulation in CQ treated cells. Solid lines indicate the line of best fit, dashed lines indicate the 95% confidence interval of each line. All error bars indicate SEM. 2 independent experiments per treatment.

Autophagosome / lysosome characteristics

Autophagosome size and abundance

A commonly used method to investigate autophagy is the analysis of autophagic bodies in cells using fluorescence microscopy. LC3 is routinely used to identify autophagosomes because LC3-II concentrates on autophagosome membranes. To monitor autophagosome size and abundance, U2OS cells transiently transfected with GFP-LC3 and either RFP, survivin$^{wild\text{-}type}$-RFP or survivin^{F61AL64A}RFP were treated with RAP and CQ for 2 h to accumulate autophagosomes, then imaged live. Cells expressing particularly high levels of LC3 were rejected so that the potential formation of non-autophagic LC3 aggregates[165] could be excluded.

Both average size and abundance of GFP-LC3 puncta in cells expressing RFP (control) increased significantly after RAP/CQ treatment (figure 3.2.3 A and B), indicating that autophagosomes are maturing and accumulating; both signs of robust autophagic flux.

The abundance of GFP-LC3 puncta in cells expressing RFP, survivin$^{wild\text{-}type}$-RFP or survivin^{F61A,L64A}-RFP was similar, as was the average size of puncta pre-treatment. However, after RAP/CQ treatment the puncta in both survivin$^{wild\text{-}type}$-RFP and survivin^{F61A,L64A}-RFP -expressing cells did not increase in size to the same extent as those in control cells (figure 3.2.3 A and B). This suggests that survivin impairs autophagosome maturation and that the LIR F_{61}KEL is **not** required for this effect.

A summary of the data collected from these experiments is shown in table 3.2.1.

Expressed construct	Control		RAP/CQ treated cells	
	Size (μm^2)	Abundance (per cell)	Size (μm^2)	Abundance (per cell)
RFP	0.21	12	0.32	20
Survivin-RFP	0.20	15	**0.27**	22
survivin^{F61A,L64A}-RFP	0.2	11	**0.28**	17

Table 3.2.1: Mean size and abundance of LC3 puncta

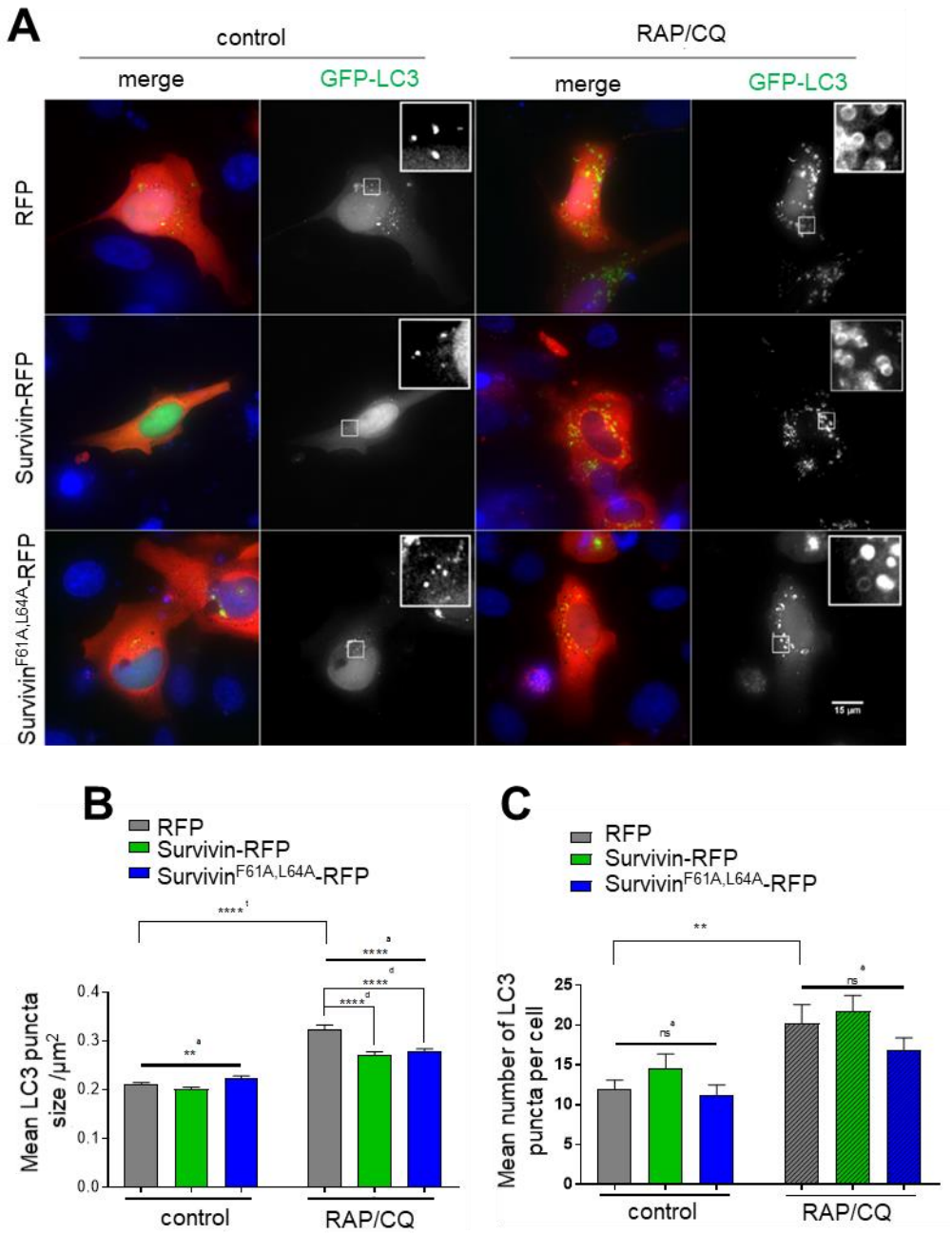


Figure 3.2.3: Size and abundance of LC3 puncta: Data from figure 3.1.6 was further analysed: (A) U2OS cells transiently expressing RFP, survivin$^{wild\text{-}type}$-RFP or survivin^{F61A,L64A}-RFP, and GFP-LC3 were treated with RAP/CQ for 2 h prior to live cell imaging to accumulate autophagosomes. (B) Mean GFP-LC3 puncta size was measured per condition, n>500 puncta over 4 independent experiments. (C) Mean number of GFP-LC3 puncta per cell was measured per condition, n>35 cells over 3 independent experiments. All error bars indicate SEM. *P<0.05 **P<0.005, ****P<0.0001. t=students' t-test, a=one-way ANOVA, d=Dunnett's multiple comparisons test.

Lysosome size and abundance

The acidic environment of the lysosomal and autolysosomal lumina facilitates their identification using the cell-permeable lysosomotrophic dye LysoTracker. Both the abundance and size of lysosomes and autolysosomes provide us with a measure of the state of autophagy in a cell, allowing us to draw conclusions about the regulation of autophagy.

To monitor autolysosome/lysosome abundance and size, U2OS cells stably expressing GFP, survivin-GFP or survivin^{F61AL64A}-GFP were treated with CQ for 2 h to inhibit late-stage autophagy, incubated with LysoTracker, and imaged live.

The average size of acidic puncta in cells expressing GFP (control) increased significantly after CQ treatment (figure 3.2.4 A and B), suggesting that either lysosomes themselves are swelling, or that autolysosomes are accumulating. The abundance of acidic puncta reduced significantly post-treatment (figure 3.2.4 A and C), and two possible explanations are that multiple lysosomes fuse with existing autolysosomes, or that lysosome generation through either nascent production or the ALR process is inhibited.

The abundance of acidic puncta was similar between GFP, survivin-GFP, and survivin^{F61A,L64A}-GFP -expressing cells, yet both wild-type and mutant survivin -expressing cells contained significantly larger puncta, both before and after treatment, to controls (figure 3.2.4 A and B). This suggests that survivin either impairs autolysosome clearance, or causes lysosomal swelling, and that the LIR F_{61}KEL is **not** required for this effect. A summary of the data collected from these experiments is shown in table 3.2.2.

Expressed construct	Control		RAP/CQ treated cells	
	Size (µm^2)	Abundance	Size (µm^2)	Abundance
GFP	0.28	66	0.45	47
Survivin$^{wild\text{-}type}$-GFP	**0.34**	67	**0.65**	40
survivin^{F61A,L64A}-GFP	**0.35**	62	**0.64**	39

Table 3.2.2: Mean size and abundance of acidic puncta

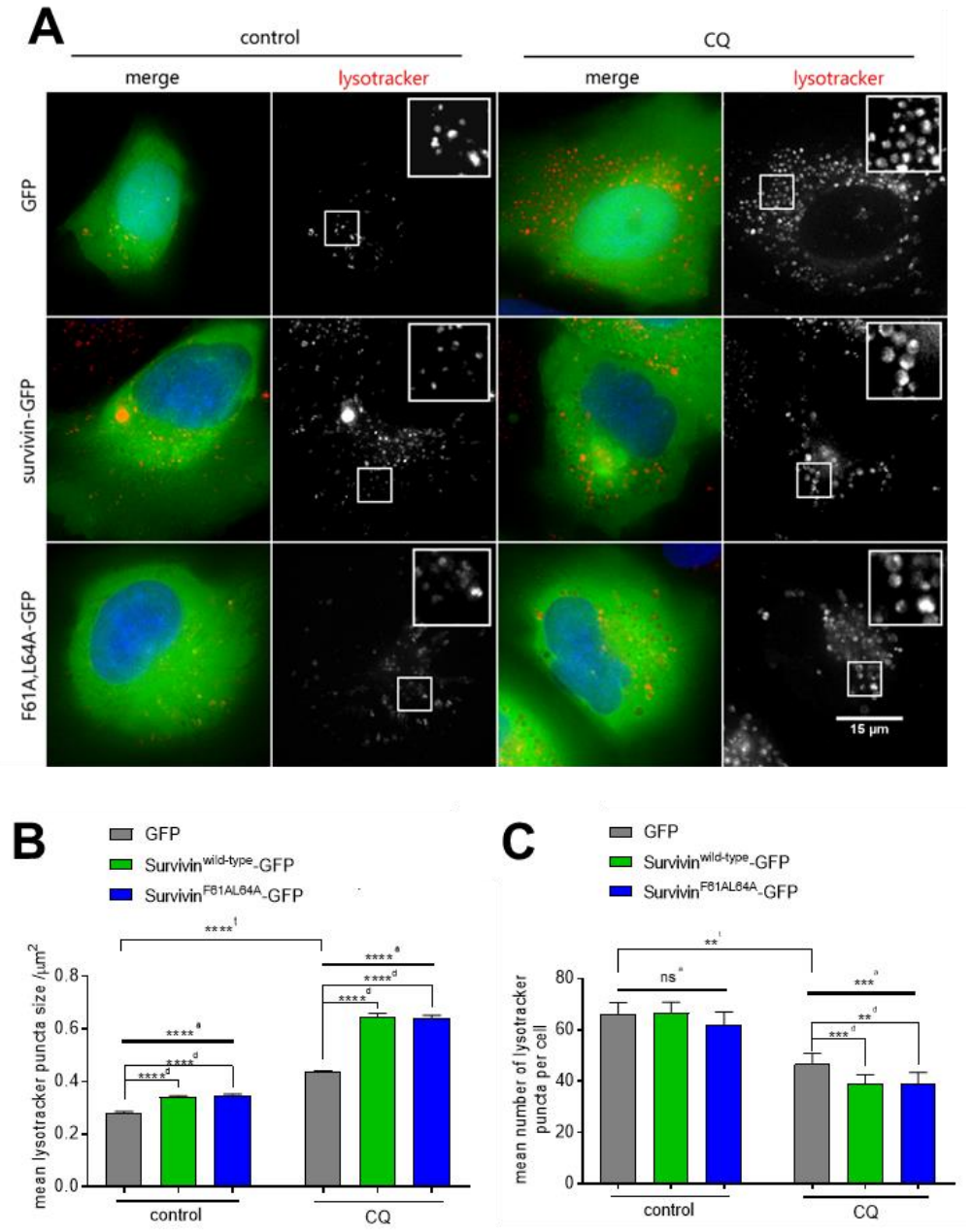


Figure 3.2.4: Size and abundance of acidic puncta: (A) U2OS cells stably expressing GFP or survivin-GFP were incubated with Lysotracker Red to highlight acidic compartments, and CQ for 2 h prior to live cell imaging. (B) Mean acidic puncta size was measured per condition, n>1500 puncta across more than 30 cells over three independent experiments. (C) Mean number of acidic puncta per cell was measured per condition, n>30 cells over three independent experiments. All error bars indicate SEM. **P<0.005,***P<0.0005, ****P<0.0001. t=students' t-test, a=one-way ANOVA, d=Dunnett's multiple comparisons test.

In summary, U2OS cells contained many, small acidic puncta pre-treatment, which were similar in size to autophagosomes yet much more abundant, and treatment with CQ resulted in few, large acidic puncta.

Summary of autophagosome / lysosome characteristics

A model for autophagic inhibition by survivin and CQ to explain these findings is shown in figure 3.2.5. It is reasonable to suppose that fusion of the immature autophagosome with endosomes to form amphisomes[166] increases the size of the organelle, and that fusion of the amphisome with lysosomes increases the size further, due to the accumulation of membrane material.

An interesting extension to these studies would be to design an experiment to allow the measurement of LC3 puncta and acidic puncta concurrently, perhaps with a dual-tagged LC3 construct where one tag does not fluoresce in the acidic lysosome environment. This would enable autophagosomes and lysosomes to be distinguished from autolysosomes, and more clearly indicate whether autophagosome/endosome/lysosome fusion is impaired.

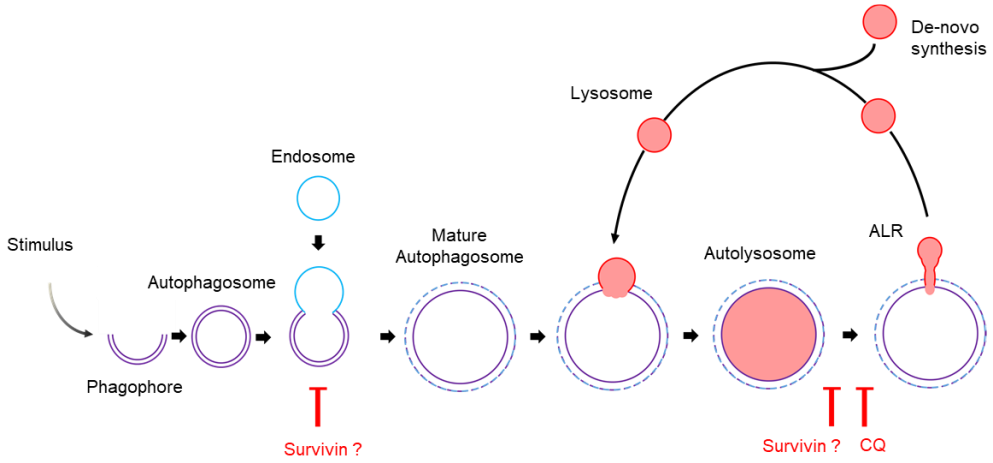


Figure 3.2.5: A model for autophagic inhibition by survivin and CQ. CQ raises the pH of lysosomes reducing the activity of the degradative enzymes they contain, thus preventing the breakdown of autolysosome content and consequently both dissolution of autolysosomes and the autolysosome reformation (ALR), leading to an accumulation of large acidic puncta. Survivin inhibits both the maturation of autophagosomes and the final phase of autophagy, leading to reduced autophagosome size, and an accumulation of large acidic puncta.

Survival under autophagic stress

To investigate whether the regulation of autophagy by survivin has an impact upon cell survival, both clonogenic and resazurin assays were performed. Clonogenic survival assays provide a means to determine how well cells

propagate after stress. The resazurin assay relies on mitochondrial respiration as a marker of cell viability over a period of days[167].

In these studies, clonogenic survival of GFP and survivin-GFP cells grown in starvation conditions (HBSS) was assessed. The average number of GFP-expressing cells producing a colony during starvation was 39% of those producing a colony in normal growth conditions, indicating that starvation had a negative impact on cell growth (figure 3.2.6). Starvation appeared to have a reduced impact on cells expressing survivin-GFP (51%) However, the impact was highly variable between samples and this meant that this reduced impact was not statistically significant (figure 3.2.6).

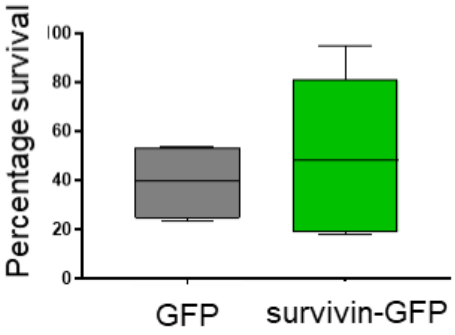


Figure 3.2.6: Clonogenic survival during starvation: U2OS cells stably expressing GFP or survivin$^{wild\text{-}type}$-GFP were treated with RAP for 2 hours, then incubated for 2 weeks in complete media. Survival is expressed as colonies on treated plates as a percentage of colonies on untreated plates. The mid-line indicates the median, and the upper and lower extremes of the box indicate Q3 and Q2 respectively. Whiskers represent the upper and lower extreme values of the data. Three replicates in each of two independent experiments.

Resazurin assays were performed to assess the impact of serum-free media; PBS (serum, amino-acid and glucose -free media); H_2O_2 media (to induce mitochondrial stress) and growth after 2 h of RAP treatment upon viability of U2OS cells expressing GFP, survivin-GFP or survivin^{F61A,L64A}-GFP (figure 3.2.7).

Results indicated that all cells had the highest viability in complete media, and the lowest in H_2O_2 and PBS medium, where very little mitochondrial respiration could be detected after 1 day (figure 3.2.7 A-C). All cell lines showed a 50% reduction in viability when grown in serum-free media compared to complete media (figure 3.2.7 A-C), yet the response to RAP treatment varied significantly

(figure 3.2.7 D-E). Survivin-GFP appeared to be particularly sensitive to RAP with a reduction in viability of around 60% while GFP and survivin^{F61A,L64A}-GFP -expressing cells only showed a 40% reduction (figure 3.2.7 D-E).

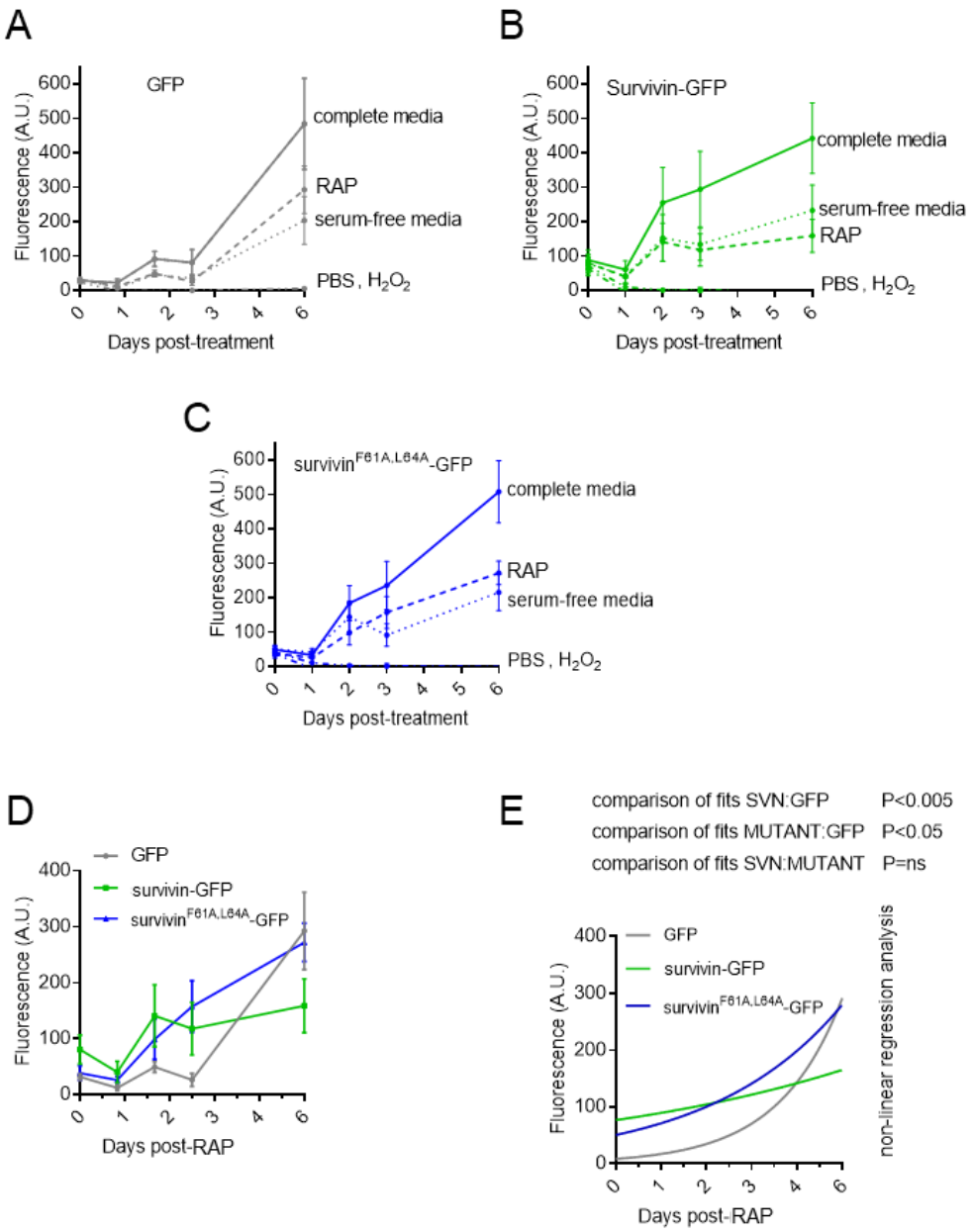


Figure 3.2.7. Viability under autophagic stress: U2OS cells stably expressing GFP, survivin$^{wild\text{-}type}$-GFP or survivin^{F61A,L64A}-GFP were treated with RAP for 2 h or grown in various media for 6 days and assessed for viability, n=3. (A) Viability of cells expressing GFP and grown various media. (B) Viability of cells expressing survivin$^{wild\text{-}type}$-GFP and grown various media. (C) Viability of cells expressing survivin^{F61A,L64A}-GFP and grown various media. (D) Viability of each cell line after in RAP treatment. (E) Non-linear best fit of data from (D). All error bars indicate SEM.

Both the clonogenic and resazurin experiments showed that starvation had a similar effect on the viability of cells expressing GFP, survivin-GFP, yet inhibition of mTOR and associated autophagy induction was more detrimental to cells expressing high levels of wild-type survivin. This suggests that the long-term effect of mTOR inhibition on cell viability in cells expressing high levels of survivin are partially due to the LIR F[61]KEL, since mutations at F61 and L64 showed a viability similar to cells expressing GFP alone.

At first it may seem surprising that RAP and starvation have different effects on cell viability, since both treatments induce autophagy. However, literature suggests that RAP and starvation do indeed have different effects on cellular processes[168–170]. For example, in murine macrophages infected with *B.pseudomallai* bacteria , the RAP response is beclin-1 independent whereas the starvation response is beclin-1 dependent[168]. Thus, the studies in this section indicate that wild-type survivin overexpression has a negative impact on cell growth when mTOR is inhibited, but not in starvation conditions.

Importantly, aside from nutrient and growth factor levels, mTOR is regulated by DNA damage. Since survivin-expression is related to cell survival[2], it is possible that mTOR inhibition by RAP may be suppressing cell division in cells with high levels of survivin. Following DNA damage, temporary suppression of cell division could have a positive impact on the long-term survival of the cell. Indeed, recent research suggests that quiescence is a major factor in cell survival following cancer therapy[171].

RESIDUES F61 AND L64 ARE REQUIRED FOR MITOTIC LOCALISATION OF SURVIVIN

Localisation of survivin^{F61A,L64A}

At interphase survivin assumes a diffuse, predominantly cytoplasmic localisation. As a member of the chromosomal passenger complex, survivin binds to phosphorylated histone H3 at the centromeres and guides the chromosomes during early mitosis. At anaphase, survivin decorates the midzone while chromosomes migrate towards opposing spindle-poles, and at telophase it localises to the midbody[40].

To investigate whether the LIR F_{61}KEL is required for the localisation of survivin, U2OS cell lines stably expressing GFP, survivin-GFP or survivin^{F61A,L64A}-GFP were imaged live by fluorescence microscopy. To obtain images at different stages of mitosis, cells were arrested at prometaphase using an Eg5 inhibitor overnight, then released prior to imaging (figure 3.3.1). To confirm the location of survivin relative to the mitotic spindle and chromosomes, cells were fixed and immunostained for tubulin and counterstained with DAPI (figure 3.3.2).

As previously reported, wild-type survivin tagged with GFP adopted a diffuse, predominantly cytoplasmic distribution at interphase, localised with centromeres at prophase and metaphase, and at the midzone in anaphase and telophase. However, although survivin^{F61A,L64A}-GFP localised as wild-type at interphase and telophase, it failed to localise normally at prophase, metaphase and anaphase where it adopted a diffuse distribution (figures 3.3.1 and 3.3.2).

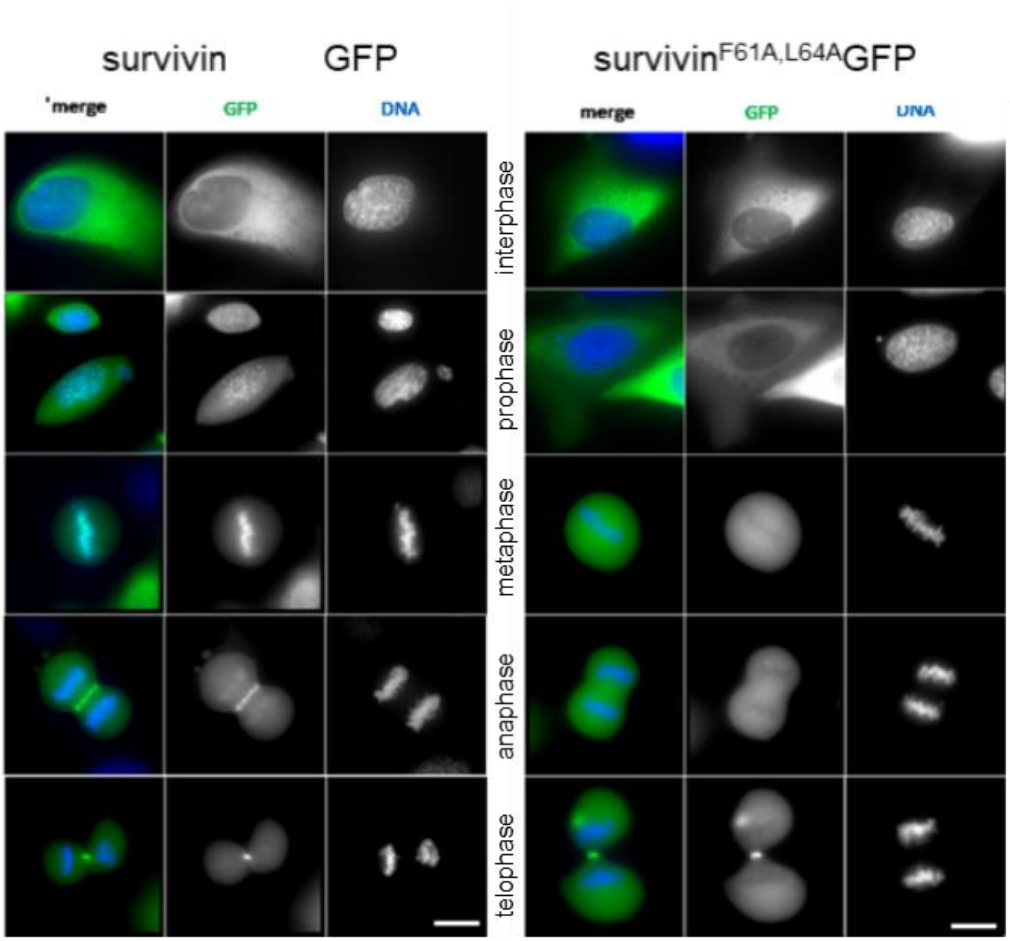


Figure 3.3.1: Localisation of survivin during the cell cycle. U2OS cells stably expressing survivin-GFP or survivin^{F61A,L64A}-GFP (green) were subjected to live fluorescence imaging. DNA stained by Hoechst (blue). Examples of cells at different mitotic stages are presented. Scale bar 10 µm. Images are representative of multiple cells visualised in a single experiment.

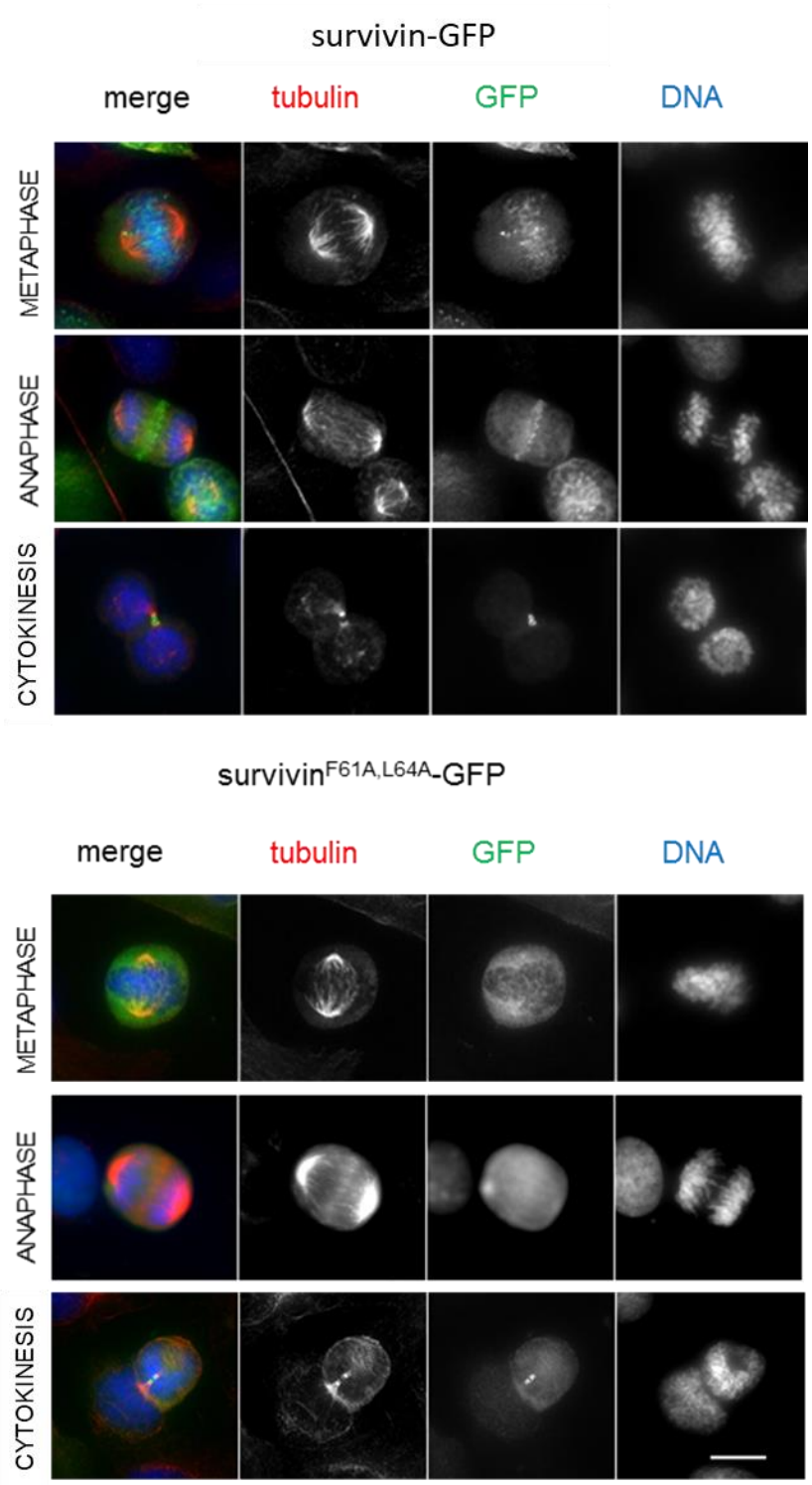


Figure 3.3.2: Localisation of survivin relative to the mitotic spindle during the cell cycle. U2OS cells stably expressing GFP, survivin$^{wild\text{-}type}$-GFP or survivin^{F61A,L64A}-GFP (green) were stained with Hoechst (blue) to visualise DNA, then fixed with formaldehyde and permeabilised with Triton X100 before immunostaining for tubulin (red) to visualise the mitotic spindle. Examples of cells at different life cycle stages are presented. Scale bar 15 µm. Images are representative of multiple cells visualised in a single experiment

Results from these experiments indicate that Survivin^{F61A,L64A}-GFP not only fails to localise to centromeres during early mitosis but is unable to localise to the midzone in anaphase.

Failure to localise to centromeres could be explained by location of the survivin mutations. As illustrated in figure 3.3.3, the F_{61}KEL sequence lies within a pocket in the BIR domain that forms the interaction surface for histone H3 pT^{3}. This interaction is critical for the centromeric localisation of the CPC at prophase and metaphase[44].

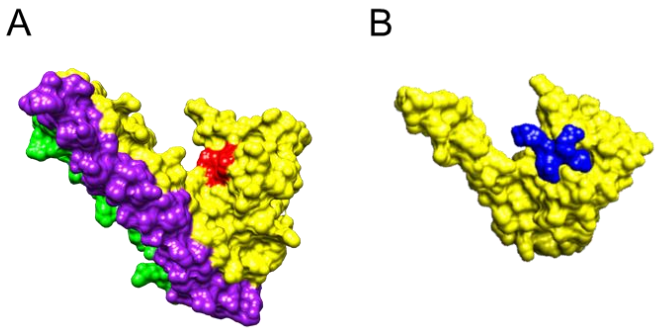


Figure 3.3.3: Location of the LC3-binding pocket. A: Crystal structure of borealin (green) and the n-terminus of INCENP (purple) bound to survivin (yellow) (PDB:2QFA) with the F_{61}KEL sequence highlighted in red showing that this surface is exposed in the CPC complex. B: Crystal structure of survivin (yellow) bound to the tail of histone H3 (blue) (PDB:3UED). Images generated using UCSF Chimera[29].

However, interference with the histone-survivin interaction does not explain the failure of Survivin^{F61A,L64A}-GFP to localise to the midzone at anaphase, since at this point survivin has dissociated from the chromosomes. Dephosphorylation of histone H3 with subsequent dissociation from survivin is required for the CPC to dissociate from chromosomes at the metaphase-to-anaphase transition[44]. This suggests that the failure to bind to LC3 could be the cause of this mislocalisation, perhaps through the interaction between LC3 and microtubules[137].

Co-immunoprecipitation of survivin and histone H3 pT3

As part of the CPC, survivin binds to the H3 tail of histone, phosphorylated at threonine 3 (histone H3 p^{T3}) to regulate the congression of chromosomes at the spindle midzone during mitosis. To further investigate why survivin^{F61A,L64A} fails to localise to the centromeres at prophase and metaphase, the association of this mutant with histone H3 was analysed by co-immunoprecipitation.

Hek 293T cells expressing GFP-LC3 were transfected with flag-tagged survivin constructs and incubated for 24 h, then lysed and proteins immunoprecipitated with anti-flag M2 affinity gel. Immunoprecipitates were immunoblotted for histone H3 p^{T3} (figure 3.3.4).

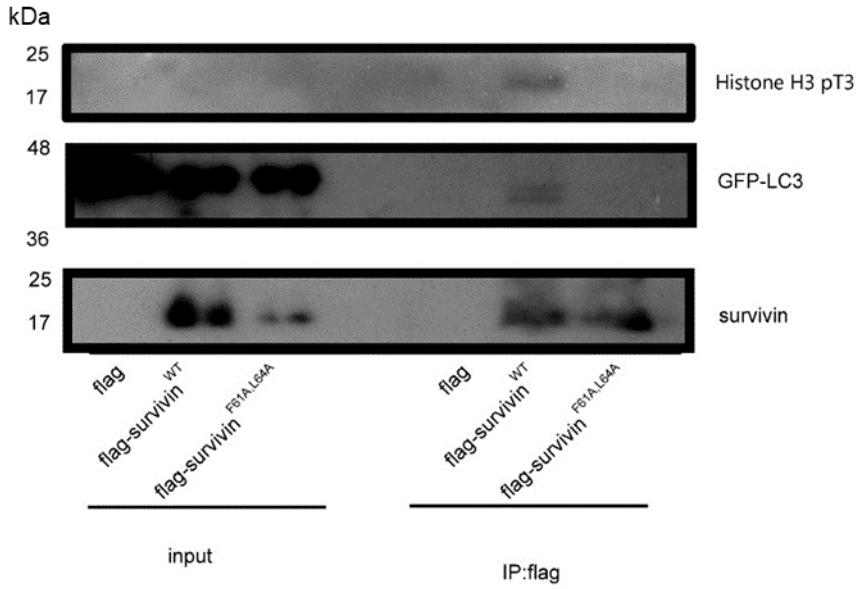


Figure 3.3.4: Histone H3 pT3 does not co-immunoprecipitate with survivin^{F61A,L64A}. Hek 293T cells expressing GFP-LC3 were transfected with flag-tagged survivin constructs, lysed and immunoprecipitated with anti-flag M2 affinity gel, and immunoblotted for histone H3 $p^{T3.}$ Image taken from a single experiment.

Flag-survivin$^{wild\text{-}type}$ and flag-survivin^{F61A,L64A} proteins both precipitated with anti-flag matrix but histone H3 pT3 only co-immunoprecipitated with wild-type survivin which indicates that residues F61 and L64 of survivin are critical for this interaction. This aligns with findings in section 3.3 which demonstrate that

unlike wild-type survivin, survivin^{F61A,L64A} fails to localise to the centromeres. In support of these findings, figure 3.3.3 illustrated that the crystal structure of survivin bound to the tail of histone H3 indicates that histone H3 and LC3 bind to the same pocket on the surface of the BIR domain of survivin. It seems reasonable to hypothesise that both proteins could not bind to survivin simultaneously and may therefore compete for this site, though further study such as saturation binding is required to confirm this. Mitotic arrest before co-immunoprecipitation may also improve this experiment by increasing the availability of Histone H3 pT3.

DISCUSSION

CONCLUSIONS

As its name implies, survivin is a protein that promotes cell viability[172]. It is well established that survivin is essential for mitosis[43,173] and inhibits apoptosis by reducing caspase activity[172,174]. Overexpression of survivin in cancer correlates with increased resistance to chemotherapy[60] and irradiation[17], and poor prognosis for the patient. This correlation is reproduced in cell culture[17,35,175]. Interestingly, it was recently discovered that in addition to inducing DNA damage, irradiation stimulates autophagy[176]. It has also been reported that survivin co-immunoprecipiates with the autophagic proteins, LC3[4], beclin1[26], LAMTOR5/HBXIP[14] and Atg5[177] and that survivin expression is linked to autophagy and cell death. This thesis aimed to discover whether survivin expression could regulate autophagy to prevent autophagic cell death.

The data presented herein establishes the following:

Survivin regulates autophagic flux, autophagosome and acidic puncta size independent of its association with LC3.
Survivin does not co-localise with autophagic puncta.
Survivin contains an LIR at residues 61-64 which is essential to the association with LC3.
Survivin increases sensitivity to rapamycin treatment in a manner that is partly dependent upon residues F61 and L64.

In addition to these main findings, this study revealed an unusual localisation of the survivin^{pent} mutant, which localised to the periphery of highly lobular nuclei after combined RAP and CQ treatment, in a pattern suggestive of the nuclear lamina. Further study is required to identify which of the five point mutations in survivin^{pent} are responsible for this aberrant localisation, and whether there is a connection to the autophagy of the nuclear lamina[178] or progeria syndrome; a condition caused by a mutant form of lamin A which

changes the structure of the nuclear lamina and affects the localisation of ran[179]; a GTPase known to interact with survivin[24].

Survivin regulates autophagic flux, autophagosome and acidic puncta size independent of its association with LC3.

Data presented in this thesis indicate that both LC3-II and P62 accumulate more gradually after CQ treatment in survivin-overexpressing cells, which implies that autophagic flux is reduced in cells overexpressing survivin. This finding is in line with a studies using the survivin inhibitor YM155 which showed that survivin suppression induced autophagy-dependent cell death in both prostate cancer cells[180] and adenoid cystic carcinoma cells[181]. Impairment in autophagic flux has been associated with neurodegenerative diseases such as Alzheimer's disease; muscular and cardiovascular diseases; immune-mediated diseases, in which autophagy mediates pathogen clearance or inflammation; and cancer, where autophagy can be associated with tumour suppression but also chemoresistance[182]. Dysregulation of autophagy by survivin may constitute part of the mechanism by which tumourigenesis occurs.

Survivin overexpression was also associated with reduced autophagosome size. The apparent contradiction with a recent research paper which reported that survivin-depleted murine erythroblasts harboured smaller cytoplasmic vacuoles compared to control cells, may be explained by the use of different model organisms[151]. In this study, we found that autophagosomes were smaller in cells overexpressing survivin than in control cells, yet their size still increased with CQ treatment. This suggests that survivin restricts autophagosome size but does not prevent cells from reaching late-stage autophagy, where CQ causes the accumulation of mature autophagosomes and autolysosomes.

The acidic lumina of lysosomes and autolysosomes were visualised with a cell-permeable lysotrophic dye. These experiments showed that survivin overexpression was associated with increased average acidic puncta size. Canonical lysosomes are by nature the smaller of these two vesicles

(lysosomes: 50-500 nm in diameter[183]; autophagosomes 500-1500 nm[184]), and therefore larger acidic puncta are more likely to be autolysosomes created by the fusion of autophagosomes with lysosomes. CQ treatment also resulted in increased average puncta size, caused by the accumulation of late-stage autophagosomes/autolysosomes and indicating that these vesicles are unable to complete the degradation stage of autophagy. It seems possible therefore, that survivin is having a similar effect on autophagy, and inhibiting final-stage autophagy.

Surprisingly, the mutation of the LIR site in the primary sequence of survivin from F_{61}KEL to A_{61}KEA had no impact of the regulation of autophagosome or acidic puncta size or number. This finding suggests that the association of survivin with LC3 is not responsible for autophagic regulation, and that an alternative mechanism must be involved (further discussed in section 4.2).

Survivin does not co-localise with autophagic puncta.

The association of survivin with LC3 initially suggests they may co-localise at autophagosomes, yet no evidence of co-localisation was found. This implies that rather than associating with LC3 on autophagosomes, survivin interacts with LC3 elsewhere in the cell in an autophagosome-independent manner (further discussed in section 4.3)

Survivin contains an LIR at residues 61-64 which is essential to the association with LC3.

The iLIR integrated bioinformatics service[185] identifies five putative LC3 interaction regions (LIRs) in the survivin primary sequence. Only one region, F_{61}KEL, is well conserved and located on a flexible strand, making it more likely to interact with the beta-sheet of LC3[135]. Using site-directed mutation and co-immunoprecipitation techniques this research has shown that this LIR is essential to the association of survivin with LC3.

Survivin increases sensitivity to RAP treatment in a manner that is dependent upon residues F61 and L64.

Cells overexpressing survivin are particularly sensitive to RAP treatment. Decreased cell viability could indicate a higher incidence of cell death, or reduced cell division. Cells maintained in a non-proliferating quiescent state for long time intervals is a frequent clinical phenomenon in cancer biology[186]. The quiescent state protects these cells from anti-proliferating agents and is therefore an important factor of resistance to chemotherapy[186]. It is possible that mTOR inhibition triggers quiescence in cells with high levels of survivin, and this may promote the survival of these cells in the long-term. Concurrent with this possibility, survivin has recently been identified as a marker for quiescent breast cancer stem cells, where it favours metastasis[187]. The mutation of the LIR site F_{61}KEL reduced sensitivity to RAP treatment, implying that the long-term effect of mTOR inhibition on cells expressing high levels of survivin are partially due to the LIR F_{61}KEL or interaction with LC3.

UNDERSTANDING THE MECHANISM AND PURPOSE OF AUTOPHAGIC INHIBITION BY SURVIVIN.

One possible mechanism is the regulation of immature autophagosome fusion with endosomes to form amphisomes[26], a process that increases the size of the resulting vesicle. Survivin could regulate fusion via the interaction with LAMTOR5/HBXIP on the lysosome surface. Another possibility is that building blocks required for autophagosome expansion, such as Atg5 and beclin1, both of which interact with survivin, are less readily available in cells expressing high levels of survivin. In support of this theory, recent research in the Wheatley lab has found that mitochondrial survivin regulates the activity of phosphatidylserine decarboxylase, the enzyme responsible for conversion of phosphatidylserine to PE (unpublished data), and PE is conjugated to LC3 to form the LC3II on the autophagosome surface (unpublished data).

Since survivin-LC3 interaction has been excluded as the mechanism by which survivin regulates autophagy, the question of how survivin achieves this regulation remains to be determined. Survivin has been shown to interact with three other proteins involved in autophagosome formation; beclin1[26], Atg5[150], and LAMTOR5/HBXIP[14]. Beclin1 is important for the localization of autophagic proteins to the phagophore and is also involved in membrane trafficking[91] and Atg5 is involved in the extension of the phagophore and LC3 lipidation and associates with survivin in the nucleus following DNA damage[150]. Thus, survivin may inhibit phagophore formation and extension via these proteins. LAMTOR5 forms part of the ragulator complex responsible for locating mTORC1 at the lysosome surface when amino acids are abundant, thus enabling its activation and subsequent autophagic inhibition. In addition, Survivin has been shown to interact with clathrin in enucleating murine erythroblasts[151]. Clathrin is required for the formation of coated vesicles, including those used to transport acid hydrolases to the lysosome, and also plays a role in ALR regulation and therefore autophagosome homeostasis[155]. One or more of these interactions could be involved in the regulation of autophagy by survivin. A summary of

potential mechanisms for the inhibition of autophagy by survivin is illustrated in figure 4.2.

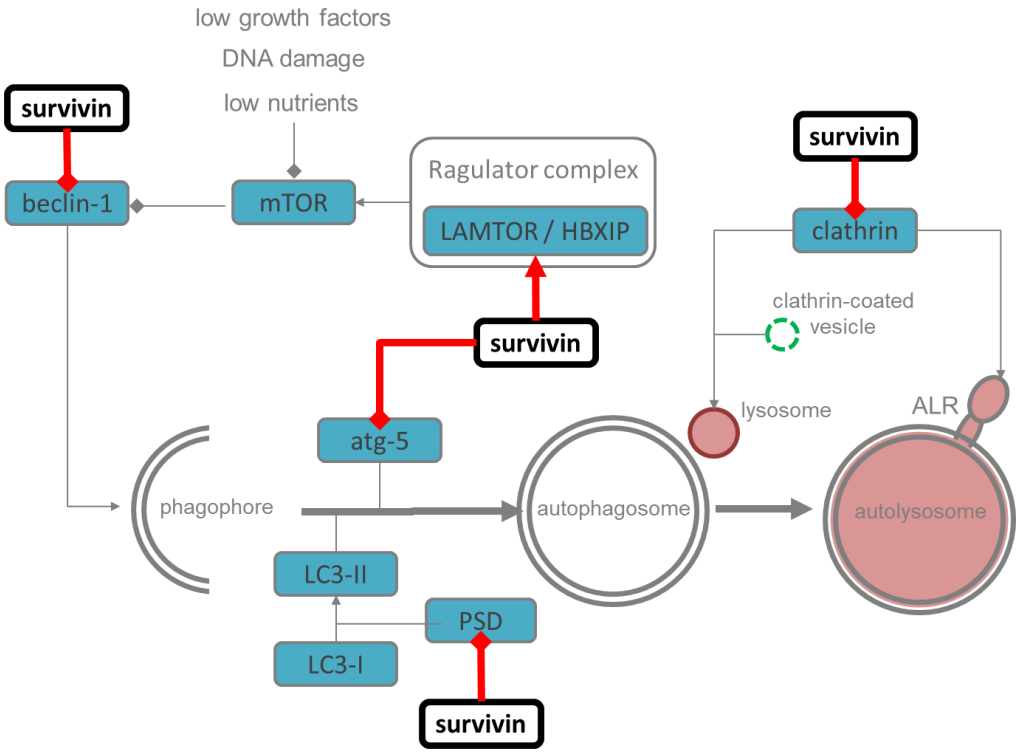


Figure 4.2: Potential mechanisms for the inhibition of autophagy by survivin: Survivin has been shown to interact with beclin1, Atg-5, clathrin, LAMTOR/HBXIP and PSD, all proteins which have a role in autophagy.

Interestingly, recent research has found that mTOR can upregulate survivin[151,152]. This suggests that autophagic suppression by survivin would be favoured in healthy cells with active mTOR, but not in cells under stress. In confirmation of a link between the mTOR pathway and tumourigenesis, a paper published earlier this year found that hyperactivation of mTOR activity caused by the loss of tumour-suppressor RNF168 is associated with the accumulation of unrepaired DNA and genome instability[188]. Together these papers suggest that overexpression of survivin can promote tumourigenesis via genome instability, perhaps through reduced degradation of damaged DNA by autophagy.

One model to explain the purpose of autophagic inhibition by survivin is that survivin expression, restricted to mitosis in normal cells, suppresses autophagy to protect vulnerable chromatin from autophagic degradation in the absence of nuclear compartmentalisation, and to protect mitochondria from mitophagy while they are fragmented in preparation for their segregation into daughter cells. Elevated levels of survivin during interphase could lead to increased cell survival after DNA damage, leading to genome instability, and increased survival in extreme conditions where excessive autophagy might normally lead to cell death, such as the hypoxic environment of a tumour, or metastatic migration through the blood or lymph system.

UNDERSTANDING AND PURPOSE OF THE ASSOCIATION BETWEEN SURVIVIN AND LC3.

This study has found that association between survivin and LC3 is not required for the regulation of autophagic vesicle size. Since LC3 can bind directly to microtubules[124] and the protein FYCO1 to mediate vesicle transport[105], it may be that LC3 has roles in intracellular trafficking beyond those of autophagy and that interaction with survivin is required for these roles. Intriguingly, in addition to abrogating LC3 interaction, the survivin^{F61A,L64A} mutant failed to localize to the centromeres at prophase and metaphase, and the midzone at anaphase, which corroborates the finding that survivin interacts with both histone H3 pT3 and LC3 through the same site. One intriguing possibility for the LC3-survivin association is that the migration of survivin as part of the CPC from chromosomal centromeres to the spindle midzone at the metaphase-anaphase transition involves the dissociation of survivin from histone H3 pT3 and the association of survivin with LC3 using the same binding site (figure 6.2). The involvement of LC3 during mitosis is supported by the recent finding that LC3-I levels are raised during mitosis[189]. This hypothesis could explain a novel aspect of mitosis regulation and is worthy of further investigation.

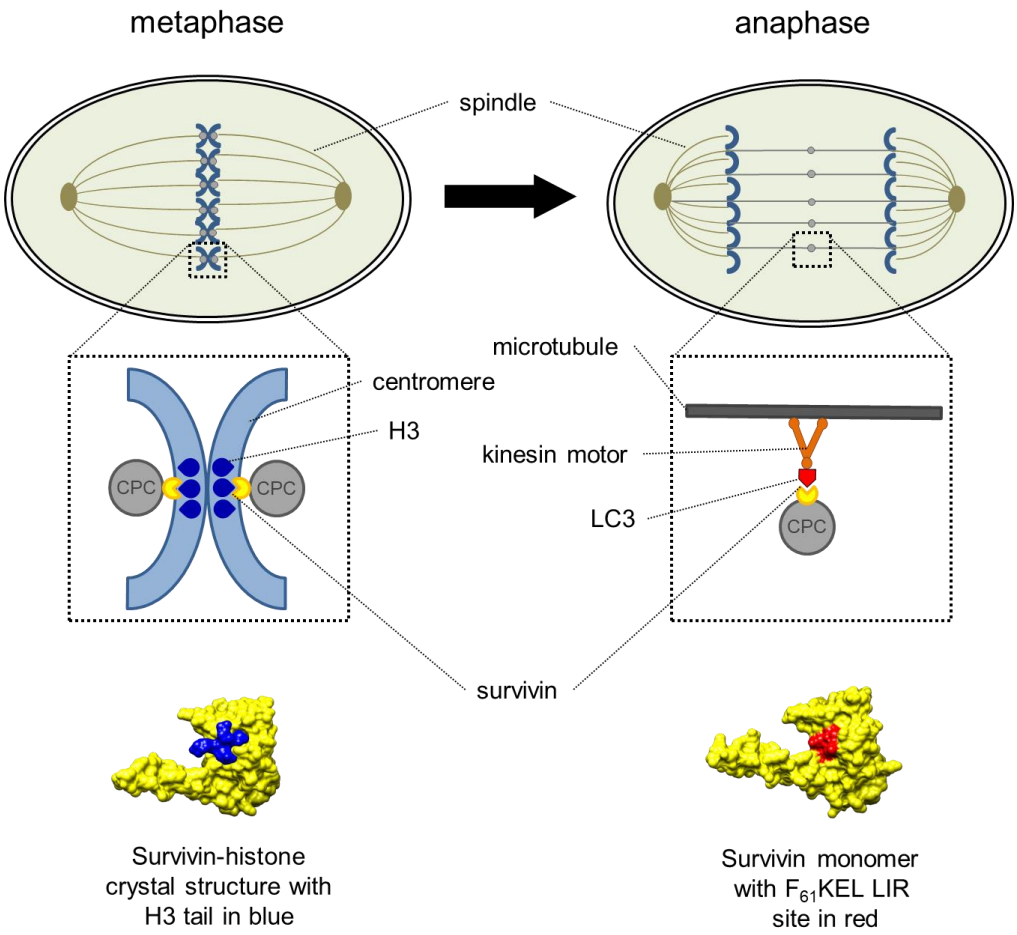


Figure 6.2: Proposed model for the relocation of the CPC at the metaphase-anaphase transition. The binding of survivin to phosphorylated histone H3 pT3 at metaphase could be replaced by an interaction with LC3 in early anaphase. LC3 has been shown to bind to kinesins for intracellular transport and could potentially be involved in localisation of the CPC to the spindle midzone at anaphase in preparation for cytokinesis.

OUTLOOK.

The data presented in this thesis, combined with recent research, suggest that survivin restricts autophagic flux by regulating autophagosome maturation. Further studies are needed to determine which stages of autophagy are regulated by survivin and the mechanism through which this occurs. Studies which downregulate survivin would also be helpful to confirm the role of survivin in autophagy. The possibility that overexpression of survivin may induce quiescence following mTOR inhibition is also worthy of further investigation.

In addition, these data show that survivin associates with LC3, through a site also required for Histone H3 pT3 interaction, in a manner requiring residues F61 and L64. Since data also indicate that this association is not required for autophagic regulation, an intriguing possibility has arisen that this association may be involved in the relocation of survivin from the centromere to the spindle midzone at metaphase-anaphase transition. Further research to investigate this hypothesis should include the use of LC3 mutants which are unable to bind to LIR sites, and the localisation of LC3 throughout mitosis.

Control of cellular life and death is tightly regulated and involves complex signalling pathways. Elucidating the exact roles of survivin in the cell will increase our understanding of its role in not only cancer, but in other pathologies associated with survivin dysregulation, including lung, heart and autoimmune disease.

REFERENCES

1. Uren, AG, Wong, L, Pakusch, M, Fowler, KJ, Burrows, FJ, Vaux, DL, *et al.* (2000). Survivin and the inner centromere protein INCENP show similar cell-cycle localization and gene knockout phenotype. *Curr. Biol.* **10**: 1319–1328.
2. Tamm, I, Wang, Y, Sausville, E, Scudiero, DA, Vigna, N, Oltersdorf, T, *et al.* (1998). IAP-Family Protein Survivin Inhibits Caspase Activity and Apoptosis Induced by Fas (CD95), Bax, Caspases, and Anticancer Drugs. *Cancer Res.* **58**: 5315–5320.
3. Yonekawa, T and Thorburn, A (2013). Autophagy and Cell Death. *Essays Biochem.* **55**: 105–117.
4. Roca, H, Varsos, Z and Pienta, KJ (2008). CCL2 protects prostate cancer PC3 cells from autophagic death via phosphatidylinositol 3-kinase/AKT-dependent survivin up-regulation. *J. Biol. Chem.* **283**: 25057–25073.
5. Ambrosini, G, Adida, C, Sirugo, G and Altieri, DC (1998). Induction of Apoptosis and Inhibition of Cell Proliferation by survivin Gene Targeting. *J. Biol. Chem.* **273**: 11177–11182.
6. Zody, MC, Garber, M, Adams, DJ, Sharpe, T, Harrow, J, Lupski, JR, *et al.* (2006). DNA sequence of human chromosome 17 and analysis of rearrangement in the human lineage. *Nature* **440**: 1045–1049.
7. Li, F, Ambrosini, G, Chu, EY, Plescia, J, Tognin, S, Marchisio, PC, *et al.* (1998). Control of apoptosis and mitotic spindle checkpoint by survivin. *Nature* **396**: 580–584.
8. Zwicker, J, Lucibello, FC, Wolfraim, LA, Gross, C, Truss, M, Engeland, K, *et al.* (1995). Cell cycle regulation of the cyclin A, cdc25C and cdc2 genes is based on a common mechanism of transcriptional repression. *EMBO J.* **14**: 4514–4522.
9. Zhao, J, Tenev, T, Martins, LM, Downward, J and Lemoine, NR (2000). The ubiquitin-proteasome pathway regulates survivin degradation in a cell cycle-dependent manner. *J. Cell Sci.* **113 Pt 23**: 4363–4371.
10. Ambrosini, G, Adida, C and Altieri, DC (1997). A novel anti-apoptosis gene, survivin, expressed in cancer and lymphoma. *Nat. Med.* **3**: 917–921.
11. Chantalat, L, Skoufias, DA, Kleman, J-P, Jung, B, Dideberg, O and Margolis, RL (2000). Crystal Structure of Human Survivin Reveals a Bow Tie–Shaped Dimer with Two Unusual α-Helical Extensions. *Mol. Cell* **6**: 183–189.
12. Muchmore, SW, Chen, J, Jakob, C, Zakula, D, Matayoshi, ED, Wu, W, *et al.* (2000). Crystal structure and mutagenic analysis of the inhibitor-of-apoptosis protein survivin. *Mol. Cell* **6**: 173–182.
13. Dunajová, L, Cash, E, Markus, R, Rochette, S, Townley, AR and Wheatley, SP (2016). The NH2 terminus of survivin is a mitochondrial targeting sequence and C-Src regulator. *J Cell Sci*: jcs.183277doi:10.1242/jcs.183277.
14. Marusawa, H, Matsuzawa, S-I, Welsh, K, Zou, H, Armstrong, R, Tamm, I, *et al.* (2003). HBXIP functions as a cofactor of survivin in apoptosis suppression. *EMBO J.* **22**: 2729–2740.

15. Barrett, RMA, Colnaghi, R and Wheatley, SP (2011). Threonine 48 in the BIR domain of survivin is critical to its mitotic and anti-apoptotic activities and can be phosphorylated by CK2 in vitro. *Cell Cycle Georget. Tex* **10**: 538–548.
16. Cao, L, Yan, X, Wu, Y, Hu, H, Li, Q, Zhou, T, *et al.* (2006). Survivin mutant (Surv-DD70, 71AA) disrupts the interaction of Survivin with Aurora B and causes multinucleation in HeLa cells. *Biochem. Biophys. Res. Commun.* **346**: 400–407.
17. Colnaghi, R, Connell, CM, Barrett, RMA and Wheatley, SP (2006). Separating the Anti-apoptotic and Mitotic Roles of Survivin. *J. Biol. Chem.* **281**: 33450–33456.
18. Engelsma, D, Rodriguez, JA, Fish, A, Giaccone, G and Fornerod, M (2007). Homodimerization antagonizes nuclear export of survivin. *Traffic Cph. Den.* **8**: 1495–1502.
19. Wheatley, SP, Henzing, AJ, Dodson, H, Khaled, W and Earnshaw, WC (2004). Aurora-B Phosphorylation in Vitro Identifies a Residue of Survivin That Is Essential for Its Localization and Binding to Inner Centromere Protein (INCENP) in Vivo. *J. Biol. Chem.* **279**: 5655–5660.
20. Wang, H, Holloway, MP, Ma, L, Cooper, ZA, Riolo, M, Samkari, A, *et al.* (2010). Acetylation directs survivin nuclear localization to repress STAT3 oncogenic activity. *J. Biol. Chem.* **285**: 36129–36137.
21. Aljaberi, AM, Webster, JR and Wheatley, SP (2014). Analysis of the functional repertoire of a mutant form of survivin, K129E, which has been linked to lung cancer. *Cancer Cell Int.* **14**: 78.
22. Jeyaprakash, AA, Klein, UR, Lindner, D, Ebert, J, Nigg, EA and Conti, E (2007). Structure of a Survivin–Borealin–INCENP Core Complex Reveals How Chromosomal Passengers Travel Together. *Cell* **131**: 271–285.
23. Elkins, JM, Santaguida, S, Musacchio, A and Knapp, S (2012). Crystal structure of human aurora B in complex with INCENP and VX-680. *J. Med. Chem.* **55**: 7841–7848.
24. Xia, F, Canovas, PM, Guadagno, TM and Altieri, DC (2008). A Survivin-Ran Complex Regulates Spindle Formation in Tumor Cells. *Mol. Cell. Biol.* **28**: 5299–5311.
25. O'Connor, DS, Grossman, D, Plescia, J, Li, F, Zhang, H, Villa, A, *et al.* (2000). Regulation of apoptosis at cell division by p34cdc2 phosphorylation of survivin. *Proc. Natl. Acad. Sci.* **97**: 13103–13107.
26. Niu, T-K, Cheng, Y, Ren, X and Yang, J-M (2010). Interaction of Beclin 1 with survivin regulates sensitivity of human glioma cells to TRAIL-induced apoptosis. *FEBS Lett.* **584**: 3519–3524.
27. Song, Z, Yao, X and Wu, M (2003). Direct Interaction between Survivin and Smac/DIABLO Is Essential for the Anti-apoptotic Activity of Survivin during Taxol-induced Apoptosis. *J. Biol. Chem.* **278**: 23130–23140.
28. Fackler Marc, Wolter Patrick and Gaubatz Stefan (2014). The GAR domain of GAS2L3 mediates binding to the chromosomal passenger complex and is required for localization of GAS2L3 to the constriction zone during abscission. *FEBS J.* **281**: 2123–2135.
29. Pettersen, EF, Goddard, TD, Huang, CC, Couch, GS, Greenblatt, DM, Meng, EC, *et al.* (2004). UCSF Chimera--a visualization system for exploratory research and analysis. *J. Comput. Chem.* **25**: 1605–1612.

30. Colnaghi, R and Wheatley, SP (2010). Liaisons between Survivin and Plk1 during Cell Division and Cell Death. *J. Biol. Chem.* **285**: 22592–22604.
31. O'Connor, DS, Wall, NR, Porter, ACG and Altieri, DC (2002). A p34cdc2 survival checkpoint in cancer. *Cancer Cell* **2**: 43–54.
32. Wheatley, SP, Barrett, RM, Andrews, PD, Medema, RH, Morley, SJ, Swedlow, JR, *et al.* (2007). Phosphorylation by Aurora-B Negatively Regulates Survivin Function During Mitosis. *Cell Cycle* **6**: 1220–1230.
33. Rodríguez, JA, Span, SW, Ferreira, CGM, Kruyt, FAE and Giaccone, G (2002). CRM1-mediated nuclear export determines the cytoplasmic localization of the antiapoptotic protein Survivin. *Exp. Cell Res.* **275**: 44–53.
34. Stauber, RH, Rabenhorst, U, Rekik, A, Engels, K, Bier, C and Knauer, SK (2006). Nucleocytoplasmic shuttling and the biological activity of mouse survivin are regulated by an active nuclear export signal. *Traffic Cph. Den.* **7**: 1461–1472.
35. Connell, CM, Colnaghi, R and Wheatley, SP (2008). Nuclear Survivin Has Reduced Stability and Is Not Cytoprotective. *J. Biol. Chem.* **283**: 3289–3296.
36. Dallaglio, K, Petrachi, T, Marconi, A, Truzzi, F, Lotti, R, Saltari, A, *et al.* (2014). Expression of nuclear survivin in normal skin and squamous cell carcinoma: a possible role in tumour invasion. *Br. J. Cancer* **110**: 199–207.
37. Dohi, T, Beltrami, E, Wall, NR, Plescia, J and Altieri, DC (2004). Mitochondrial survivin inhibits apoptosis and promotes tumorigenesis. *J. Clin. Invest.* **114**: 1117–1127.
38. Beltrami, E, Plescia, J, Wilkinson, JC, Duckett, CS and Altieri, DC (2004). Acute Ablation of Survivin Uncovers p53-dependent Mitotic Checkpoint Functions and Control of Mitochondrial Apoptosis. *J. Biol. Chem.* **279**: 2077–2084.
39. Li, F, Yang, J, Ramnath, N, Javle, MM and Tan, D (2005). Nuclear or cytoplasmic expression of survivin: What is the significance? *Int. J. Cancer J. Int. Cancer* **114**: 509–512.
40. Skoufias, DA, Mollinari, C, Lacroix, FB and Margolis, RL (2000). Human Survivin Is a Kinetochore-Associated Passenger Protein. *J. Cell Biol.* **151**: 1575–1582.
41. Wheatley, SP, Carvalho, A, Vagnarelli, P and Earnshaw, WC (2001). INCENP is required for proper targeting of Survivin to the centromeres and the anaphase spindle during mitosis. *Curr. Biol. CB* **11**: 886–890.
42. Bolton, MA, Lan, W, Powers, SE, McCleland, ML, Kuang, J and Stukenberg, PT (2002). Aurora B kinase exists in a complex with survivin and INCENP and its kinase activity is stimulated by survivin binding and phosphorylation. *Mol. Biol. Cell* **13**: 3064–3077.
43. Carvalho, A, Carmena, M, Sambade, C, Earnshaw, WC and Wheatley, SP (2003). Survivin is required for stable checkpoint activation in taxol-treated HeLa cells. *J. Cell Sci.* **116**: 2987–2998.
44. Kelly, AE, Ghenoiu, C, Xue, JZ, Zierhut, C, Kimura, H and Funabiki, H (2010). Survivin reads phosphorylated histone H3 threonine 3 to activate the mitotic kinase Aurora B. *Science* **330**: 235–239.
45. Niedzialkowska, E, Wang, F, Porebski, PJ, Minor, W, Higgins, JMG and Stukenberg, PT (2012). Molecular basis for phosphospecific recognition of

histone H3 tails by Survivin paralogues at inner centromeres. *Mol. Biol. Cell* **23**: 1457–1466.
46. Samejima, K, Platani, M, Wolny, M, Ogawa, H, Vargiu, G, Knight, PJ, *et al.* (2015). The Inner Centromere Protein (INCENP) Coil Is a Single α-Helix (SAH) Domain That Binds Directly to Microtubules and Is Important for Chromosome Passenger Complex (CPC) Localization and Function in Mitosis. *J. Biol. Chem.* **290**: 21460–21472.
47. Potapova, T and Gorbsky, GJ (2017). The Consequences of Chromosome Segregation Errors in Mitosis and Meiosis. *Biology* **6**.
48. Barnum, KJ and O'Connell, MJ (2014). Cell Cycle Regulation by Checkpoints. *Methods Mol. Biol. Clifton NJ* **1170**: 29–40.
49. Gojo, I, Zhang, B and Fenton, RG (2002). The Cyclin-dependent Kinase Inhibitor Flavopiridol Induces Apoptosis in Multiple Myeloma Cells through Transcriptional Repression and Down-Regulation of Mcl-1. *Clin. Cancer Res.* **8**: 3527–3538.
50. Elmore, S (2007). Apoptosis: A Review of Programmed Cell Death. *Toxicol. Pathol.* **35**: 495–516.
51. Li, F, Ackermann, EJ, Bennett, CF, Rothermel, AL, Plescia, J, Tognin, S, *et al.* (1999). Pleiotropic cell-division defects and apoptosis induced by interference with survivin function. *Nat. Cell Biol.* **1**: 461–466.
52. Guzman, JR, Fukuda, S and Pelus, LM (2009). Inhibition of caspase-3 by Survivin prevents Wee1 Kinase degradation and promotes cell survival by maintaining phosphorylation of p34Cdc2. *Gene Ther. Mol. Biol.* **13B**: 264–273.
53. Shin, S, Sung, BJ, Cho, YS, Kim, HJ, Ha, NC, Hwang, JI, *et al.* (2001). An anti-apoptotic protein human survivin is a direct inhibitor of caspase-3 and -7. *Biochemistry (Mosc.)* **40**: 1117–1123.
54. Banks, DP, Plescia, J, Altieri, DC, Chen, J, Rosenberg, SH, Zhang, H, *et al.* (2000). Survivin does not inhibit caspase-3 activity. *Blood* **96**: 4002–4003.
55. Li, J, Xing, M, Zhu, M, Wang, X, Wang, M, Zhou, S, *et al.* (2008). Glycogen synthase kinase 3β induces apoptosis in cancer cells through increase of survivin nuclear localization. *Cancer Lett.* **272**: 91–101.
56. Chandele, A, Prasad, V, Jagtap, JC, Shukla, R and Shastry, PR (2004). Upregulation of survivin in G2/M cells and inhibition of caspase 9 activity enhances resistance in staurosporine-induced apoptosis. *Neoplasia N. Y. N* **6**: 29–40.
57. Pavlyukov, MS, Antipova, NV, Balashova, MV, Vinogradova, TV, Kopantzev, EP and Shakhparonov, MI (2011). Survivin Monomer Plays an Essential Role in Apoptosis Regulation. *J. Biol. Chem.* **286**: 23296–23307.
58. Dohi, T, Okada, K, Xia, F, Wilford, CE, Samuel, T, Welsh, K, *et al.* (2004). An IAP-IAP Complex Inhibits Apoptosis. *J. Biol. Chem.* **279**: 34087–34090.
59. Liu, T, Brouha, B and Grossman, D (2004). Rapid induction of mitochondrial events and caspase-independent apoptosis in Survivin-targeted melanoma cells. *Oncogene* **23**: 39–48.
60. Paik, S, Shak, S, Tang, G, Kim, C, Baker, J, Cronin, M, *et al.* (2004). A multigene assay to predict recurrence of tamoxifen-treated, node-negative breast cancer. *N. Engl. J. Med.* **351**: 2817–2826.

61. Fukuda, S and Pelus, LM (2006). Survivin, a cancer target with an emerging role in normal adult tissues. *Mol. Cancer Ther.* **5**: 1087–1098.
62. Talbot, DC, Blackhall, FH, Kowalski, D, Ramlau, R, Bepler, G, Grossi, F, *et al.* (2013). A randomized open-label phase II study evaluating antitumor activity of the survivin antisense oligonucleotide LY2181308 (LY) in combination with docetaxel (DO) for second-line treatment of patients with non-small cell lung cancer (NSCLC) using change in tumor size (CTS). *J. Clin. Oncol.* **31**: 8051–8051.
63. Wiechno, PJ, Chlosta, P, Pikiel, J, Somer, BG, Mellado, B, Duran Martinez, I, *et al.* (2013). Randomized phase II study with window-design to evaluate anti-tumor activity of the survivin antisense oligonucleotide (ASO) ly2181308 in combination with docetaxel for first-line treatment of castrate-resistant prostate cancer (CRPC). *J. Clin. Oncol.* **31**: 5019–5019.
64. Clemens, MR, Gladkov, OA, Gartner, E, Vladimirov, V, Crown, J, Steinberg, J, *et al.* (2015). Phase II, multicenter, open-label, randomized study of YM155 plus docetaxel as first-line treatment in patients with HER2-negative metastatic breast cancer. *Breast Cancer Res. Treat.* **149**: 171–179.
65. Kudchadkar, R, Ernst, S, Chmielowski, B, Redman, BG, Steinberg, J, Keating, A, *et al.* A phase 2, multicenter, open-label study of sepantronium bromide (YM155) plus docetaxel in patients with stage III (unresectable) or stage IV melanoma. *Cancer Med.* **4**: 643–650.
66. Cortes, JE, Faderl, S, Pagel, J, Jung, CW, Yoon, S-S, Koh, Y, *et al.* (2015). Phase 1 study of CWP232291 in relapsed/refractory acute myeloid leukemia (AML) and myelodysplastic syndrome (MDS). *J. Clin. Oncol.* **33**: 7044–7044.
67. Ellebaek, E, Iversen, TZ, Junker, N, Donia, M, Engell-Noerregaard, L, Met, Ö, *et al.* (2012). Adoptive cell therapy with autologous tumor infiltrating lymphocytes and low-dose Interleukin-2 in metastatic melanoma patients. *J. Transl. Med.* **10**: 169.
68. Mehrotra, S, Britten, CD, Chin, SH, Salem, ML, Cloud, C, Nelson, MH, *et al.* (2016). A feasibility and safety study of vaccination with Poly-ICLC and peptide-pulsed dendritic cells in patients with advanced pancreatic adenocarcinoma. *J. Clin. Oncol.* **34**: e14579–e14579.
69. Svane, IM, Pedersen, AE, Johnsen, HE, Nielsen, D, Kamby, C, Gaarsdal, E, *et al.* (2004). Vaccination with p53-peptide-pulsed dendritic cells, of patients with advanced breast cancer: report from a phase I study. *Cancer Immunol. Immunother. CII* **53**: 633–641.
70. Fenstermaker, RA, Ciesielski, MJ, Qiu, J, Yang, N, Frank, CL, Lee, KP, *et al.* (2016). Clinical study of a survivin long peptide vaccine (SurVaxM) in patients with recurrent malignant glioma. *Cancer Immunol. Immunother.* **65**: 1339–1352.
71. Rapoport, AP, Aqui, NA, Stadtmauer, EA, Vogl, DT, Fang, H-B, Cai, L, *et al.* (2011). Combination immunotherapy using adoptive T-cell transfer and tumor antigen vaccination on the basis of hTERT and survivin after ASCT for myeloma. *Blood* **117**: 788–797.
72. Villella, JA, Wilson, MK, Berinstein, NL, Karkada, M, Quinton, T, Butler, MO, *et al.* (2016). Determination of optimal dose and treatment schedule of the immunotherapeutic vaccine, DPX-Survivac, for combination immunotherapy

treatment of ovarian, fallopian tube or peritoneal cancer (OC): A phase Ib study. *J. Clin. Oncol.* **34**: e14577–e14577.
73. Gravina, G, Wasén, C, Garcia-Bonete, MJ, Turkkila, M, Erlandsson, MC, Töyrä Silfverswärd, S, *et al.* (2017). Survivin in autoimmune diseases. *Autoimmun. Rev.* **16**: 845–855.
74. de Souza, HSP, West, GA, Rebert, N, de la Motte, C, Drazba, J and Fiocchi, C (2012). Increased Levels of Survivin, via Association With Heat Shock Protein 90, in Mucosal T Cells From Patients With Crohn's Disease. *Gastroenterology* **143**: 1017-1026.e9.
75. Chun-Lai, T, Murad, S, Erlandsson, MC, Hussein, H, Sulaiman, W, Dhaliwal, JS, *et al.* (2015). Recognizing rheumatoid arthritis: oncoprotein survivin opens new possibilities: a population-based case-control study. *Medicine (Baltimore)* **94**: e468.
76. Jenko, B, Praprotnik, S, Čučnik, S, Rotar, Ž, Tomšič, M and Dolžan, V (2015). Survivin polymorphism is associated with disease activity in rheumatoid arthritis patients. *Pharmacogenomics* **17**: 45–9.
77. Marković, D, Jevtović-Stoimenov, T, Ćosić, V, Stošić, B, Dinić, V, Marković-Živković, B, *et al.* (2018). Clinical Utility of Survivin (BIRC5), Novel Cardiac Biomarker, as a Prognostic Tool Compared to High-Sensitivity C-Reactive Protein, Heart-Type Fatty Acid Binding Protein and Revised Lee Score in Elderly Patients Scheduled for Major Non-Cardiac Surgery: A Prospective Pilot Study. *J. Med. Biochem.* **37**: 110–120.
78. Assaf, HA, Abdel-Maged, WM, Elsadek, BEM, Hassan, MH, Adly, MA and Ali, SA (2016). Survivin as a Novel Biomarker in the Pathogenesis of Acne Vulgaris and Its Correlation to Insulin-Like Growth Factor-I. *Dis. Markers*doi:10.1155/2016/7040312.
79. Ju, L, Zhang, X, Deng, Y, Han, J, Yang, J, Chen, S, *et al.* (2017). Enhanced expression of Survivin has distinct roles in adipocyte homeostasis. *Cell Death Dis.* **8**: e2533.
80. Bossios, A, Ekerljung, L, Turkkila, M, Malmhäll, C, Erlandsson, M, Silfverswärd, ST, *et al.* (2015). Survivin in patients with chronic obstructive pulmonary disease. *Eur. Respir. J.* **46**: PA3347.
81. AbouAlaiwi, WA, Muntean, BS, Ratnam, S, Joe, B, Liu, L, Booth, RL, *et al.* (2014). Survivin-Induced Abnormal Ploidy Contributes to Cystic Kidney and Aneurysm Formation. *Circulation* **129**: 660–672.
82. Stefano, JT, Oliveira, C, Corrêa-Giannella, ML, C Soares, I, Kubrusly, M, Bellodi-Privato, M, *et al.* (2011). Decreased immunoexpression of survivin could be a potential marker in human non-alcoholic fatty liver disease progression? *Liver Int. Off. J. Int. Assoc. Study Liver* **31**: 377–85.
83. Lilienbaum, A (2013). Relationship between the proteasomal system and autophagy. *Int. J. Biochem. Mol. Biol.* **4**: 1–26.
84. Klionsky, DJ (2008). Autophagy revisited: A conversation with Christian de Duve. *Autophagy* **4**: 740–743.
85. Mizushima, N, Yamamoto, A, Matsui, M, Yoshimori, T and Ohsumi, Y (2004). In Vivo Analysis of Autophagy in Response to Nutrient Starvation Using Transgenic Mice Expressing a Fluorescent Autophagosome Marker. *Mol. Biol. Cell* **15**: 1101–1111.

86. Maiuri, MC, Zalckvar, E, Kimchi, A and Kroemer, G (2007). Self-eating and self-killing: crosstalk between autophagy and apoptosis. *Nat. Rev. Mol. Cell Biol.* **8**: 741–752.
87. Eskelinen, E-L, Prescott, AR, Cooper, J, Brachmann, SM, Wang, L, Tang, X, *et al.* (2002). Inhibition of autophagy in mitotic animal cells. *Traffic Cph. Den.* **3**: 878–893.
88. Furuya, T, Kim, M, Lipinski, M, Li, J, Kim, D, Lu, T, *et al.* (2010). Negative regulation of Vps34 by Cdk mediated phosphorylation. *Mol. Cell* **38**: 500–511.
89. Mijaljica, D, Prescott, M and Devenish, RJ (2011). Microautophagy in mammalian cells: revisiting a 40-year-old conundrum. *Autophagy* **7**: 673–682.
90. Massey, A, Kiffin, R and Cuervo, AM (2004). Pathophysiology of chaperone-mediated autophagy. *Int. J. Biochem. Cell Biol.* **36**: 2420–2434.
91. Kang, R, Zeh, HJ, Lotze, MT and Tang, D (2011). The Beclin 1 network regulates autophagy and apoptosis. *Cell Death Differ.* **18**: 571–580.
92. Liang, XH, Jackson, S, Seaman, M, Brown, K, Kempkes, B, Hibshoosh, H, *et al.* (1999). Induction of autophagy and inhibition of tumorigenesis by beclin 1. *Nature* **402**: 672–676.
93. Russell, RC, Tian, Y, Yuan, H, Park, HW, Chang, Y-Y, Kim, J, *et al.* (2013). ULK1 induces autophagy by phosphorylating Beclin-1 and activating Vps34 lipid kinase. *Nat. Cell Biol.* **15**.
94. Cebollero, E, van der Vaart, A, Zhao, M, Rieter, E, Klionsky, DJ, Helms, JB, *et al.* (2012). Phosphatidylinositol-3-Phosphate Clearance Plays a Key Role in Autophagosome Completion. *Curr. Biol.* **22**: 1545–1553.
95. Tooze, SA and Yoshimori, T (2010). The origin of the autophagosomal membrane. *Nat. Cell Biol.* **12**: 831–835.
96. Mizushima, N, Noda, T, Yoshimori, T, Tanaka, Y, Ishii, T, George, MD, *et al.* (1998). A protein conjugation system essential for autophagy. *Nature* **395**: 395–398.
97. Fujita, N, Itoh, T, Omori, H, Fukuda, M, Noda, T and Yoshimori, T (2008). The Atg16L complex specifies the site of LC3 lipidation for membrane biogenesis in autophagy. *Mol. Biol. Cell* **19**: 2092–2100.
98. Pankiv, S, Clausen, TH, Lamark, T, Brech, A, Bruun, J-A, Outzen, H, *et al.* (2007). p62/SQSTM1 binds directly to Atg8/LC3 to facilitate degradation of ubiquitinated protein aggregates by autophagy. *J. Biol. Chem.* **282**: 24131–24145.
99. Wong, YC and Holzbaur, ELF (2014). Optineurin is an autophagy receptor for damaged mitochondria in parkin-mediated mitophagy that is disrupted by an ALS-linked mutation. *Proc. Natl. Acad. Sci. U. S. A.* **111**: E4439-4448.
100. Razi, M, Chan, EYW and Tooze, SA (2009). Early endosomes and endosomal coatomer are required for autophagy. *J. Cell Biol.* **185**: 305–321.
101. Klionsky, DJ, Eskelinen, E-L and Deretic, V (2014). Autophagosomes, phagosomes, autolysosomes, phagolysosomes, autophagolysosomes… Wait, I'm confused. *Autophagy* **10**: 549–551.
102. Rong, Y, McPhee, CK, McPhee, C, Deng, S, Huang, L, Chen, L, *et al.* (2011). Spinster is required for autophagic lysosome reformation and mTOR reactivation following starvation. *Proc. Natl. Acad. Sci. U. S. A.* **108**: 7826–7831.

103. Monastyrska, I, Rieter, E, Klionsky, DJ and Reggiori, F (2009). Multiple roles of the cytoskeleton in autophagy. *Biol. Rev.* **84**: 431–448.
104. Wijdeven, RH, Janssen, H, Nahidiazar, L, Janssen, L, Jalink, K, Berlin, I, *et al.* (2016). Cholesterol and ORP1L-mediated ER contact sites control autophagosome transport and fusion with the endocytic pathway. *Nat. Commun.* **7**: 11808.
105. Pankiv, S, Alemu, EA, Brech, A, Bruun, J-A, Lamark, T, Øvervatn, A, *et al.* (2010). FYCO1 is a Rab7 effector that binds to LC3 and PI3P to mediate microtubule plus end–directed vesicle transport. *J. Cell Biol.* **188**: 253–269.
106. Korolchuk, VI, Saiki, S, Lichtenberg, M, Siddiqi, FH, Roberts, EA, Imarisio, S, *et al.* (2011). Lysosomal positioning coordinates cellular nutrient responses. *Nat. Cell Biol.* **13**: 453–460.
107. Jiang, P, Nishimura, T, Sakamaki, Y, Itakura, E, Hatta, T, Natsume, T, *et al.* (2014). The HOPS complex mediates autophagosome-lysosome fusion through interaction with syntaxin 17. *Mol. Biol. Cell* **25**: 1327–1337.
108. Tian, Y, Li, Z, Hu, W, Ren, H, Tian, E, Zhao, Y, *et al.* (2010). C. elegans Screen Identifies Autophagy Genes Specific to Multicellular Organisms. *Cell* **141**: 1042–1055.
109. Zhen, Y and Li, W (2015). Impairment of autophagosome-lysosome fusion in the buff mutant mice with the VPS33A(D251E) mutation. *Autophagy* **11**: 1608–1622.
110. Liu, N-A, Sun, J, Kono, K, Horikoshi, Y, Ikura, T, Tong, X, *et al.* (2015). Regulation of homologous recombinational repair by lamin B1 in radiation-induced DNA damage. *FASEB J. Off. Publ. Fed. Am. Soc. Exp. Biol.* **29**: 2514–2525.
111. Furuta, N and Amano, A (2012). SNARE mediates autophagosome–lysosome fusion. *J. Oral Biosci.* **54**: 83–85.
112. Shen, H-M and Mizushima, N (2014). At the end of the autophagic road: an emerging understanding of lysosomal functions in autophagy. *Trends Biochem. Sci.* **39**: 61–71.
113. Jahreiss, L, Menzies, FM and Rubinsztein, DC (2008). The Itinerary of Autophagosomes: From Peripheral Formation to Kiss-and-Run Fusion with Lysosomes. *Traffic Cph. Den.* **9**: 574–587.
114. Levine, B and Kroemer, G (2008). Autophagy in the Pathogenesis of Disease. *Cell* **132**: 27–42.
115. Wong, ASL, Cheung, ZH and Ip, NY (2011). Molecular machinery of macroautophagy and its deregulation in diseases. *Biochim. Biophys. Acta BBA - Mol. Basis Dis.* **1812**: 1490–1497.
116. Nixon, RA, Wegiel, J, Kumar, A, Yu, WH, Peterhoff, C, Cataldo, A, *et al.* (2005). Extensive involvement of autophagy in Alzheimer disease: an immuno-electron microscopy study. *J. Neuropathol. Exp. Neurol.* **64**: 113–122.
117. Pickford, F, Masliah, E, Britschgi, M, Lucin, K, Narasimhan, R, Jaeger, PA, *et al.* (2008). The autophagy-related protein beclin 1 shows reduced expression in early Alzheimer disease and regulates amyloid β accumulation in mice. *J. Clin. Invest.* **118**: 2190–2199.
118. Luciani, A, Villella, VR, Esposito, S, Brunetti-Pierri, N, Medina, D, Settembre, C, *et al.* (2010). Defective CFTR induces aggresome formation and

lung inflammation in cystic fibrosis through ROS-mediated autophagy inhibition. *Nat. Cell Biol.* **12**: 863–875.
119. Travassos, LH, Carneiro, LAM, Ramjeet, M, Hussey, S, Kim, Y-G, Magalhães, JG, *et al.* (2010). Nod1 and Nod2 direct autophagy by recruiting ATG16L1 to the plasma membrane at the site of bacterial entry. *Nat. Immunol.* **11**: 55–62.
120. Su, M, Mei, Y and Sinha, S (2013). Role of the Crosstalk between Autophagy and Apoptosis in Cancer. *J. Oncol.* **2013**.
121. Aita, VM, Liang, XH, Murty, VVVS, Pincus, DL, Yu, W, Cayanis, E, *et al.* (1999). Cloning and Genomic Organization of Beclin 1, a Candidate Tumor Suppressor Gene on Chromosome 17q21. *Genomics* **59**: 59–65.
122. Tsukada, M and Ohsumi, Y (1993). Isolation and characterization of autophagy-defective mutants of Saccharomyces cerevisiae. *FEBS Lett.* **333**: 169–174.
123. Kirisako, T, Baba, M, Ishihara, N, Miyazawa, K, Ohsumi, M, Yoshimori, T, *et al.* (1999). Formation Process of Autophagosome Is Traced with Apg8/Aut7p in Yeast. *J. Cell Biol.* **147**: 435–446.
124. Mann, SS and Hammarback, JA (1994). Molecular characterization of light chain 3. A microtubule binding subunit of MAP1A and MAP1B. *J. Biol. Chem.* **269**: 11492–11497.
125. Kabeya, Y, Mizushima, N, Ueno, T, Yamamoto, A, Kirisako, T, Noda, T, *et al.* (2000). LC3, a mammalian homologue of yeast Apg8p, is localized in autophagosome membranes after processing. *EMBO J.* **19**: 5720–5728.
126. Schoenfeld, TA, McKerracher, L, Obar, R and Vallee, RB (1989). MAP 1A and MAP 1B are structurally related microtubule associated proteins with distinct developmental patterns in the CNS. *J. Neurosci. Off. J. Soc. Neurosci.* **9**: 1712–1730.
127. Feng, Y, Yao, Z and Klionsky, DJ (2015). How to control self-digestion: transcriptional, post-transcriptional, and post-translational regulation of autophagy. *Trends Cell Biol.* **25**: 354–363.
128. Behrends, C, Sowa, ME, Gygi, SP and Harper, JW (2010). Network organization of the human autophagy system. *Nature* **466**: 68–76.
129. Tanida, I, Ueno, T and Kominami, E (2004). LC3 conjugation system in mammalian autophagy. *Int. J. Biochem. Cell Biol.* **36**: 2503–2518.
130. He, H, Dang, Y, Dai, F, Guo, Z, Wu, J, She, X, *et al.* (2003). Post-translational Modifications of Three Members of the Human MAP1LC3 Family and Detection of a Novel Type of Modification for MAP1LC3B. *J. Biol. Chem.* **278**: 29278–29287.
131. Wu, J, Dang, Y, Su, W, Liu, C, Ma, H, Shan, Y, *et al.* (2006). Molecular cloning and characterization of rat LC3A and LC3B--two novel markers of autophagosome. *Biochem. Biophys. Res. Commun.* **339**: 437–442.
132. Sou, Y, Waguri, S, Iwata, J, Ueno, T, Fujimura, T, Hara, T, *et al.* (2008). The Atg8 conjugation system is indispensable for proper development of autophagic isolation membranes in mice. *Mol. Biol. Cell* **19**: 4762–4775.
133. Nguyen, TN, Padman, BS, Usher, J, Oorschot, V, Ramm, G and Lazarou, M (2016). Atg8 family LC3/GABARAP proteins are crucial for autophagosome-lysosome fusion but not autophagosome formation during PINK1/Parkin mitophagy and starvation. *J. Cell Biol.* **215**: 857–874.

134. Klionsky, DJ and Schulman, BA (2014). Dynamic regulation of macroautophagy by distinctive ubiquitin-like proteins. *Nat. Struct. Mol. Biol.* **21**: 336–345.
135. Noda, NN, Ohsumi, Y and Inagaki, F (2010). Atg8-family interacting motif crucial for selective autophagy. *FEBS Lett.* **584**: 1379–1385.
136. Kouno, T, Mizuguchi, M, Tanida, I, Ueno, T, Kanematsu, T, Mori, Y, *et al.* (2005). Solution Structure of Microtubule-associated Protein Light Chain 3 and Identification of Its Functional Subdomains. *J. Biol. Chem.* **280**: 24610–24617.
137. Faller, EM, Villeneuve, TS and Brown, DL (2009). MAP1a associated light chain 3 increases microtubule stability by suppressing microtubule dynamics. *Mol. Cell. Neurosci.* **41**: 85–93.
138. Heckmann, BL, Boada-Romero, E, Cunha, LD, Magne, J and Green, DR (2017). LC3-Associated Phagocytosis and Inflammation. *J. Mol. Biol.* **429**: 3561–3576.
139. de Haan, CAM, Molinari, M and Reggiori, F (2010). Autophagy-independent LC3 function in vesicular traffic. *Autophagy* **6**: 994–996.
140. Yoshioka, A, Miyata, H, Doki, Y, Yamasaki, M, Sohma, I, Gotoh, K, *et al.* (2008). LC3, an autophagosome marker, is highly expressed in gastrointestinal cancers. *Int. J. Oncol.* **33**: 461–468.
141. Tang, J-Y, Hsi, E, Huang, Y-C, Hsu, NC-H, Chu, P-Y and Chai, C-Y (2013). High LC3 expression correlates with poor survival in patients with oral squamous cell carcinoma. *Hum. Pathol.* **44**: 2558–2562.
142. Jiang, Z-F, Shao, L-J, Wang, W-M, Yan, X-B and Liu, R-Y (2012). Decreased expression of Beclin-1 and LC3 in human lung cancer. *Mol. Biol. Rep.* **39**: 259–267.
143. Wang, L, Chen, M, Yang, J and Zhang, Z (2013). LC3 fluorescent puncta in autophagosomes or in protein aggregates can be distinguished by FRAP analysis in living cells. *Autophagy* **9**: 756–769.
144. Deng, Q, Wang, Z, Wang, L, Zhang, L, Xiang, X, Wang, Z, *et al.* (2013). Lower mRNA and protein expression levels of LC3 and Beclin1, markers of autophagy, were correlated with progression of renal clear cell carcinoma. *Jpn. J. Clin. Oncol.* **43**: 1261–1268.
145. Liang, XH, Kleeman, LK, Jiang, HH, Gordon, G, Goldman, JE, Berry, G, *et al.* (1998). Protection against fatal Sindbis virus encephalitis by beclin, a novel Bcl-2-interacting protein. *J. Virol.* **72**: 8586–8596.
146. Rubinstein, AD, Eisenstein, M, Ber, Y, Bialik, S and Kimchi, A (2011). The Autophagy Protein Atg12 Associates with Antiapoptotic Bcl-2 Family Members to Promote Mitochondrial Apoptosis. *Mol. Cell* **44**: 698–709.
147. Tasdemir, E, Maiuri, MC, Galluzzi, L, Vitale, I, Djavaheri-Mergny, M, D'Amelio, M, *et al.* (2008). Regulation of autophagy by cytoplasmic p53. *Nat. Cell Biol.* **10**: 676–687.
148. Wang, Q, Wu, PC, Roberson, RS, Luk, BV, Ivanova, I, Chu, E, *et al.* (2011). Survivin and escaping in therapy-induced cellular senescence. *Int. J. Cancer* **128**: 1546–1558.
149. Wang, J, Pan, X-L, Ding, L-J, Liu, D-Y, Da-Peng Lei, null and Jin, T (2013). Aberrant expression of Beclin-1 and LC3 correlates with poor prognosis of human hypopharyngeal squamous cell carcinoma. *PloS One* **8**: e69038.

150. Simon, H-U and Friis, R (2014). ATG5: a distinct role in the nucleus. *Autophagy* **10**: 176–177.
151. Keerthivasan, G, Liu, H, Gump, JM, Dowdy, SF, Wickrema, A and Crispino, JD (2012). A novel role for survivin in erythroblast enucleation. *Haematologica* **97**: 1471–1479.
152. Zhao, P, Meng, Q, Liu, L-Z, You, Y-P, Liu, N and Jiang, B-H (2010). Regulation of survivin by PI3K/Akt/p70S6K1 pathway. *Biochem. Biophys. Res. Commun.* **395**: 219–224.
153. Bar-Peled, L, Schweitzer, LD, Zoncu, R and Sabatini, DM (2012). Ragulator Is a GEF for the Rag GTPases that Signal Amino Acid Levels to mTORC1. *Cell* **150**: 1196–1208.
154. Sancak, Y, Bar-Peled, L, Zoncu, R, Markhard, AL, Nada, S and Sabatini, DM (2010). Ragulator-Rag complex targets mTORC1 to the lysosomal surface and is necessary for its activation by amino acids. *Cell* **141**: 290–303.
155. Rong, Y, Liu, M, Ma, L, Du, W, Zhang, H, Tian, Y, *et al.* (2012). Clathrin and phosphatidylinositol-4,5-bisphosphate regulate autophagic lysosome reformation. *Nat. Cell Biol.* **14**: 924–934.
156. Braulke, T and Bonifacino, JS (2009). Sorting of lysosomal proteins. *Biochim. Biophys. Acta BBA - Mol. Cell Res.* **1793**: 605–614.
157. Sharifi, MN, Mowers, EE, Drake, LE, Collier, C, Chen, H, Zamora, M, *et al.* (2016). Autophagy promotes focal adhesion disassembly and cell motility of metastatic tumor cells through the direct interaction of paxillin with LC3. *Cell Rep.* **15**: 1660–1672.
158. Chu, X-Y, Chen, L-B, Wang, J-H, Su, Q-S, Yang, J-R, Lin, Y, *et al.* (2012). Overexpression of survivin is correlated with increased invasion and metastasis of colorectal cancer. *J. Surg. Oncol.* **105**: 520–528.
159. NCBI:BLASTat <https://blast.ncbi.nlm.nih.gov/Blast.cgi?PROGRAM=blastn&PAGE_TYPE=BlastSearch&LINK_LOC=blasthome>.
160. Schneider, CA, Rasband, WS and Eliceiri, KW (2012). NIH Image to ImageJ: 25 years of image analysis. *Nat. Methods* **9**: 671–675.
161. *FASTA*, EMBL:EBIat <https://www.ebi.ac.uk/Tools/sss/fasta/>.
162. Schneider, TD and Stephens, RM (1990). Sequence logos: a new way to display consensus sequences. *Nucleic Acids Res.* **18**: 6097–6100.
163. ClustalW2at <https://www.ebi.ac.uk/Tools/msa/clustalw2/>.
164. WebLogoat <https://weblogo.berkeley.edu/logo.cgi>.
165. Kuma, A, Matsui, M and Mizushima, N (2007). LC3, an autophagosome marker, can be incorporated into protein aggregates independent of autophagy: caution in the interpretation of LC3 localization. *Autophagy* **3**: 323–328.
166. Gordon, P (1988). Prelysosomal convergence of autophagic and endocytic pathwaysat <https://www.ncbi.nlm.nih.gov/pubmed/3126737/>.
167. Ambrose, M, Goldstine, JV and Gatti, RA (2007). Intrinsic mitochondrial dysfunction in ATM-deficient lymphoblastoid cells. *Hum. Mol. Genet.* **16**: 2154–2164.
168. Li, M, Khambu, B, Zhang, H, Kang, J-H, Chen, X, Chen, D, *et al.* (2013). Suppression of Lysosome Function Induces Autophagy via a Feedback Down-

regulation of MTOR Complex 1 (MTORC1) Activity. *J. Biol. Chem.* **288**: 35769–35780.
169. Miyazawa, MR, Melatto, AR, Silene, M and Nobuko, Y (2011). Starvation and rapamycin differentially regulate host cell lysosome exocytosis and invasion by Trypanosoma cruzi metacyclic forms. *Cell. Microbiol.* **13**: 943–954.
170. Wong, P-M, Feng, Y, Wang, J, Shi, R and Jiang, X (2015). Regulation of autophagy by coordinated action of mTORC1 and protein phosphatase 2A. *Nat. Commun.* **6**: 8048.
171. Moore, N and Lyle, S (2010). Quiescent, Slow-Cycling Stem Cell Populations in Cancer: A Review of the Evidence and Discussion of Significance. *J. Oncol.* **2011**: e396076.
172. Altieri, DC (2008). Survivin, cancer networks and pathway-directed drug discovery. *Nat. Rev. Cancer* **8**: 61–70.
173. Lens, SMA, Wolthuis, RMF, Klompmaker, R, Kauw, J, Agami, R, Brummelkamp, T, *et al.* (2003). Survivin is required for a sustained spindle checkpoint arrest in response to lack of tension. *EMBO J.* **22**: 2934–2947.
174. Wheatley, SP and McNeish, IA (2005). Survivin: a protein with dual roles in mitosis and apoptosis. *Int. Rev. Cytol.* **247**: 35–88.
175. Chakravarti, A, Zhai, GG, Zhang, M, Malhotra, R, Latham, DE, Delaney, MA, *et al.* (2004). Survivin enhances radiation resistance in primary human glioblastoma cells via caspase-independent mechanisms. *Oncogene* **23**: 7494–7506.
176. Nam, HY, Han, MW, Chang, HW, Lee, YS, Lee, M, Lee, HJ, *et al.* (2013). Radioresistant cancer cells can be conditioned to enter senescence by mTOR inhibition. *Cancer Res.* **73**: 4267–4277.
177. Maskey, D, Yousefi, S, Schmid, I, Zlobec, I, Perren, A, Friis, R, *et al.* (2013). ATG5 is induced by DNA-damaging agents and promotes mitotic catastrophe independent of autophagy. *Nat. Commun.* **4**: 2130.
178. Dou, Z, Xu, C, Donahue, G, Shimi, T, Pan, J-A, Zhu, J, *et al.* (2015). Autophagy mediates degradation of nuclear lamina. *Nature* **527**: 105–109.
179. Kelley, JB, Datta, S, Snow, CJ, Chatterjee, M, Ni, L, Spencer, A, *et al.* (2011). The Defective Nuclear Lamina in Hutchinson-Gilford Progeria Syndrome Disrupts the Nucleocytoplasmic Ran Gradient and Inhibits Nuclear Localization of Ubc9. *Mol. Cell. Biol.* **31**: 3378–3395.
180. Wang, Q, Chen, Z, Diao, X and Huang, S (2011). Induction of autophagy-dependent apoptosis by the survivin suppressant YM155 in prostate cancer cells. *Cancer Lett.* **302**: 29–36.
181. Wang, Y-F, Zhang, W, He, K-F, Liu, B, Zhang, L, Zhang, W-F, *et al.* (2013). Induction of autophagy-dependent cell death by the survivin suppressant YM155 in salivary adenoid cystic carcinoma. *Apoptosis Int. J. Program. Cell Death*doi:10.1007/s10495-013-0960-1.
182. Zhang, X, Chen, S, Huang, K and Le, W (2013). Why should autophagic flux be assessed? *Acta Pharmacol. Sin.* **34**: 595–599.
183. Alberts, B, Bray, D, Lewis, J, Raff, M and Roberts, K (1994). *Molecular Biology of the Cell.*, New York: Garland Publishing.
184. Mizushima, N, Ohsumi, Y and Yoshimori, T (2002). Autophagosome formation in mammalian cells. *Cell Struct. Funct.* **27**: 421–429.

185. Kalvari, I, Tsompanis, S, Mulakkal, NC, Osgood, R, Johansen, T, Nezis, IP, *et al.* (2014). iLIR: A web resource for prediction of Atg8-family interacting proteins. *Autophagy* **10**: 913–925.
186. Chen, W, Dong, J, Haiech, J, Kilhoffer, M-C and Zeniou, M (2016). Cancer Stem Cell Quiescence and Plasticity as Major Challenges in Cancer Therapy. *Stem Cells Int.* **2016**.
187. Siddharth, S, Das, S, Nayak, A and Kundu, CN (2016). SURVIVIN as a marker for quiescent-breast cancer stem cells-An intermediate, adherent, pre-requisite phase of breast cancer metastasis. *Clin. Exp. Metastasis* **33**: 661–675.
188. Xie, X, Hu, H, Tong, X, Li, L, Liu, X, Chen, M, *et al.* (2018). The mTOR–S6K pathway links growth signalling to DNA damage response by targeting RNF168. *Nat. Cell Biol.* **20**: 320–331.
189. Li, Z, Ji, X, Wang, D, Liu, J and Zhang, X (2016). Autophagic flux is highly active in early mitosis and differentially regulated throughout the cell cycle. *Oncotarget* **7**: 39705–39718.

APPENDIX

CLONING PRIMERS

Desired construct	Primer nucleotide sequence
survivin^{F61A,L64A}	Forward: CTTCTGCGCCAAGGAGGCGCAAGGCTGGG Reverse: CCCAGCCTTCCGCCTCCTTGGCGCAGAAG
survivin^{F61A,L64A}GFP	Forward: TTTCTTCTGCGCCAAGGAGGCGG Reverse: CACTGGGCCAAGTCTGGC
survivin^{F61A,L64A}RFP	Forward: TTTCTTCTGCGCCAAGGAGGCGG Reverse: CACTGGGCCAAGTCTGGC
flag-survivin^{F61A,L64A}	Forward: TTTCTTCTGCGCCAAGGAGGCGG Reverse: CACTGGGCCAAGTCTGGC

BUFFERS AND SOLUTIONS.

Reagent	Components
Fixation solution	4% formaldehyde in PBS
Triton X-100 solution	0.15% Triton X-100 in PBS.
Blocking solution	1% BSA in PBS
Laemmli running buffer	25 mM Trizma, 192 mM Glycine, 0.1% SDS
Towbin transfer buffer	24 mM Trizma, 195 mM Glycine, 0.5% SDS, 10% methanol
RIPA lysis buffer	200 nM tris-HCl pH 8.0, 137 mM NaCl, 0.5 mM EDTA, 10% Glycerol, 1% CA-630 (NP-40), 0.1% SDS, 1% Sodium deoxycholate, 1 µg/ml CLAP (chymostatin, leupeptin, antipain and pepstatin A), 2 mM β-glycerophosphate, 100 µM AEBSF

Anti-Flag M2 lysis buffer	50 mM tris-HCl pH 7.4, 150 mM NaCl, 1 mM EDTA, 1% Triton x-100, 1 µg/ml CLAP (chymostatin, leupeptin, antipain and pepstatin A), 100 µM AEBSF
GFP-Trap lysis buffer	10 mM tris-HCl pH 7.5, 150 mM NaCl, 0.5 mM EDTA, 0.5% CA-630 (NP-40), 1 µg/ml CLAP (chymostatin, leupeptin, antipain and pepstatin A), 1mM PMSF
Methylene blue dye	1% methylene blue (w/v) in ethanol.
Tris-Buffered Saline (TBS)	50 mM tris-HCl pH 7.4, 150 mM NaCl
SDS sample buffer	250 mM tris pH 6.8, 10% SDS, 50% glycerol, 0.5% bromophenol blue, 500mM β-mercaptoethanol
Anti-flag M2 sample buffer.	125 mM tris-HCl pH 6.8, 4% SDS, 20% glycerol, 0.004% bromophenol blue.
GFP Trap sample buffer	120 mM tris-HCl pH 6.8, 20% glycerol, 4% SDS, 0.04% bromophenol blue, 10% β-mercaptoethanol
GFP Trap dilution buffer	10 mM tris-HCl pH 7.5, 150 mM NaCl, 0.5 mM EDTA
Agarose gel	0.8% (w/v) agarose in TAE buffer, 1:10,000 SYBR Safe DNA stain.
TAE buffer	40 mM tris-acetate, 1 mM EDTA

ANTIBIOTIC CONCENTRATIONS

Antibiotic	Working concentration
Geneticin (G418)	500 µg/ml
Ampicillin	100 µg/ml
Kanamycin	30 µg/ml

METHODOLOGIES

DNA purification.

The Qiagen QIAPrep Miniprep kit used to purify plasmid DNA from bacteria during this research relied on the principle that denatured proteins and genomic dna will precipitate in acidic potassium acetate, and that plasmid DNA will precipitate in ethanol.

Buffer P1 is used to resuspend the bacterial cell pellet and supplies RNase. Buffer P2 contains SDS detergent to solubilise the bacterial cell membrane leading to lysis, and sodium hydroxide to temporarily denature proteins and DNA. During this step, RNase A digests cellular RNA. Buffer N3 contains acidic potassium acetate and causes the cell debris to become trapped in salt-detergent complexes and precipitate. Plasmid DNA is smaller and will renature in these conditions, remaining in solution. After removing the precipitate by centrifugation, the cell lysate supernatant is applied to the Qiagen QIAfilter; designed to bind plasmid DNA, while allowing cell debris to flow through. The filter is then washed with PE buffer which contains ethanol to precipitate the plasmid DNA, ensuring that it is retained on the filter during this wash step. Sterile distilled water can then be used to resuspend the plasmid DNA, allowing it to pass through the filter.

Polymerase Chain Reaction (PCR)

This technique uses the principle that polymerase will bind to single stranded DNA in the presence of a primer and free nucleotides and generate the complementary strand of DNA. Repeated cycles of heating and cooling allow the exponential amplification of a specific region of DNA by a thermostable polymerase. PCR primers are single stranded fragments of DNA complementary to the termini of a DNA region of interest. They can be designed with 5' overhangs to allow the introduction of new nucleotides, for example to enable subsequent restriction digestion of the amplified DNA sequence.

Site-directed mutagenesis

For mutagenesis of plasmid DNA, primers are designed to be complementary to a sequence of DNA spanning the target site, with mismatch nucleotides to modify the codon for a single amino acid residue. Primers can be designed to be overlapping; forward and reverse primers are designed to ensure that both sense and anti-sense DNA strands are amplified to include the mutation. Another approach is to design primers to sit 'back-to-back'; the forward primer includes the required mutation and the reverse primer is designed to sit 'back-to-back' with it on the antisense DNA strand. This means the resulting PCR reaction performs exponential amplification, rather than linear amplification as performed by overlapping primers. However, kinase is required in this second approach to anneal the ends of the double-stranded DNA product and re-create a circular plasmid prior to transformation.

Generation of stable cell lines

A cell line stably expressing a protein of interest can be generated by maintaining selection pressure on a transiently transfected cell. Stable cell lines have the advantage of consisting almost entirely of cells expressing the protein where transient plasmid transfection more commonly results in 30-50% of cells expressing the protein. In addition, stable cell lines expressing fluorescent proteins can be sorted by the fluorescence of each individual cell using a specialised cell sorter, resulting in sub-lines with high, medium or low levels of fluorescence. Finally, transient transfection can induce a level of stress in the cell resulting from the introduction of foreign material from which the stable cell line has recovered.

Bradford protein assay

Total protein concentration of cell lysate can be assessed using the Bradford protein assay invented by Marion Bradford in 1976. The principle of the assay takes advantage of a change in Coomassie Brilliant Blue G-250 dye from red to blue when it binds to protein in acidic conditions. The increase in absorbance

of the dye at 595 nm is proportional to the amount of bound dye and therefore to the concentration of protein in the sample.

SDS Polyacrylamide gel electrophoresis

Sodium dodecyl sulphate polyacrylamide gel electrophoresis (SDS-PAGE) is an experimental technique used to separate proteins by size. The principle of this technique is that proteins are unfolded and given a negative charge proportional to their size allowing them to be drawn through a gel at a rate dependent on their molecular weight.

Cell lysates are prepared by boiling in sample buffer containing the detergent SDS which denatures the proteins, reducing them to their linear peptide sequences. Sample buffer may also contain a reducing agent such as β-mercaptoethanol to remove di-sulphide bonds. The SDS in the buffer will also coat the proteins with a uniform negative charge, masking the charge of individual amino acid residues. This results in a charge which is approximately proportional to the molecular weight of the protein. When protein samples buffered in this way are drawn through a polyacrylamide gel matrix by an applied electric field, the friction with the gel combined with the charge on each protein effects the rate with which the protein migrates towards the anode. When the samples reach the end of the gel and the electric field removed, proteins will remain static at the point they reached within the gel. When a control sample with proteins of known sizes (a protein 'ladder') is run alongside experimental protein samples, it is possible to estimate the size of proteins identified in the gel.

Immunoblotting

To identify specific proteins following SDS PAGE, proteins held within the gel are transferred to a membrane such as polyvinylidene fluoride (PVDF) using an electric field applied across the gel. The hydrophobicity of this membrane and its small pore size means the proteins attach firmly. This membrane can then be probed with primary antibodies which recognise the protein of interest, and subsequently with secondary antibodies raised to recognise the Fc domain of

the primary antibody. These secondary antibodies are commonly conjugated to the enzyme horseradish peroxidase (HRP), enabling their detection using a chemiluminescent substrate such as luminol and photographic film. The primary antibody can also be directly conjugated to HRP, removing the need for a secondary antibody step, or the secondary antibody can be conjugated to an infrared dye enabling recognition with a suitable detector.

P62 degradation assay for autophagic flux

P62 is a long-lived adaptor protein which binds to ubiquitinated material in the cytoplasm and to LC3 on the membrane of autophagosomes. In this way it targets ubiquitinated material to the autophagosome for degradation by autophagy. P62 is degraded itself in the process of autophagy, and this phenomenon can be exploited to assess the rate of autophagy, or 'autophagic flux'. When autophagy is stimulated in cell culture, P62 levels should fall in a time-dependant manner. When autophagy is inhibited P62 levels should rise. By studying P62 levels over time during autophagic stimulation or inhibition, we can determine the rate of P62 degradation, and infer the relative rate of autophagic flux between cell lines or growth conditions.

Co-immunoprecipitation.

Co-immunoprecipitation can be used to identify proteins which associate together within a cell. The principle of immunoprecipitation is to isolate a protein from cell lysate by binding it to a specific antibody fused to a substrate, commonly a magnetic or agarose bead. Un-bound cell components can then be removed by gentle washing. In co-immunoprecipitation, the isolated protein acts as 'bait' and other proteins which remain in association with it after washing are described as 'prey'. These 'prey' proteins can then be identified by western blotting or protein sequencing, giving us information about proteins which associate with the 'prey' either directly or as part of a complex, within the cell. It is important to remember that cell lysis by nature will extinguish compartmentalization within the cell, which may allow the association of proteins which would not normally encounter each-other.

Overexpression of tagged 'bait' proteins is a useful technique both to simplify the isolation of the protein onto a substrate pre-coated with antibodies against the tag and to increase the likelihood of detecting protein association. However, excessive overexpression could potentially cause aggregation of a protein, which may lead to false positives if centrifugation is used to isolate the immunoprecipitation substrate and for this reason it is important to include negative controls.

Clonogenic Survival Assay

Clonogenic survival assays provide a means to determine how well cells deal with stress, using the principle that a single cell from an immortal cell line will divide exponentially to produce a colony over a period of several weeks, provided it survives the initial insult.

Standard Error of the Mean

Indicates how far a sample mean deviates from the population mean. A large SEM relative to the value of the sample mean indicates that the sample mean is not closely representative of the mean of the whole population

Students' t-test

This statistical test tells us the probability of any difference between the means of two data sets being due to chance, i.e. the likelihood of the sample data being an inaccurate representation of the population. A low probability such as $P < 0.05$ (less than 5% chance) or less tells us that we can be confident that the difference between the means of two sample data sets is true of the population. Where the test returns a P value of $P > 0.05$ (more than 5% chance) we should assume that any apparent difference between the compared sample means is due to chance and is therefore not significant.

MACROS

Batch Processing images to measure red puncta, green puncta and co-localised puncta.

```
//This is a batch file designed for analyzing colocalised red and green
autophagosome-sized puncta in widefield fluorescence microscopy at 1024x1024,
bin 1x1
//Author: Nicola Humphry, University of Nottingham, 27.12.2017. Modified from
an original macro by Dan Shiwarski, Duvvuri Lab 2010
//NB - size is gated by um assuming SET_SCALE has been set to an appropriate
raw data file (eg dv image) and size (diameter) is recorded as um based on the
set scale in imagej
//on a dv image taken at x100 1024x1024 bin 1x1 15.5497 pixels/um - 10-1000
gates at 0.6-64um. Need 4.5-30 to get 0.3-2um
//on a dv image taken at x60 1024x1024 bin 1x1 9.3985 pixels/um - 10-1000 gates
at 1-106um. Need 3-20 or similar to get 0.3-2um
// (refs say 0.5-1.5um for autophagosomes)
// (refs say 0.1-1.2um for lysosomes)

macro "RedAndGreenPunctaBatch_v5 [F5]" {
wait(100);
dir = getDirectory("Choose Source Directory ");
list = getFileList(dir);
run("Bio-Formats Macro Extensions");
setBatchMode(true);

for (i=0; i<list.length; i++)
{
        showProgress(i+1, list.length);

        if (endsWith(toLowerCase(list[i]), ".tif"))
        {
                open(dir+list[i]);
                origname=getTitle;
                print(" directory is "+dir);
                print(" file is "+origname);

                print(" split channels");
                run("Split Channels");

                run("Window/Level...");
                print(" enhance contrast");
                run("Enhance Contrast", "saturated=0.35");
                setMinAndMax(25, 96);
                saveAs("Tiff", "C:\\coloc\\Blue.tif");
                close();

                run("Window/Level...");
                run("Enhance Contrast", "saturated=0.35");
                setMinAndMax(25, 96);
                saveAs("Tiff", "C:\\coloc\\Green.tif");
                close();

                run("Enhance Contrast", "saturated=0.35");
                setMinAndMax(25, 96);
                saveAs("Tiff", "C:\\coloc\\Red.tif");
                close();

                open("C:\\coloc\\Red.tif");
                open("C:\\coloc\\Green.tif");

                selectWindow("Red.tif");
                run("Subtract Background...", "rolling=14");
                selectWindow("Green.tif");
                run("Subtract Background...", "rolling=14");
                selectWindow("Red.tif");

                print(" autothreshold");
                setAutoThreshold("RenyiEntropy");
                setAutoThreshold("RenyiEntropy dark");
                run("Convert to Mask");
                selectWindow("Green.tif");
```

```
                setAutoThreshold("RenyiEntropy");
                setAutoThreshold("RenyiEntropy dark");
                print(" convert to mask");
                run("Convert to Mask");

run("Merge Channels...", "red=Red.tif green=Green.tif blue=*None* gray=*None*
create");
                run("Stack to RGB");
                run("Split Channels");

print("counting particles 0.1-2um diameter puncta. NB you must have SET_SCALE
to the appropriate dv file first!! lysosomes and autolysosomes are 0.1-1.5um
wide.");

                selectWindow("Composite (RGB) (green)");
                run("Make Binary");
run("Analyze Particles...", "size=0.1-2 circularity=0.60-1.00  show=Masks
display summarize");

                selectWindow("Composite (RGB) (red)");
                run("Make Binary");
run("Analyze Particles...", "size=0.1-2 circularity=0.60-1.00  holes show=Masks
display summarize");

                print("analysing colocalisation");
        run("Colocalization ", "channel_1=[Mask of Composite (RGB) (red)]
channel_2=[Mask of Composite (RGB) (green)] ratio=30 threshold_channel_1=15
threshold_channel_2=15 display=255  colocalizated");

                selectWindow("Colocalizated points (8-bit) ");
                run("Make Binary");
run("Analyze Particles...", "size=0.1-2 circularity=0.30-1.00 holes show=Masks
display summarize");

                //save data
                selectWindow("Mask of Composite (RGB) (green)");
                name=origname+"_green_points_mask_v5";
                path = dir+name;
                print("saving "+name);
                saveAs("jpg", path);

                selectWindow("Results");
                results_name=origname+"_red-green-results_v5";
                path = dir+results_name;
                print("saving "+results_name);
                saveAs("text", path);

                selectWindow("Summary");
                summary_name=origname+"_summary_v5";
                path = dir+summary_name;
                print("saving "+summary_name);
                saveAs("text", path);

                print("closing windows");
                selectWindow(summary_name+".txt");
                run("Close");
                selectWindow("Results");
                run("Close");
                while (nImages>0)  {
                selectImage(nImages); close();
        }
}

}
print("Batch processing completed!.");
```

Batch processing to measure red lysosome puncta.

```
//This is a batch file designed for analyzing red lysosome-sized puncta in
widefield fluorescence microscopy at 1024x1024, bin 1x1
//Author: Nicola Humphry, University of Nottingham, 09.01.2018

//NB - size is gated by um assuming SET_SCALE has been set to an appropriate
raw data file (eg dv image) and size (diameter) is recorded as um based on the
set scale in imagej
//on a dv image taken at x100 1024x1024 bin 1x1 15.5497pixels/um - 10-1000
gates at 0.6-64um. Need 4.5-30 to get 0.3-2um, 1.55-30 to get 0.1 to 2um
//on a dv image taken at x60 1024x1024 bin 1x1 9.3985pixels/um - 10-1000 gates
at 1-106um. Need 1-20 or similar to get 0.1-2.1um

// (refs say 0.5-1.5um for autophagosomes)
// (refs say 0.1-1.2um for lysosomes)

macro "RedLysosomesPunctaBatch_v1 [F5]" {
wait(100);

dir = getDirectory("Choose Source Directory ");
list = getFileList(dir);
run("Bio-Formats Macro Extensions");
setBatchMode(true);

for (i=0; i<list.length; i++) {
        showProgress(i+1, list.length);

        if (endsWith(toLowerCase(list[i]), ".tif"))
        {
                open(dir+list[i]);
                origname=getTitle;
                print(" directory is "+dir);
                print(" file is "+origname);

                print(" split channels");
                run("Split Channels");

                close();
                close();

                run("Enhance Contrast", "saturated=0.35");
                setMinAndMax(25, 96);
                saveAs("Tiff", "C:\\\coloc\\red.tif");
                close();
                open("C:\\\coloc\\red.tif");

                run("Subtract Background...", "rolling=14");
                setAutoThreshold("RenyiEntropy");
                setAutoThreshold("RenyiEntropy dark");
                run("Convert to Mask");


print("counting particles 0.1-2um diameter puncta. NB you must have SET_SCALE
to the appropriate dv file first!! lysosomes and autolysosomes are 0.1-1.5um
wide.");
run("Make Binary");
run("Analyze Particles...", "size=0.1-2 circularity=0.30-1.00  holes show=Masks
display summarize");

        //save data
        selectWindow("Results");
        name=origname+"_RedLysoPunctaResults";
        path = dir+name;
        print("saving "+name);
        saveAs("text", path);

}
}
selectWindow("Summary");
path = dir+"_RedLysoPunctaSummary";
print("saving RedLysoPunctaSummary");
saveAs("text", path);
print("Batch processing completed!");
}
```

ABBREVIATIONS

Abbreviation	Full name
AIF	Apoptosis Inducing Factor
AIM	Atg-8 interaction motif. The yeast equivalent of the LIR
AKT	Protein kinase B
AMP	Adenosine monophosphate Adenosine monophosphate
AMPK	5' AMP-activated protein kinase
Apaf-1	Apoptotic protease activating factor 1
Atg8	Yeast homologue of LC3
BubR1	budding uninhibited by benzimidazole-related 1
CDK-1	Cyclin-dependent kinase 1
CQ	Chloroquine, a lysosomotrophic drug used to inhibit autophagy
DMEM	Dulbecco's Modified Eagle's Medium – a growth medium for cell culture.
DMSO	Dimethyl Sulphoxide, a solvent.
Epg5	Ectopic P-Granules Autophagy Protein 5 Homolog
Erk	Extracellular-signal regulated kinase
Erm1	Ezrin-radixin-moesin family protein 1
Fas	Fas ligand (CD95L) expressed on T-lymphocytes binds to Fas receptor (CD95) on target cells to induce apoptosis.
FASTA	A protein and dna sequence alignment software package using the FASTA Format.
FASTA Format	A standardized format used to represent an amino acid or nucleotide sequence in bioinformatics.
FCS	Foetal calf serum, a mixture of proteins from calf blood used in cell culture to provide growth factors.
GAS2L3	Growth arrest-specific protein –like 3
GTPase	Enzyme capable of binding to and hydrolyzing guanosine triphosphate

HEPES	4-(2-Hydroxyethyl)piperazine-1-ethanesulfonic acid, N-(2-Hydroxyethyl)piperazine-N'-(2-ethanesulfonic acid). A buffer with adequate CO_2-buffering capacity for mammalian cell culture.
HOPS	Hsp70-Hsp90 Organizing Protein
INCENP	Inner centromere protein.
LC3	Microtubule associated protein light chain 3. Protein lipidated for encorporation into autophagosome membranes.g
LIR	LC3 interacting region.
Mad2	Mitotic Arrest Deficient Protein 2
MAP	Microtubule associated protein.
MAPK	Mitogen-activated protein kinase.
MTOR	Mechanistic target of rapamycin
PAGE	polyacrylamide gel electrophoresis, a technique in combination with SDS to separate proteins by molecular weight.
PAS	Phagophore assembly site
PBS	Phosphate-buffered saline.
PI	Phosphatidylinositol
PI3P (PtdIns3K)	Phosphatidylinositol 3-phosphate
Ran	Ras-related nuclear protein
RAP/CQ	Combined rapamycin and chloroquine treatment.
SDS	Sodium dodecyl sulphate, a detergent
SEM	Standard Error of the Mean
SMAC/DIABLO	Second mitochondria-derived activator of caspases, also called Direct IAP-binding protein with low PI.
SNAP29	Synaptosome Associated Protein 29
STX17	Syntaxin 17
TAE	Tris-acetate EDTA buffer

TNF	tumour necrosis factor
TRAIL	TNF-related apoptosis-inducing ligand
ULK-1	Unc-51 like autophagy activating kinase
VAMP8	Vesicle-associated membrane protein 8
VPS34	Vacuolar protein sorting 23. A phosphatidylinositol 3-kinase

© 2018. Published by The Company of Biologists Ltd | Biology Open (2018) 7, bio037374. doi:10.1242/bio.037374

RESEARCH ARTICLE

Survivin inhibits excessive autophagy in cancer cells but does so independently of its interaction with LC3

Nicola J. Humphry and Sally P. Wheatley*

ABSTRACT

Survivin expression is pivotal to life and death at the cellular level. For the past decade its pro-survival activity has been attributed to its essential role in cell proliferation and its ability to inhibit apoptosis. However, a growing body of evidence suggests that it may also contribute to cell viability through an as yet undefined role in autophagy. We report that survivin overexpression in osteosarcoma (U2OS) cells is associated with increased LC3-II expression, smaller autophagosomes, enlarged lysosomes and reduced autophagic flux. We also demonstrate that survivin binds LC3 directly through a canonical LC3-interacting region (LIR) in its baculovirus inhibitors of apoptosis protein (IAP) repeat BIR domain, mutation of which inhibits the interaction, but does not abrogate its influence on autophagy. Collectively these data suggest that survivin expression restricts autophagic flux, thereby inhibiting late-stage autophagy and preventing cell death, but does so independently of LC3.

KEY WORDS: Survivin, Birc5, Autophagy, Lysosome, LC3

INTRODUCTION

Implicit in its name survivin is a protein that promotes cell survival. It is overexpressed in cancer (Ambrosini et al., 1997) where its presence correlates with increased resistance to chemotherapy (Paik et al., 2004) and irradiation (Colnaghi et al., 2006), treatments aimed at killing cancer cells. Thus its expression is a biomarker of poor patient prognosis and survivin itself is a promising target for cancer therapy.

Survivin is both essential for mitosis and can suppress cell death (Altieri, 2008; Wheatley and McNeish, 2005). It has a baculovirus inhibitors of apoptosis protein (IAP) repeat (BIR) domain that assigns it membership to the IAP family. Although expression of survivin is cytoprotective (Ambrosini et al., 1997), and its depletion increases apoptosis (Li et al., 1999; Ambrosini et al., 1998), the exact mechanism by which it inhibits cell death remains uncertain. In terms of apoptotic inhibition, several models have been suggested, including inhibition of the mitochondrial apoptosis promoting factor Smac/DIABLO (Pavlyukov et al., 2011; Song et al., 2003); stabilization of X-linked inhibitor of pro-apoptotic protein (XIAP) (Dohi et al., 2004); and induction of the mitochondrial-nuclear translocation of apoptosis inducing factor (Ambrosini et al., 1997).

School of Life Sciences, Faculty of Medicine and Health Sciences, Queen's Medical Centre, University of Nottingham, Nottingham NG7 2UH, UK.

*Author for correspondence (sally.wheatley@nottingham.ac.uk)

S.P.W., 0000-0002-9550-8979

This is an Open Access article distributed under the terms of the Creative Commons Attribution License (http://creativecommons.org/licenses/by/3.0), which permits unrestricted use, distribution and reproduction in any medium provided that the original work is properly attributed.

Received 26 July 2018; Accepted 23 August 2018

Recently, several lines of evidence have suggested that survivin may aid the evasion of cell death in ways distinct from apoptosis, one of which is manipulation of autophagy, a catabolic process in which intracellular components are broken down and re-used. Briefly, autophagy targets specific intracellular components for degradation by encasing them in a double-membraned vesicle, called an 'autophagosome' that is rich in the human Atg8 homologue, microtubule-associated protein light chain 3 (MAP-LC3 or LC3) bound to phosphatidylethanolamine (PE), LC3-II (Kabeya et al., 2000). Autophagosomes can fuse with endosomes to form amphisomes before fusing either transiently, or completely, with a lysosome to form an autolysosome (Jahreiss et al., 2008). The autophagosome contents are degraded by hydrolytic enzymes that favour an acidic environment before the sub-components are released back into the cytoplasm. Nascent lysosomes can reform from the autolysosome by a process of budding termed 'autophagic lysosome reformation' (ALR) (Yu et al., 2010). Basal levels of autophagy are required for cellular homeostasis but, under stress, including radiation
treatment, autophagy is induced to promote cell survival. However, intracellular re-cycling cannot continue ad infinitum and excessive autophagy ultimately results in cell death (Maiuri et al., 2007).

Emerging data point to several aspects of autophagy that may involve survivin. Firstly, it co-immunoprecipitates with the key autophagic protein, LC3B (Roca et al., 2008); secondly, its expression is upregulated by the autophagic suppressor, mTOR, within the PI3K/Akt pathway (Roca et al., 2008; Zhao et al., 2010); and finally, it interacts with the autophagic regulators Beclin 1 (Niu et al., 2010) and Atg5 (Maskeyet al., 2013). Using live fluorescence imaging, immunoblotting and immunoprecipitation assays, here we report that overexpression of survivin increases LC3-II levels, reduces autophagosome size, enlarges lysosomes, and causes an overall reduction in autophagic flux. We also show that expressing a mutant version, survivin^{F61AL64A}, that cannot bind to LC3, yields similar outcomes. Thus, in addition to its roles in mitosis and apoptosis, we show that survivin can also act in a pro-survival manner by preventing excessive autophagy, but it does so independently of its interaction with LC3.

RESULTS AND DISCUSSION

When survivin is overexpressed in cancer it is hugely detrimental to human health: its abundance correlates with tumour resistance to radiation, and this is recapitulated in cell culture (Colnaghi et al., 2006; Connell et al., 2008; Chakravarti et al., 2004). X-irradiation kills cells by inducing DNA damage and apoptosis, but it also promotes autophagy (Jin et al., 2015; Chen et al., 2015). Therefore we hypothesised that survivin may also protect cells against death by limiting excessive autophagy.

Survivin reduces autophagic flux

To understand how survivin affects autophagy, we first measured the level of LC3-II in U2OS cells overexpressing survivin with and without chloroquine (CQ). CQ is commonly used to assess autophagic flux (Klionsky et al., 2016): it inhibits late stage autophagy causing

Downloaded from http://bio.biologists.org/ by guest on October 22, 2018

Biology Open (2018) 7, bio037374. doi:10.1242/bio.037374

accumulation of autophagosomes. High LC3-II levels suggest either increased autophagic flux or inhibition of latestage autophagy. CQ can help discriminate between these two alternatives as it freely diffuses into lysosomes, but gets trapped there where it inhibits degradative enzymes (Solomon and Lee, 2009; Kunze et al., 1982). If flux is increased CQ will further increase LC3-II levels, however, if late-stage autophagy has been inhibited, no difference will be seen (Klionsky et al., 2016). The use of rapamycin (RAP) in combination with CQ allows us to study autophagic flux above basal levels.

To investigate any potential effects that survivin has on autophagy we chose to use U2OS cells stably expressing survivin^{WT}GFP (green fluorescent protein) or GFP (control). These were treated

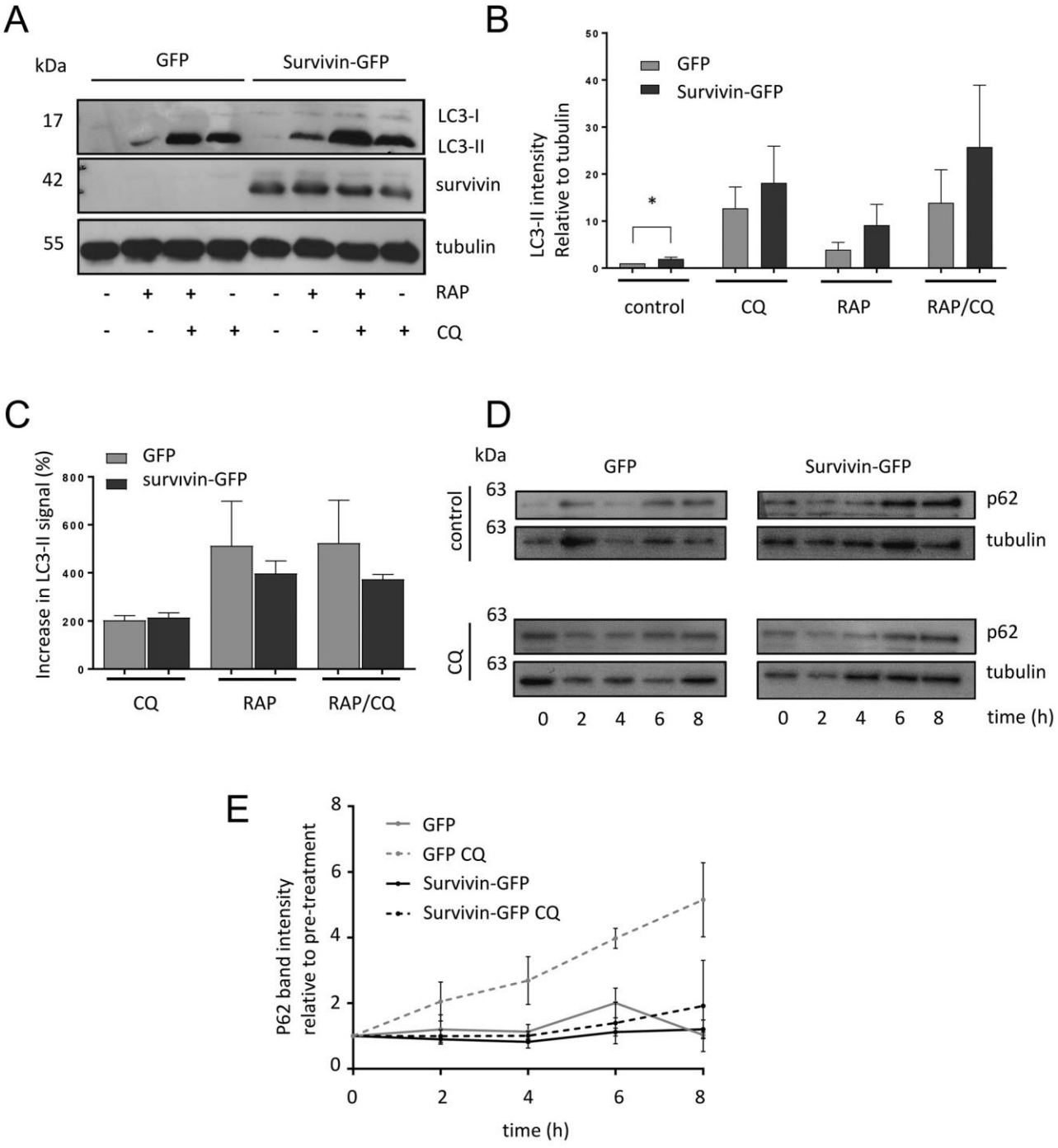


Fig. 1. Survivin regulates autophagic flux. (A) U2OS cells stably expressing survivin^{WT}GFP or GFP alone were treated with RAP (200 nM) and CQ (120 µM) for 2 h, then lysed and immunoblotted with anti-LC3, anti-survivin and anti-tubulin antibodies. Immunoblot shown is representative of four independent experiments. (B) ImageJ quantitation of LC3II signals in (A), normalised against tubulin control and expressed as band intensity relative to untreated GFP cells. (C) Data from (B) expressed as a percentage increase in LC3II between CQ treated and untreated cells to indicate autophagic flux. (D) The above cell lines were treated with CQ (50 µM) for 8 h and p62 levels assessed by immunoblotting at 2 h intervals. Blot shown is representative of three independent experiments. (E) ImageJ quantitation of p62 signals in (D) normalised against tubulin and expressed as band intensity relative to untreated GFP cells. Error bars indicate s.e.m., N=3. *P<0.05.

BiologyOpen

Downloaded from http://bio.biologists.org/ by guest on October 22, 2018

Biology Open (2018) 7, bio037374. doi:10.1242/bio.037374

simultaneously with RAP and/or CQ for 2 h, and LC3II abundance quantified by immunoblotting of whole cell lysates (Fig. 1A). Basal levels of LC3-II in survivin^{WT}GFP cells were significantly higher than in control cells (Fig. 1B). LC3II levels also appeared higher in survivin^{WT}GFP cells after treatment with CQ, RAP or RAP/CQ, however, this did not achieve statistical significance in a Student's t-test. To determine whether this was due to induction or inhibition of autophagic flux, we plotted the increase in LC3II signal (Fig. 1C) and found that the increase was similar in both GFP and survivin^{WT}GFP cells, thus we concluded that survivin inhibits flux, possibly in the same manner as CQ.

To confirm this finding, we assayed p62 levels in these cells. p62 is an adaptor protein that facilitates autophagic degradation by binding to ubiquitinated targets in the cytosol, and to LC3-II on the autophagosome. As a result, p62 itself is degraded by autophagy and this phenomenon can be used to monitor autophagic flux (Klionsky et al., 2016). U2OS cells stably expressing survivin^{WT}GFP or GFP were treated with CQ and p62 expression was assessed at regular intervals from 0-8 h by immunoblotting. In this experiment p62 accumulated significantly more slowly in cells expressing survivin than in control cells, supported by linear regression analysis of treated cell lines ($P<0.0001$; Fig. 1D,E), further substantiating the hypothesis that survivin reduces autophagic flux.

Survivin decreases the size of LC3-positive puncta

To investigate whether survivin alters the number or size of autophagosomes, we measured these parameters in LC3-positive puncta within the cell before and after RAP/CQ treatment. U2OS cells transiently expressing GFP-LC3 and either red fluorescent protein (RFP) or survivin-RFP were imaged live. RAP/CQ treatment caused an increase in the size of LC3-puncta in both RFP and survivin-RFP expressing cells, but those in cells expressing survivin-RFP were significantly smaller (Fig. 2A,B). The number of autophagosomes was similar in both conditions and increased approximately twofold after RAP/CQ treatment (Fig. S1A). These results suggest that survivin regulates autophagosome maturation, potentially by inhibiting fusion with endosomes (Huotari and Helenius, 2011; Eskelinen, 2005).

Survivin increases the size of acidic puncta Fusion of the autophagosome with lysosomes creates an autolysosome with an acidic lumen, allowing lysosomal proteases to digest autophagosomal cell debris. To investigate whether survivin has an impact on lysosomes and autolysosomes, we measured the size and number of acidic puncta within the cell using the cell permeable fluorescent dye, LysoTracker Red, which accumulates in acidic compartments and thus highlights lysosomes and autolysosomes.

To observe the difference in acidic compartments before and after CQ inhibition, U2OS cells stably expressing survivin^{WT}GFP or GFP (control) were treated with CQ for 2 h and imaged live using fluorescent microscopy. In both cell sub-lines, CQ treatment increased the average size of acidic puncta, suggesting an accumulation of autolysosomes and a concurrent reduction in nascent lysosomes formation (Fig. 2C,D). Cells expressing survivin^{WT}GFP had significantly larger acidic puncta both preand post-treatment compared to cells expressing GFP (Fig. 2C,D). No significant difference in the numberof acidic puncta between the sub-lines was observed (Fig. S1B), suggesting that like CQ, survivin causes an accumulation of autolysosomes and a concurrent reduction in nascent lysosomes formation. However, since effects were cumulative when survivin overexpression and CQ treatment were combined, this suggests that survivin operates in a different pathway from CQ.

One potential mechanism by which survivin could work is by inhibiting autophagosome-lysosome fusion, as this causes an increase in lysosome (acidic puncta) size (Chen, 2011). Alternatively it may regulate ALR, a process that is triggered by the reactivation of mTOR at the end of the autophagic pathway, which involves the budding of proto-lysosomes from the autolysosome, which then acquire lysosomal hydrolases and mature into lysosomes (Yu et al., 2010). Inhibition of ALR would decrease the number of small, nascent autolysosomes resulting in an increase in mean lysosome size, similar to our observations in survivin-expressing cells.

SurvivininteractsdirectlywithLC3viaaconservedLIRinthe BIR domain

Having established that survivin suppresses autophagic flux, restricts the size of LC3 puncta and increases the size of acidic puncta, we next asked whether this inhibition was due to association with LC3, with which it is known to co-immunoprecipitate (Roca et al., 2008).

The binding of proteins to LC3 usually occurs via canonical LC3 interaction regions (LIR), which are defined as tetrapeptides with an aromatic residue at position one, and a hydrophobic residue at position four: W/F/Y×X L/I/V (where X is any residue) (Noda et al., 2008). Sequence analysis using iLIR (http://repeat.biol.ucy.ac.cy/ iLIR/) revealed that survivin has five putative LIR motifs, which are highlighted in the primary sequence and the crystal structure (Fig. 3A,B). The first three of these sequences are located within the BIR domain; the fourth in the central linker between residues 90 and 98; and the fifth at the start of the C-terminal alpha helix. Regression analysis of FASTA alignments (CLUSTAL W2, 10 iterations) of survivin homologues from several mammals (EMBL-EBI: www. ebi.ac.uk), was used to generate a sequence logo using (http:// weblogo.berkeley.edu) which showed that all five sites are highly conserved (Fig. 3A). However, since functional LIRs are more frequently associated with exposed beta strands (Noda et al., 2010), we next looked at the position of these five sites in relation to beta strands using UniProt (https://www.uniprot.org/). This stratagem revealed that only F^{61}KEL within the BIR domain conforms to this rule, which is highlighted in the blue ribbon (Fig. 3B). Thus we hypothesized that F^{61}KEL was a bona fide LIR.

To test this hypothesis, we generated a mutant in which residues at positions one and four of the putative LIR, F^{61}KEL, were mutated to an alanine, survivin^{F61A,L64A}, tagged with either GFP, RFP or flag, and the immunoprecipitation and fluorescence experiments were repeated. Unlike survivin^{WT}, survivin^{F61A,L64A} does not associate with LC3 in either an immunoprecipitation of flagsurvivin or an immunoprecipitation of GFP-LC3, clearly

demonstrating that this is a functional and unique LIR in survivin (Fig. 3A,B). However, expression of survivin^{F61A,L64A} had the same effect as the wild-type protein on LC3 puncta and acidic puncta size suggesting that interaction with LC3 is not required for these phenomena (Fig. 3E,F; see representative images in Fig. S1-C).

Consistent with this we also noted that there was no significant co-localisation of survivin at LC3-positive puncta suggesting that survivin does not accumulate on the membranes or in the lumen of autophagosomes (data not shown).

Collectively these data demonstrate that survivin inhibits autophagic flux through a mechanism that restricts autophagosome size but it does so independently of its interaction with LC3 and in a manner distinct from CQ. In addition to LC3, survivin interacts with two other proteins involved in autophagosome formation;

BiologyOpen

Downloaded from http://bio.biologists.org/ by guest on October 22, 2018

Biology Open (2018) 7, bio037374. doi:10.1242/bio.037374

Beclin 1 (Niu et al., 2010), which is involved in membrane trafficking and localizing autophagic proteins to the phagophore (Kang et al., 2011); and atg5 (Maskey et al., 2013) which extends the phagophore and facilitates LC3 lipidation. Consistent with this, it has been reported that depletion of survivin from erythroblasts causes defects in endosome/lysosomal trafficking, which ultimately manifests as an increase in autophagosomes and can be rescued by expression of vacuolin-1, a protein that promotes endosome-lysosome fusion (Keerthivasan et al., 2012). Survivin has also been shown to bind to HBXIP/ LAMTOR5 (Marusawa et al., 2003), a component of the ragulator complex that activates mTOR on the lysosome surface (Bar-Peled et al., 2012), and with clathrin (Keerthivasan et al., 2012) which is included in the membrane of many intracellular vesicles (Royle, 2006) and is also known to regulate ALR (Rong et al., 2012).

We have shown that the inhibitory influence that survivin has on autophagy is independent of its interaction with LC3, which proves that not all LIR motifs and LC3 interactions are autophagy-relevant. So, is there a non-canonical function to the survivin-LC3 interaction? LC3 was initially identified as a protein that interacts with a microtubule-binding protein, and its interaction between a neuronal Ca^{2+}-sensor called 'caldendrin' appears to be related to microtubule association (Seidenbecher et al., 2004; Mann and Hammarback, 1994). It also binds to FYVE and coiled-coil (CC) domain-containing protein 1 (FYCO1) to mediate microtubule plusend directed vesicle transport (Pankiv et al., 2010), so one possibility may be that its liaison with LC3 relates to its influence on microtubule dynamics (Rosa et al., 2006). We are currently investigating this possibility.

Conclusions

In summary, the data herein presented show that survivin can restrict excessive autophagy by reducing autophagic flux and restricting autophagosome maturation. We also identify F_{61}KEL as a function LIR in the BIR domain of survivin, and show that its inhibition of excessive autophagy is independent of its interaction with LC3.

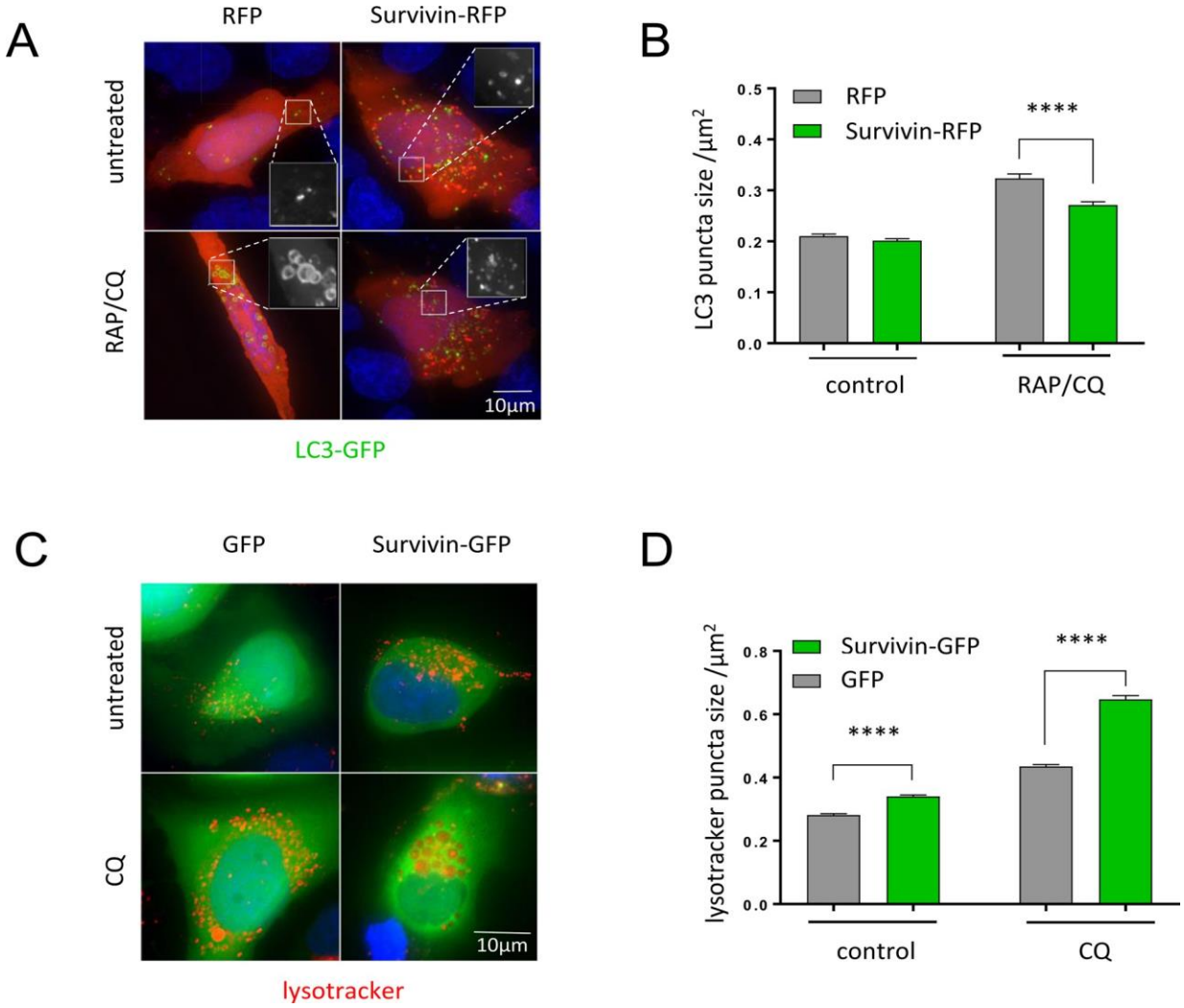


Fig. 2. Survivin regulates autophagosome and lysosome size. (A) Representative images of U2OS cells transiently expressing survivin-RFP and LC3GFP treated with RAP (200 nM) and CQ (120 µM) for 2 h then imaged live. (B) Mean GFP-LC3 puncta size was measured using ImageJ, N>500 puncta, >35 cells over four independent experiments. (C) Live U2OS cells stably expressing GFP or survivin-GFP were stained with LysoTracker Red to highlight acidic compartments. (D) Mean acidic puncta size was measured using ImageJ, N>1500 puncta for>30 cells for each condition in three independent experiments All error bars indicate s.e.m. ****P<0.0001.

BiologyOpen

Downloaded from http://bio.biologists.org/ by guest on October 22, 2018

Biology Open (2018) 7, bio037374. doi:10.1242/bio.037374

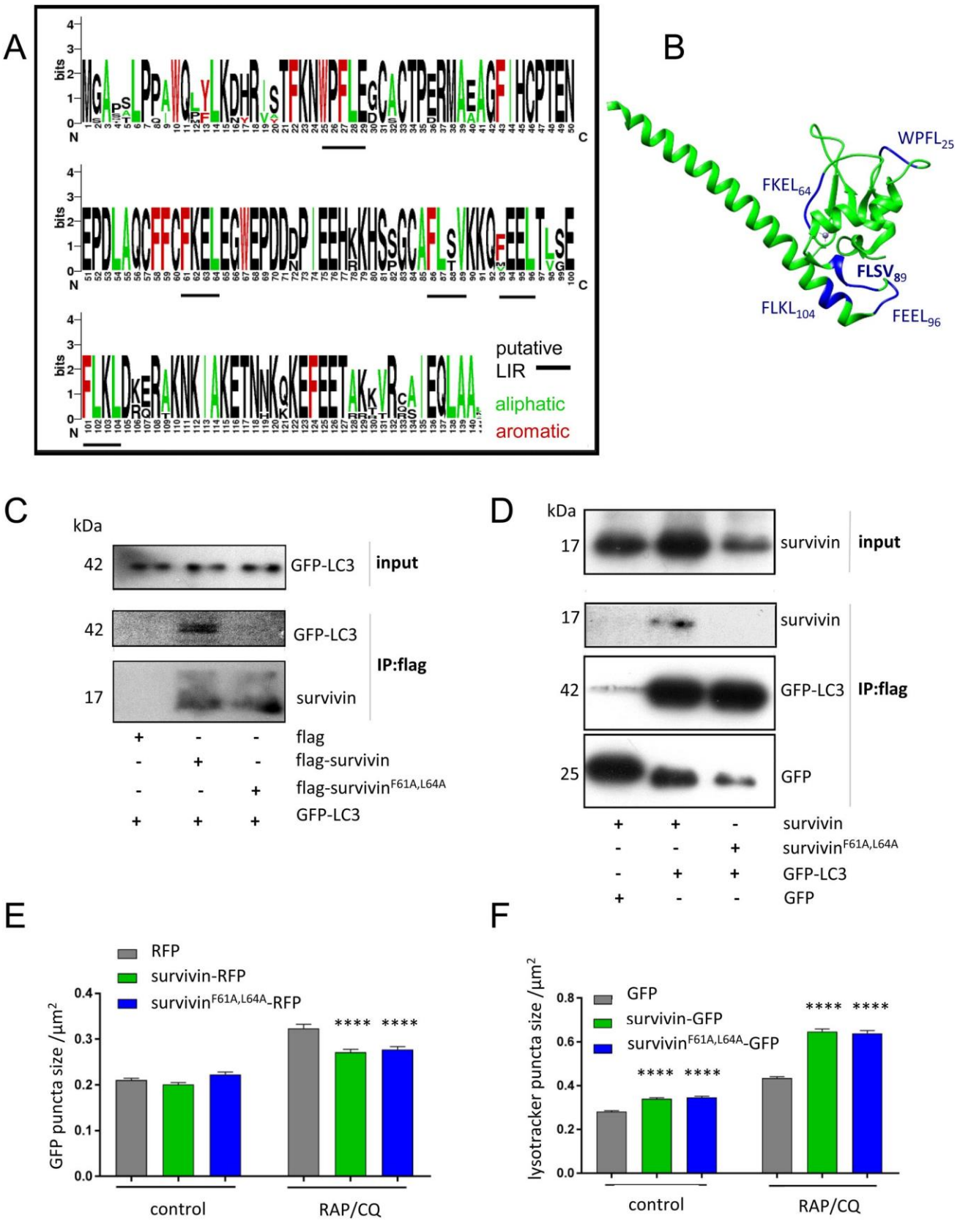


Fig. 3. See next page for legend.

Downloaded from http://bio.biologists.org/ by guest on October 22, 2018

BiologyOpen

Biology Open (2018) 7, bio037374. doi:10.1242/bio.037374

Fig. 3. Survivin F^{61}KEL is a canonical LIR but is not required for autophagy inhibition. (A) The primary sequence of survivin contains five putative LIR motifs, underscored in black within this sequence logo (Schneider and Stephens, 1990) generated from several mammalian homologues of survivin using WebLogo (http://weblogo.berkeley.edu). One stack represents a single position in the sequence, stack height indicates the sequence conservation, and the height of each symbol in the stack indicates the relative frequency of each amino acid at that position. (B) Location of the five putative LIR sites (blue) within the tertiary structure of survivin [PDB 1E31, graphic produced using UCSF Chimera, San Francisco (Pettersen et al., 2004)]. Only F^{61}KEL overlaps a beta strand (blue ribbon). (C) HEK293T cells expressing GFP-LC3 were transiently transfected with either Flag, Flagsurvivin^{WT} or Flag-survivin^{F61A,L64A}. Lysates were immunoprecipitated with anti-Flag antibodies and analysed by immunoblotting for survivin and LC3, N=2. (D) HEK293T cells expressing GFP or GFP-LC3 were transiently transfected with survivin^{WT} or survivin^{F61A,L64A}. Lysates were immunoprecipitated with anti-GFP antibodies and analysed by immunoblotting for survivin and GFP. (E) U2OS cells transiently expressing RFP, survivin^{WT}RFP or survivin^{F61A,L64A}-RFP and LC3-GFP were treated with RAP (200 nM) and CQ (120 µM) for 2 h prior to live cell imaging. Average GFP-LC3 puncta size was measured using ImageJ for each condition N>500 puncta over three independent experiments. (F) Living U2OS cells expressing GFP, survivinGFP or survivin^{F61A,L64A}-GFP were stained with LysoTracker Red to highlight acidic compartments and CQ (120 µM) for 2 h, then imaged live. Average size of acidic puncta was measured using ImageJ for each condition, n>1400 puncta. All experiments representative of N=3. Error bars indicate s.e.m. ****P<0.0001.

MATERIALS AND METHODS

Unless otherwise stated all reagents were obtained from Sigma-Aldrich.

Cell culture

Human osteosarcoma cells and human embryonic kidney (HEK 293T) cells were cultured at 37°C, with 5% CO_2 in Dulbecco's Modified Eagle's Medium (DMEM D6429) supplemented with 10% FCS (Hyclone; PAA Labs). U2OS cells stably expressing GFP or survivin-GFP cells were generated as described in (Jin et al., 2015) and medium supplemented with 50 µg/ml G418 (Geneticin) to maintain expression. Transient transfections were performed using Torpedo transfection reagent (Ibidi) using DNA diluted in PBS as per manufacturer's instructions.

Plasmid constructs

RFP (pDsRed1), survivin-RFP (pDsRed1, survivin insert), survivinF61AL64A-RFP (pDsRed1, survivinF61AL64A insert), flag (pcDNA3.1, flag insert), flag-survivin (pcDNA3.1, flag-survivin insert), flag-survivinF61AL64A (pcDNA3.1, flag-survivinF61AL64A insert), GFP (pcDNA3.1, GFP insert), survivin-GFP (pcDNA3.1, survivin-GFP insert), survivinF61AL64A-GFP (pcDNA3.1 survivinF61AL64A-GFP), GFP-LC3 (pEGFP-N1, LC3 insert).

Drug treatments

To induce autophagy cells were treated for 2 h at 37°C with 200 nM RAP (PHZ1235; Thermo Fisher Scientific). Working stocks of 200 µM lyophilized RAP dissolved in DMSO were stored in aliquots at −20°C.

To inhibit autophagic flux, cells were treated with 120 µM CQ (C6628; Sigma-Aldrich) for 2 h at 37°C or 50 µM CQ for >2 h incubation. Working stocks of 100 mM CQ diphosphate salt dissolved in water were stored in aliquots at −20°C.

Immunoblotting

Standard procedures were used for SDS-PAGE and transfer to PVDF (Amersham Hybond 0.2 µm; GE Healthcare) membrane. Membranes were blocked in 5% (w/v) milk in PBS with 0.1% (w/v) Tween-20. The following primary antibodies were diluted in blocking solution and used to immunoprobe membranes: anti-LC3, which recognises LC3A and LC3B (1:2000; Sigma-Aldrich, L8918), anti-tubulin (1:2000; Sigma-Aldrich, T5168), anti-GFP (1:2000; Sigma-Aldrich, G1546), anti-survivin (1:1000; Novus, NB500-201), anti-histone H3 pT3 (1:2000; 159 Novus, NBP261546), anti-p62 (1:1000; Enzo Life Sciences, BML-PW9860). Horseradish peroxidise-conjugated secondary antibodies (1:2000; Dako) were diluted in either PBS with 0.1% tween (anti-survivin) or blocking medium (all others) and signals detected using enhanced chemiluminescence (Amersham ECL; GE Healthcare) and X-ray film (Amersham Hyperfilm; GE Healthcare). ImageJ (Schneider et al., 2012) was used for quantification.

Fluorescence imaging

Cells were seeded onto 8-well IbiTreat chambered MicroSlides (Ibidi), incubated overnight, then transfected with relevant DNA constructs, and incubated for 24 h. Medium was replaced with HEPES buffered phenol red free DMEM with 10% FCS supplemented with 200 nM RAP, 120 µm CQ or 0.04 nM LysoTracker Red (L7528; Thermo Fisher Scientific) where applicable. Cells were imaged on an inverted fluorescence microscope (Olympus Delta Vision Elite) using oil immersion objectives: 60× (NA 1.42), or 100× (NA 1.40). Z-stacks were taken at 0.3 µm intervals, deconvolved and z-projected for maximum intensity using SoftWorx software (Applied Precision). Bespoke macros were used with ImageJ (Schneider et al., 2012) software to count and measure puncta.

Immunoprecipitations

HEK293T cells were used for all co-immunoprecipitation experiments. For immunoprecipitation of survivin, cells were seeded onto a 6-well plate and once approximately 70% confluent, transfected with plasmid constructs for GFP-LC3 and either Flag (control), Flag-Survivin or Flag-survivin^{F61A,L64A}. After 24 h, cells were washed with cold PBS and harvested by scraping into ice-cold lysis buffer (50 mM TrisHCl pH 7.5, 150 mM NaCl, 1 mM EDTA, 1% Triton x-100, 1 µg/ml CLAP containing chymostatin, leupeptin, antipain, pepstatin A and 100 µM AEBSF) and lysed on ice (30 min) with gentle pipetting. Lysates were clarified by centrifugation at 17,000 g to eliminate cell debris and DNA (10 min at 4°C) and the supernatant retained. A sample of the lysate (20 µl) was removed as an input sample and boiled in 20 µl sample buffer (125 mM TrisHCl, pH 6.8, 4% SDS, 20% glycerol, 0.004% bromophenol blue) in a heat block at 90°C for 3 min. To the remainder, Anti-flag M2 Affinity Gel (A2220; Sigma-Aldrich) was added to precipitate flag-tagged proteins as per the recommended protocol.

For immunoprecipitation of LC3, cells were seeded on a six-well plate and grown to 70% confluence, then transfected with plasmid constructs for survivin or survivin^{F61AL64A}, and either GFP (control) or GFP-LC3. After 24 h, cells were harvested and re-plated into 10 cm^2 tissue culture dishes. Once 70% confluent, cells were scraped into 1 ml cold PBS and washed twice by centrifugation at 500× g. Each cell pellet was then resuspended in 200 µl lysis buffer (10 mM Tris/Cl pH 7.5; 150 mM NaCl; 0.5 mM EDTA; 0.5% NP-40, 1 µg/ml CLAP containing chymostatin, leupeptin, antipain and pepstatin A, 100 µM AEBSF) and lysed on ice for 30 min with gentle pipetting. DNA and cell debris were pelleted as above and supernatant retained. GFP-Trap-A beads (gta20; ChromoTek) were used to precipitate GFP and GFP-tagged proteins as per the manufacturer's protocol.

Statistical methods

Data from fluorescence images were analysed using GraphPad Prism where paired immunoblots or unpaired two-tailed t-tests were performed to compare the data between conditions, and Welch's correction where sample variance was considered significant by an f-test. A $P<0.05$ for the t-test or f-test was considered significant. Outliers were removed from all fluorescence imaging measurements using the GraphPad ROUT method.

Acknowledgements

BiologyOpen

Downloaded from http://bio.biologists.org/ by guest on October 22, 2018

We thank Dr Stephen Tait for GFP-LC3; Dr Alan Huett and Professor Rob Layfield for helpful discussions. We also recognise the technical contributions of Sophie Rochette, Jamie Webster, Nikko Liceralde and Jessica Winfield. Imaging was carried out in the School of Life Sciences Imaging Facility (SLIM).

Competing interests

The authors declare no competing or financial interests.

Author contributions

Conceptualization: N.J.H., S.P.W.; Methodology: N.J.H., S.P.W.; Investigation: N.J.H., S.P.W.; Writing - original draft: N.J.H.; Writing - review & editing: S.P.W.; Supervision: S.P.W.

Funding

This research received no specific grant from any funding agency in the public, commercial or not-for-profit sectors.

Supplementary information

Supplementary information available online at http://bio.biologists.org/lookup/doi/10.1242/bio.037374.supplemental

References

Altieri, D. C. (2008). Survivin, cancer networks and pathway-directed drug discovery. Nat. Rev. Cancer 8, 61-70.

Ambrosini, G., Adida, C. and Altieri, D. C. (1997). A novel anti-apoptosis gene, survivin, expressed in cancer and lymphoma. Nat. Med. 3, 917-921.

Ambrosini, G., Adida, C., Sirugo, G. and Altieri, D. C. (1998). Induction of apoptosis and inhibition of cell proliferation by survivin gene targeting. J. Biol. Chem. 273, 11177-11182.

Bar-Peled, L., Schweitzer, L. D., Zoncu, R. and Sabatini, D. M. (2012). Ragulator is a GEF for the Rag GTPases that signal amino acid levels to mTORC1. Cell 150, 1196-1208.

Chakravarti, A., Zhai, G. G., Zhang, M., Malhotra, R., Latham, D. E., Delaney, M. A., Robe, P., Nestler, U., Song, Q. and Loeffler, J. (2004). Survivin enhances radiation resistance in primary human glioblastoma cells via caspaseindependent mechanisms. Oncogene 23, 7494-7506.

Chen, P. (2011). Chloroquine treatment of ARPE-19 cells leads to lysosome dilation and intracellular lipid accumulation: possible implications of lysosomal dysfunction in macular degeneration. Cell Biosci. 8, 1-10.

Chen, N., Wu, L., Yuan, H. and Wang, J. (2015). ROS/Autophagy/Nrf2 pathway mediated low-dose radiation induced radio-resistance in human lung adenocarcinoma A549 cell. Int. J. Biol. Sci. 11, 833-844.

Colnaghi, R., Connell, C. M., Barrett, R. M. A. and Wheatley, S. P. (2006). Separating the anti-apoptotic and mitotic roles of survivin. J. Biol. Chem. 281, 33450-33456.

Connell, C. M., Colnaghi, R. and Wheatley, S. P. (2008). Nuclear survivin has reduced stability and is not cytoprotective. J. Biol. Chem. 283, 3289-3296.

Dohi, T., Okada, K., Xia, F., Wilford, C. E., Samuel, T., Welsh, K., Marusawa, H., Zou, H., Armstrong, R., Matsuzawa, S.-I. et al. (2004). An IAP-IAP complex inhibits apoptosis. J. Biol. Chem. 279, 34087-34090.

Eskelinen, E.-L. (2005). Maturation of autophagic vacuoles in mammalian cells. Autophagy 1, 1-10.

Huotari, J. and Helenius, A. (2011). Endosome maturation. EMBO J. 30, 3481-3500.

Jahreiss, L., Menzies, F. M. and Rubinsztein, D. C. (2008). The itinerary of autophagosomes: from peripheral formation to kiss-and-run fusion with lysosomes. Traffic Cph Den. 9, 574-587.

Jin, X., Li, F., Zheng, X., Liu, Y., Hirayama, R., Liu, X., Li, P., Zhao, T., Dai, Z. and Li, Q. (2015). Carbon ions induce autophagy effectively through stimulating the unfolded protein response and subsequent inhibiting Akt phosphorylation in tumor cells. Sci. Rep. 5, 13815.

Kabeya, Y., Mizushima, N., Ueno, T., Yamamoto, A., Kirisako, T., Noda, T., Kominami, E., Ohsumi, Y. and Yoshimori, T. (2000). LC3, a mammalian homologue of yeast Apg8p, is localized in autophagosome membranes after processing. EMBO J. 19, 5720-5728.

Kang, R., Zeh, H. J., Lotze, M. T. and Tang, D. (2011). The Beclin 1 network regulates autophagy and apoptosis. Cell Death Differ. 18, 571-580.

Keerthivasan,G.,Liu,H.,Gump,J.M., Dowdy,S.F.,Wickrema,A.andCrispino, J. D. (2012). A novel role for survivin in erythroblast enucleation. Haematologica 97, 1471-1479.

Klionsky, D. J., Abdelmohsen, K., Abe, A., Abedin, M. J., Abeliovich, H., Acevedo Arozena, A., Adachi, H., Adams, C. M., Adams, P. D., Adeli, K. et al. (2016). Guidelines for the use and interpretation of assays for monitoring autophagy (3rd edition). Autophagy 12, 1-222.

Kunze, H., Hesse, B. and Bohn, E. (1982). Effects of antimalarial drugs on several rat-liver lysosomal enzymes involved in phosphatidylethanolamine catabolism. Biochim Biophys Acta. 713, 112-117.

Li, F., Ackermann, E. J., Bennett, C. F., Rothermel, A. L., Plescia, J., Tognin, S., Villa, A., Marchisio, P. C. and Altieri, D. C. (1999). Pleiotropic cell-division defects and apoptosis induced by interference with survivin function. Nat. Cell Biol. 1, 461-466.

Maiuri, M. C., Zalckvar, E., Kimchi, A. and Kroemer, G. (2007). Self-eating and self-killing: crosstalk between autophagy and apoptosis. Nat. Rev. Mol. Cell Biol. 8, 741-752.

Mann, S. S. and Hammarback, J. A. (1994). Molecular characterization of light chain 3. A microtubule binding subunit of MAP1A and MAP1B. J. Biol. Chem. 269, 11492-11497.

Marusawa, H., Matsuzawa, S.-I., Welsh, K., Zou, H., Armstrong, R., Tamm, I. and Reed, J. C. (2003). HBXIP functions as a cofactor of survivin in apoptosis suppression. EMBO J. 22, 2729-2740.

Maskey, D., Yousefi, S., Schmid, I., Zlobec, I., Perren, A., Friis, R., Simon, H. U. (2013). ATG5 is induced by DNA-damaging agents and promotes mitotic catastrophe independent of autophagy. Nat. Commun. 2, 4130.

Niu, T.-K., Cheng, Y., Ren, X. and Yang, J.-M. (2010). Interaction of Beclin 1 with survivin regulates sensitivity of human glioma cells to TRAIL-induced apoptosis. FEBS Lett. 584, 3519-3524.

Noda, N. N., Kumeta, H., Nakatogawa, H., Satoo, K., Adachi, W., Ishii, J., Fujioka, Y., Ohsumi, Y. and Inagaki, F. (2008). Structural basis of target recognition by Atg8/LC3 during selective autophagy. Genes Cells 13, 1211-1218.

Noda, N.N., Ohsumi,Y.and Inagaki,F. (2010). Atg8-family interacting motif crucial for selective autophagy. FEBS Lett. 584, 1379-1385.

Paik, S., Shak, S., Tang, G., Kim, C., Baker, J., Cronin, M., Baehner, F. L., Walker, M. G., Watson, D., Park, T. et al. (2004). A multigene assay to predict recurrence of tamoxifen-treated, node-negative breast cancer. N. Engl. J. Med. 351, 2817-2826.

Pankiv, S., Alemu, E. A., Brech, A., Bruun, J.-A., Lamark, T., Øvervatn, A., Bjørkøy, G. and Johansen, T. (2010). FYCO1 is a Rab7 effector that binds to LC3 and PI3P to mediate microtubule plus end–directed vesicle transport. J. Cell Biol. 188, 253-269.

Pavlyukov, M. S., Antipova, N. V., Balashova, M. V., Vinogradova, T. V., Kopantzev, E. P. and Shakhparonov, M. I. (2011). Survivin monomer plays an essential role in apoptosis regulation. J. Biol. Chem. 286, 23296-23307.

Pettersen, E. F., Goddard, T. D., Huang, C. C., Couch, G. S., Greenblatt, D. M., Meng, E. C. and Ferrin, T. E. (2004). UCSF Chimera–a visualization system for exploratory research and analysis. J. Comput. Chem. 25, 1605-1612.

Roca, H., Varsos, Z. and Pienta, K. J. (2008). CCL2 protects prostate cancer PC3 cells from autophagic death via phosphatidylinositol 3-kinase/AKT-dependent survivin up-regulation. J. Biol. Chem. 283, 25057-25073.

Rong, Y., Liu, M., Ma, L., Du, W., Zhang, H., Tian, Y., Cao, Z., Li, Y., Ren, H., Zhang, C. et al. (2012). Clathrin and phosphatidylinositol-4,5-bisphosphate regulate autophagic lysosome reformation. Nat. Cell Biol. 14, 924-934.

Rosa, J., Canovas, P., Islam, A., Altieri, D. C. and Doxsey, S. J. (2006). Survivin modulates microtubule dynamics and nucleation throughout the cell cycle. Mol. Biol. Cell 17, 1483-1493.

Royle, S. J. (2006). The cellular functions of clathrin. Cell Mol. Life Sci. 63, 1823-1832.

Schneider, T. D. and Stephens, R. M. (1990). Sequence logos: a new way to display consensus sequences. Nucleic Acids Res. 18, 6097-6100.

Schneider, C. A., Rasband, W. S. and Eliceiri, K. W. (2012). NIH Image to ImageJ: 25 years of image analysis. Nat. Methods 9, 671-675.

Seidenbecher, C. I., Landwehr, M., Smalla, K.-H., Kreutz, M., Dieterich, D. C., Zuschratter, W., Reissner, C., Hammarback, J. A., Bö ckers, T. M., Gundelfinger, E. D. et al. (2004). Caldendrin but not calmodulin binds to light chain 3 of MAP1A/B: an association with the microtubule cytoskeleton highlighting exclusive binding partners for neuronal Ca2+-sensor proteins. J. Mol. Biol. 336, 957-970.

Solomon, V. R. and Lee, H. (2009). Chloroquine and its analogs: A new promise of an old drug for effective and safe cancer therapies. European Journal of Pharmacology 625, 220-233.

Song, Z., Yao,X. and Wu, M. (2003). Direct interaction between Survivin and Smac/ DIABLO is essential for the anti-apoptotic activity of survivin during taxol-induced apoptosis. J. Biol. Chem. 278, 23130-23140.

Wheatley, S. P. and Mcneish, I. A. (2005). Survivin: a protein with dual roles in mitosis and apoptosis. Int. Rev. Cytol. 247, 35-88.

Yu, L., Mcphee, C. K., Zheng, L., Mardones, G. A., Rong, Y., Peng, J., Mi, N., Zhao, Y., Liu, Z., Wan, F. et al. (2010). Termination of autophagy and reformation of lysosomes regulated by mTOR. Nature 465, 942-946.

Zhao, P., Meng, Q., Liu, L.-Z., You, Y.-P., Liu, N. and Jiang, B.-H. (2010). Regulation of survivin by PI3K/Akt/p70S6K1 pathway. Biochem. Biophys. Res. Commun. 395, 219-224.

BiologyOpen

Downloaded from http://bio.biologists.org/ by guest on October 22, 2018